Tagging – die Entwicklung neuer Quantifizierungsmethoden in der NMR Spektroskopie

Dissertation zur Erlangung des naturwissenschaftlichen Doktorgrades
der Fakultät für Chemie und Pharmazie
der Julius-Maximilians-Universität Würzburg

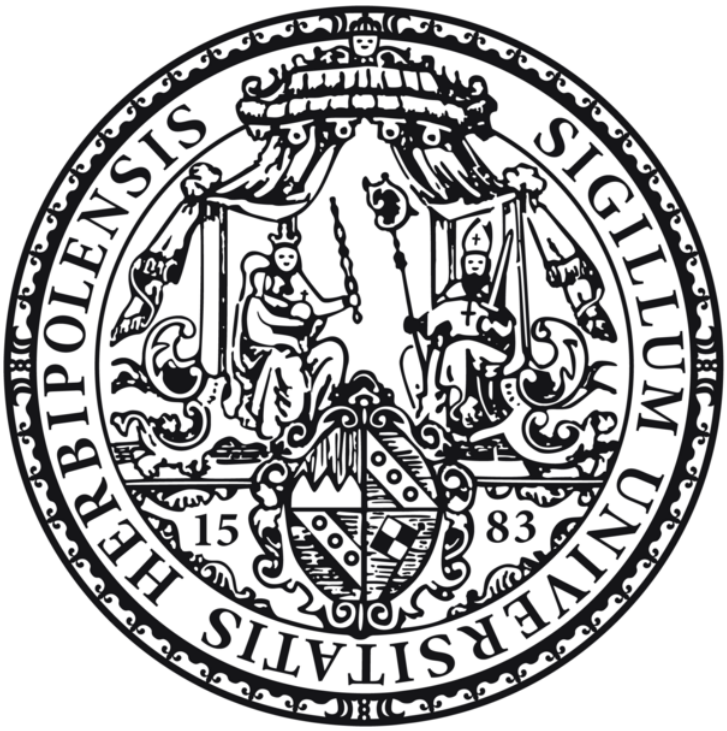

Elina Hafer, geb. Zailer

aus Atbasar, Kasachstan

Oktober, 2020

Eingereicht bei der Fakultät für Chemie und Pharmazie am: .....

Gutachter der schriftlichen Arbeit:

1. Gutachter/in: Prof. Dr. Ulrike Holzgrabe

2. Gutachter/in: .....

Datum des öffentliches Promotionskolloquiums: .....

Prüfer des öffentliches Promotionskolloquiums:

1. Prüfer/in: Prof. Dr. Ulrike Holzgrabe

2. Prüfer/in: .....

3. Prüfer/in: .....

Doktorurkunde ausgehändigt am: .....

Acknowledgements

The present study was carried out as a cooperation of the **Julius-Maximilians University**, Department of Chemistry and Pharmacy, in Würzburg and **Spectral Service AG** in Cologne, during the period 2015 and 2020.

I would like to thank my supervisor **Prof. Dr. Ulrike Holzgrabe** for her academical input, guidance, support in creating scientific papers and her valuable comments and suggestions on how to improve them. Thank you very much for sharing infinite knowledge in the field of pharmacy with me and for giving me the opportunity to learn, and to write my thesis.

I owe my most sincere thanks to **Prof. Dr. Bernd W. K. Diehl** for providing the ideo of this thesis, for his guidance, time, patience, support and trust. I hope to achieve his understanding concerning NMR spectroscopy some day in the future.

I also want to thank **Spectral Service AG** for giving me the opportunity to work on my thesis and to present my research results on conferences and congresses all over the world. Thank you very much to all my colleagues, who have supported me in the laboratory, with the NMR analyses and the spectra evaluation.

I thank all cooperation partners and co-authors who have made scientific contribution to this work, especially **James Hook, Ph. D.**, and **Kristie M. Adams, Ph. D.**, who have supported me all the years with long discussions, explanations and encouragements.

Finally, my warmest gratitude to my amazing **friends** and my big **Zailer-Hafer-Janssen family**, especially to my husband **Bastian** as well as my parents **Lisa** and **Viktor** and my sister **Luise**, who have supported me during the long journey to this doctoral degree with all the light and dark moments that every researcher encounters, and for an amazing life outside work.

Contents

1 Introduction **1**
- 1.1 Basics of qNMR spectroscopy . . . 2
  - 1.1.1 Selectivity . . . 2
  - 1.1.2 Chemical Inertness . . . 2
  - 1.1.3 Solubility . . . 3
  - 1.1.4 Sufficient Resolution . . . 3
  - 1.1.5 Relaxation . . . 4
  - 1.1.6 Stability . . . 7
- 1.2 Quantification . . . 9
  - 1.2.1 Relative Quantification Method . . . 9
  - 1.2.2 Absolute Quantification Method . . . 10
- 1.3 Applications of qNMR Spectroscopy . . . 13
  - 1.3.1 Quality Control of Heparin . . . 14
  - 1.3.2 Quality Control of Infant Milk . . . 15
  - 1.3.3 Quality Control of Oxidation in Edible Oils . . . 16
  - 1.3.4 Quality Control of Inorganic Divalent Metal Ions . . . 19
  - 1.3.5 Quality Control of Enantiomeric Products . . . 21
- 1.4 Tagging . . . 24

2 Aims of the study **25**

3 Interlaboratory Comparison Test **27**
- 3.1 Abstract . . . 27
- 3.2 Introduction . . . 27
- 3.3 Method . . . 29
  - 3.3.1 Materials . . . 29
  - 3.3.2 Sample Preparation . . . 29
  - 3.3.3 Experimental NMR Analysis Procedures . . . 29
  - 3.3.4 Experimental Data Procedures . . . 29
  - 3.3.5 NMR Data Collection . . . 30
  - 3.3.6 Statistical Data Analysis . . . 30
- 3.4 Results and Discussion . . . 32
  - 3.4.1 Vegetable Oil Analysis by ^{1}H-NMR Spectroscopy . . . 32

3.4.2 Statistical Analysis and Performance Assessment . . . 34
3.4.3 Challenging Signals . . . 42
3.4.4 Effect of the Instrument . . . 45
3.5 Conclusions . . . 46
3.6 Acknowledgments . . . 46

4 Peroxide Value **47**
4.1 Abstract . . . 47
4.2 Introduction . . . 48
4.3 Method . . . 50
4.3.1 Materials . . . 50
4.3.2 Sample Preparation . . . 51
4.3.3 Experimental NMR Analysis . . . 52
4.4 Results and Discussion . . . 53
4.4.1 Holistic NMR Method . . . 53
4.4.2 TPP ^{1}H-{^{31}P} decoupled NMR Method . . . 54
4.4.3 Comparison of titration and NMR methods . . . 60
4.4.4 Hydroperoxides in krill oil . . . 64
4.5 Conclusions . . . 65

5 Divalent Metal Cations **67**
5.1 Abstract . . . 67
5.2 Introduction . . . 68
5.3 Method . . . 69
5.3.1 Materials . . . 69
5.3.2 Sample Preparation . . . 69
5.3.3 ^{1}H NMR Measurements . . . 71
5.3.4 Calculation . . . 71
5.4 Results and Discussion . . . 72
5.4.1 pH effect on the chemical shift of EDTA . . . 72
5.4.2 Qualitative Analysis of Metal Ions and Intramolecular Exchange Processes of Met-EDTA-complexes . . . 75
5.4.3 Quantitative Analysis of Metal Ions in Artificial Salt Solutions . . . 80
5.4.4 Application in Artificial Samples: Quantitative Analysis of Lead in Water . . . 83
5.4.5 Application to Commercial samples: Quantitative Analysis of Metal Ions in Food Supplements and Pharmaceutical Products . . . 83
5.5 Conclusions . . . 86

6 Enantiomeric Excess **87**
6.1 Abstract . . . 87
6.2 Introduction . . . 87
6.3 Method . . . 91

6.3.1 Materials . . . 91
6.3.2 Sample Preparation . . . 91
6.3.3 Experimental NMR Analysis . . . 92
6.4 Results and Discussion . . . 92
6.4.1 Menthol . . . 93
6.4.2 Borneol . . . 99
6.4.3 1-Phenylethanol . . . 100
6.4.4 Linalool . . . 101
6.5 Conclusions . . . 102

7 Final Discussion **103**
7.1 Peroxides in Oils . . . 104
7.1.1 Conventional titration techniques . . . 104
7.1.2 Interlaboratory Comparison Test (ILC) . . . 105
7.1.3 ^{1}H NMR method by using TPP . . . 106
7.2 Divalent metal cations by ^{1}H NMR spectroscopy . . . 110
7.3 Enantiomeric Excess by ^{13}C NMR spectroscopy . . . 112
7.4 Conclusions . . . 115

8 Zusammenfassung **117**

9 Abstract **119**

Appendix **143**

List of Abbreviations

ANOVA	Analysis Of Variance
AOCS	American Oil Chemists' Society
AQ	Aquisition Time
BHT	Butylated Hydroxytoluene
c	Concentration
CCQM	Consultative Committee for Amount of Substance
CDA	Chiral Derivatization Agents
CE	Capillary Electrophoresis
CSA	Chiral Solvating Agent
CSR	Chiral Lanthanide Shift Reagent
δ	Delta, Chemical Shift in [ppm]
D1	Relaxation Delay
DCC	N,N'-dicyclohexylcarbodiimide
dec.	Decoupled
DGF	Deutsche Gesellschaft für Fettwissenschaft
DHA	Docosahexaenoic Acid
EMA	European Medicines Agency
EDTA	Ethylenediaminetetraacetic Acid
EDQM	European Directorate for the Quality of Medicines and Healthcare
ee	Enantiomeric Excess
EPA	Eicosapentaenoic Acid
$Eu(hfc)_3$	Tris(((Heptafluoropropyl) Hydroxy Methylene)-d-Camphorato) Europium
EXSY	Exchange Spectroscopy
FA	Fatty Acid
F-AAS	Flame Atomic Absorption Spectrometry
FAO	Food and Agriculture Organization
FDA	Food & Drug Administration
FFA	Free Fatty Acid
FT-NIR	Fourier Transform-Near Infrared
GC	Gas Chromatography
HPLC	High-Performance Liquid Chromatography
HSD	Tukey's Honest Significant Difference
Hz	Hertz

ICP-AAS	Inductively Coupled Plasma Atomic Absorption
ILC	Interlaboratory Comparison
IR	Infrared
ISO	International Organization for Standardization
LC	Liquid Chromatography
LOD	Limit of Detection
LOQ	Limit of Quantification
M	Molar
MD-GC	Multidimensional Gas Chromatography/Mass Spectrometry
Met	Metal Ion
Met-EDTA	Metal-EDTA Complex
MHz	Mega Hertz
MS	Mass Spectrometry
MTPA	α-Methoxy-α-Trifluormethyl-Phenylacetic Acid (Mosher)
MTPA-Cl	Mosher-Chloride
nFBAPTA	1,2-Bis(o-Aminophenoxy)Ethane-N, N, N',N'-Tetra Acetic Acid
NIST	National Institute of Standards and Technology
NMR	Nuclear Magnetic Resonance
OSCS	Oversulfated Chondroitin Sulfate
PC	Phosphatidylcholine
ppm	Parts Per Million
Ph. Eur.	European Pharmacopoeia
PV	Peroxide Value
qNMR	Quantitative Nuclear Magnetic Resonance
RSD	Relative Standard Deviation
SD	Standard Deviation
SI	International System of Units
si	Real Spectrum
S/N	Signal-to-Noise
SW	Spectral Width
T1	Spin-Lattice Relaxation Time
TAG	Triacylglyceride
TD	Number of Datapoints
TMS	Tetramethylsilane
TMSP	3-(Trimethylsilyl)Propionic Acid-d_4 Sodium Salt
TPP	Triphenylphosphine
TPPO	Triphenylphosphine Oxide
UN	United Nations
USP	United States Pharmacopoeia
WHO	World Health Organization
wt-%	Weight-%
$Yb(tfc)_3$	Tris[3-(Trifluoromethylhydroxymethylene)-d-Camphorato] Ytterbium

Chapter 1

Introduction

During the last almost 60 years, the nuclear magnetic resonance (NMR) spectroscopy has become more and more important in structure elucidation and quantitative analysis for purity determination and reference material analysis [1], [2], [3]. The broad applicability of NMR spectroscopy in quality assessment of food, cosmetics, personal care and pharmaceuticals has been well proven [4]. Besides that, NMR spectroscopic analysis enjoys great popularity due to its numerous advantages: it can be readily automated for a high-throughput analysis; the technique requires in most cases only little sample preparation as well as little amount of solvents, and it is highly reproducible and non-destructive [3], [5]. Consequently, the number of publications dealing with quantitative nuclear magnetic resonance (qNMR) spectroscopy, whose fundamentals are presented in chapter 1.1 and 1.2, shows a significant increase within the last 20 years [3]. This represents the potential and the growing interest in qNMR spectroscopy as an analytical tool. By way of example, five NMR methods are presented as applications for the quality control of heparin, milk, edible oils, metal ions and enantiomeric products in chapter 1.3.

In this thesis, analytical issues are solved by qNMR spectroscopy using tagging reagents, whereby *tagging* is defined in chapter 1.4. An interlaboratory comparison (ILC) test for the analysis of edible oils by using NMR spectroscopy is organized (chapter 3) and three NMR methods are developed: determination of peroxides in vegetable and animal oils (chapter 4), examination of divalent cations such as Mg^{2+}, Ca^{2+}, Sr^{2+}, Zn^{2+}, Cd^{2+}, Hg^{2+}, Sn^{2+} and Pb^{2+} (chapter 5), and study of the enantiomeric excess of chiral alcohols (chapter 6).

In chapter 7 an overview of the NMR methods including sample preparation and NMR experiment is given. Moreover, the advantages as well as the drawbacks and limits of the developed methods are discussed in detail, and prospects for future research are presented. The results of the thesis are summarized in German and English in chapter 8 and 9.

1.1 Basics of qNMR spectroscopy

NMR spectroscopy is the examination of molecules containing NMR active nuclei in a strong homogeneous magnetic field by recording the absorbtion of electromagnetic radiations at an isotope-characteristic frequency. The basics of NMR spectroscopy are well-known and explained by, among others, Timothy D.W. Claridge [6]. The current work focuses on the liquid qNMR spectroscopy, whereby solid state NMR spectroscopy is not part of this thesis.

The direct proportionality of the signal intensity I_x in the NMR spectrum to the number of nuclei N_x, responsible for the particular resonance, represents the fundamental, quantitative relationship of qNMR spectroscopy (equation 1.1). The spectrometer constant K_s is the same for all resonances in an NMR spectrum. Since the signals of only one NMR spectrum are integrated and compared, the spectrometer constant K_s does not affect the quantitative results [6], [7].

$$I_x \propto N_x, \text{ so } I_x = K_s \cdot N_x \tag{1.1}$$

The NMR spectrum is quantitative if the six rules, also known as **SCSSRS** are obeyed: **S**electivity, **C**hemical Inertness, **S**olubility, **S**ufficient Resolution, **R**elaxation, and **S**tability [6], [7], [8]. In the following, each rule of **SCSSRS** is introduced in detail.

1.1.1 Selectivity

Selectivity belongs to the critical quality attributes, presenting the ability of a method to determine all analytes of interest in parallel without interferences between them [9]. The specificity, on the other hand, enables a substance or substance class to be recorded without being falsified by other components which are present in the sample. NMR detectable components show signals in the NMR spectrum, like for example, all proton containing substances show proton signals in the ^{1}H NMR spectrum in a suitable solvent. In order to integrate the signals and, thus, to quantify the content of the substance, the signals of an internal standard as well as of the substance of interest should not interfere with other signals. To overcome signal overlapping, the following procedures can be applied: measurement on an NMR spectrometer with a different magnetic field, changing the pH value, using another signal for quantification, applying another solvent or quantifying by alternative integration procedures such as deconvolution [8].

1.1.2 Chemical Inertness

After the selection of a suitable solvent and an appropriate internal standard, the solution is checked to examine its inertness in order to avoid chemical reactions between analyte, internal standard and solvent. If any reaction is detected, different internal standard or solvent should be chosen.

1.1.3 Solubility

A prerequisite for liquid qNMR spectroscopy is the complete solubility of the substance which is examined in a suitable solvent. The choice of solvent determines the chemical shift of the signals, their visibility and coupling pattern. When analyzing substances with exchangeable protons such as hydroxy and amine groups, they often appear as broad signals which may disturb the integration. In aprotic solvents, the addition of small amounts of protic solvents such as deuterated water (D_2O) or deuterated methanol (MeOD) may be advantageous because, due to a fast hydrogen-deuterium exchange, the broad signals are no longer visible [10].

1.1.4 Sufficient Resolution

A sufficient resolution includes the signal-to-noise ratio and the digital resolution:

1. **Signal-to-noise (S/N) ratio:** The S/N ratio influences the accuracy of the quantification significantly. For a quantitative analysis of the main component, a S/N ratio of $\geq$ 150:1 [11], 200:1 [12] or 250:1 [13] of the integrated ^{1}H NMR signal is required to obtain a measurement uncertainty of <1%. High-precision determinations can be achieved when the S/N ratio reaches values of 10000:1 [14]. The S/N ratio is influenced by the quality of the NMR tube, sample concentration, concentration of solid particles (turbidity) and paramagnetic impurities as well as the hardware of the NMR spectrometer such as cryogenically cooled probe technology, and NMR measurement parameters like the number of scans (ns). According to equation (1.2) doubling the ns results in an increase of the S/N ratio of a factor $\sqrt{2} \approx 1.414$ [6]. To double the S/N ratio, it is necessary to increase the ns by a factor of 4, resulting in a four times longer experiment time.

$$S/N \propto \sqrt{ns} \tag{1.2}$$

2. **Digital resolution:** qNMR analysis requires an adequate digital resolution, which is calculated by dividing the spectral width (SW) by the number of data points (TD) [Hz/point]. The spectral resolution equals the spectral width SW divided by the size of the real spectrum (si, unit in k = 1000). A sufficient resolution is at less than 0.5 Hz/point [10], [15]. If the NMR spectrum is acquired with a low number of data points, there are not enough points to describe the Lorenzian line of the signal, leading to an inaccurate signal, and thus, to an inaccurate integral value as shown in the example of an ^{1}H NMR spectrum of Cs-EDTA in D_2O where different si values are used (figure 1.1).

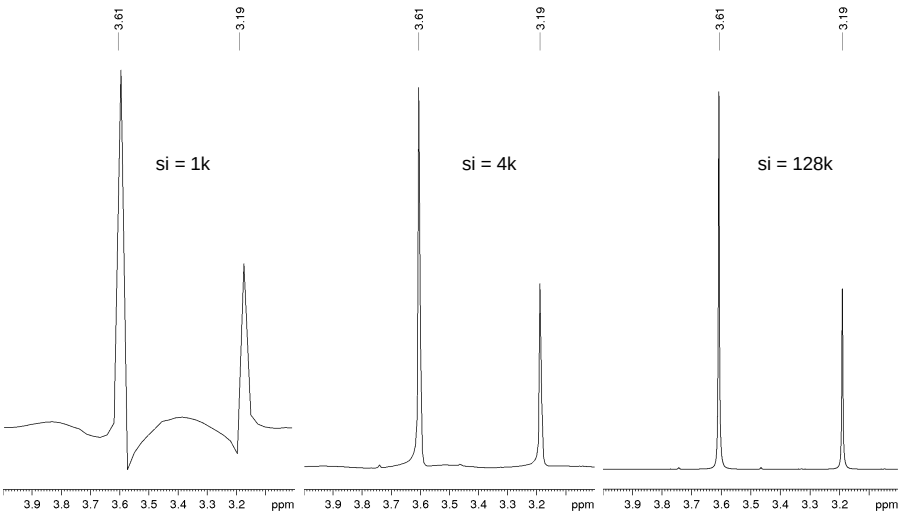

Figure 1.1: ^{1}H NMR spectra of Cs-EDTA in D_2O with si=1k, si=4k and si=128k (from left to right), 500 MHz.

1.1.5 Relaxation

When a sample is placed in a homogenous magnetic field, the spins of the nuclei align parallel or antiparallel to the magnetic field. A radio frequency pulse excits all spins to a certain angle versus the spectrometer magnetic field. After the pulse is terminated, the spins return to their original equilibrium state. This process is known as *relaxation*. The length of the relaxation delay depends on inter alia the irradiated pulse angle as well as on the longest spin-lattice relaxation time *T1* of the resonances used for integration. Protons usually have a *T1* relaxation time of $\leq$ 10 s. Small, symmetrical compounds or substances with isolated protons have significantly higher *T1* times than large, asymmetrical molecules with adjacent protons or other residues such as fluorine, hydroxy or amino groups. To determine the *T1* relaxation time, several experiments can be used. Because in this research work, the *T1* determination of protons was performed by using an *inversion-recovery sequence*, this experiment is explained in detail here (figure 1.2). By a 180° pulse, the magnetization of the protons is inverted from the +z-axis along to the -z-axis (figure 1.3: state A to state B, page 6). Without any further intervention, the magnetization relaxes from the -z-axis back toward its initial equilibrium position along the +z-axis [6].

To convert the *longitudinal* magnetization into a visible NMR signal, an additional 90°_x pulse is implemented resulting in a *transverse* magnetization (i.e., in x'y'-plane). The subsequent 90°_x pulse can be applied soon or late after the first 180°_x pulse (short or long τ). If the 90°_x pulse is carried out right after the 180°_x pulse (short τ), the magnetization will be rotated from the -z-position into the -y'-axis giving a negative signal (figure 1.3: state B to state C_{short} to D_{short}, page 6). If the evolution period τ is longer, the 90°_x pulse will be applied while the z-magnetization recedes along the -z-axis to zero value (figure 1.3: state B to state C_{long} to D_{long}, page 6). Thus, the longer the τ intervals are, the more

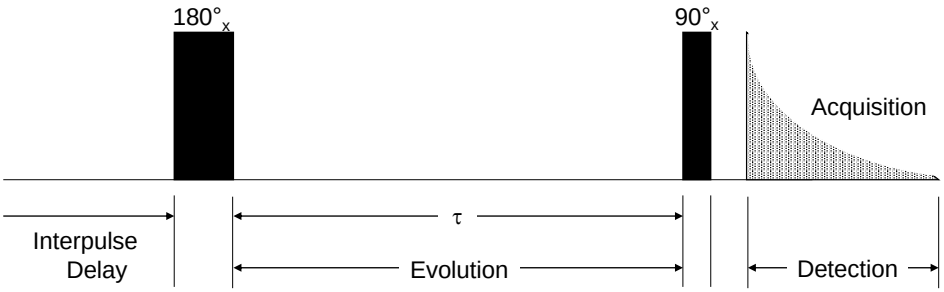

Figure 1.2: Inversion-recovery sequence [6] [Copyright (2016) Elsevier].

the magnetization rotates along the +z-axis toward its original equilibrium value (figure 1.3: state A, page 6). Within the *inversion-recovery sequence* a series of NMR spectra are produced: with negative signals for short τ, and after going through a null point, positive NMR signals for longer evolution processes τ. The successive pulse sequence is repeated n times. Here, the pulses are executed, τ and the fixed relaxation delays between successive pulses are adjusted automatically. After plotting the signal intensities as a function of the pulse width, the "zero" point, where the signal intensity is switched from a negative towards a positive value, is determined. This point is called *zero transition time* τ_0. The *zero transition time* τ_0 is used to calculate the *T1* relaxation time according the equation 1.3 [6].

$$T_1 = \frac{\tau_0[sec]}{ln(2)} = \frac{\tau_0[sec]}{0.693} \tag{1.3}$$

For an accurate quantification, it must be ensured that the resonances, which are used for the quantification, are fully relaxed. A 99.3% relaxation can be achieved by running the recycling with a time difference of 5 times the longest *T1*, by increasing the waiting time to 7 times the longest *T1*, 99.9% of the spin magnitization is totally relaxed [5], [16].

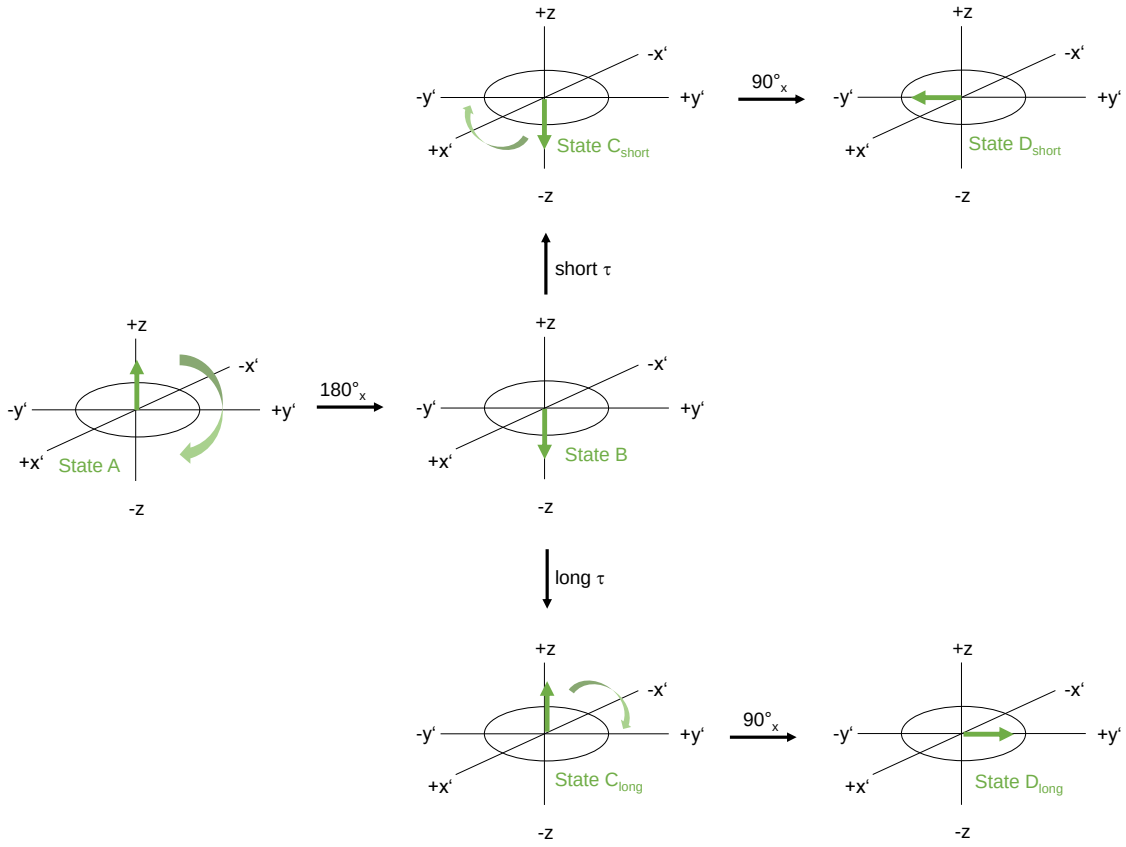

Figure 1.3: Rotation of magnetization during inversion-recovery sequence [6] [Copyright (2016) Elsevier].

1.1.6 Stability

Stability is defined as the ability of a method to provide comparable results over a specified period of time. The chemical stability of the test and reference substance in the prepared sample solution must be ensured at least for the duration of an NMR experiment or for the duration of an analytical series. To check this parameter, several prcedures are possible. One procedure is to measure a control sample several times over a previously defined period of time against a freshly prepared comparison sample of the sample stored at the defined storage conditions (e.g. room temperature, refrigerator temperature, light protection). The difference in content determines the process stability. If the test item is not stable in the solvent, the content of the active ingredient will change significantly over time [5]. In the following example, a sample with the active ingredient R-2-chloroacetate (comment: R is a rest which cannot be outlined in detail due to a non-disclosure agreement with the manufacturer of the sample) has been analyzed immediately after sample preparation, after 24 hours and after 72 hours as a six-fold determination, respectively, according to customer's request. The average content of the active ingredient R-2-chloroacetate as well as the deviations of the six-fold determination after 0 hours, 24 hours and 72 hours are presented in figure 1.5a. As shown in figure 1.5a, within 72 hours the content of the active ingredient decreased from 98.05% to 96.52%. Conversely, the amount of the degradation products increased. Degradation product 1 was identified as 2-chloroacetic acid whose amount more or less doubled from 0.28% to 0.57% (figure 1.5b, green). Additionally, an alcohol was identified as another degradation product whose amount also rose from 0.39% to 0.74% (figure 1.5b, red). Consequently, it was stated that the sample was not stable at the given parameters. After presenting the results, the customer agreed hygroscopic properties which have been studied in the past without informing us prior the validation study (figure 1.4). Thus, the active ingredient degraded at each vial opening. The example illustrated that as an analyical chemist, it is essential to have as much information of the sample as possible to provide an accurate and precise quantitative result. Additionally, this example demonstrates the importance of validation studies.

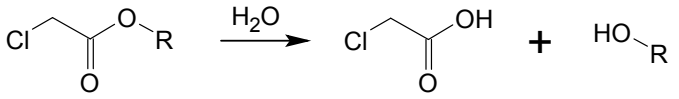

Figure 1.4: Degradation reaction of the active ingredient R-2-chloroacetate forming the two degradation products 2-chloroacetic acid and an alcohol with R (no further information on the rest R is allowed to be provided).

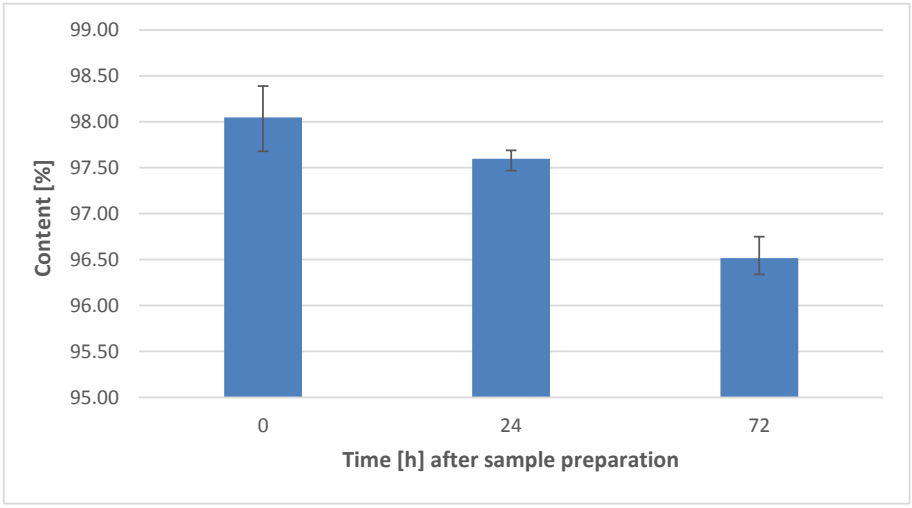

a) active ingredient R-2-chloroacetate

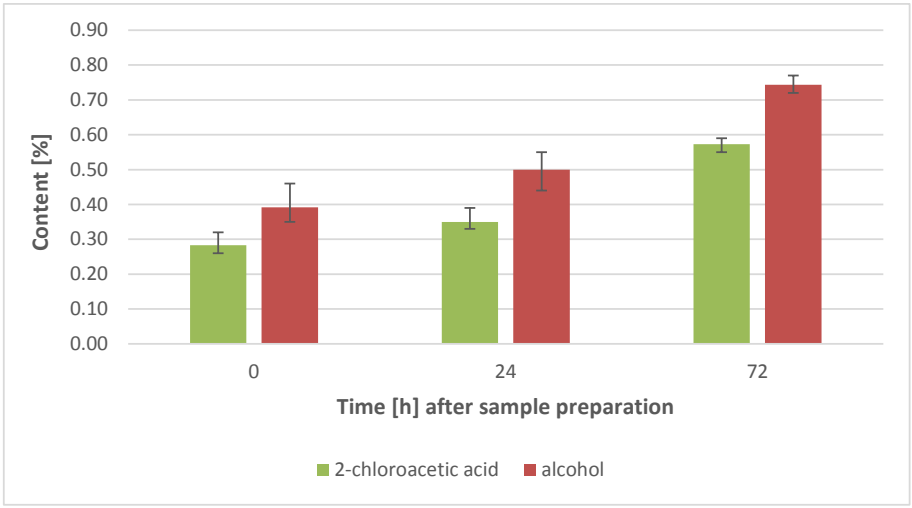

b) degradation products 2-chloroacetic acid (green) and alcohol (red)

Figure 1.5: Varying concentration of (a) the active ingredient R-2-chloroacetate, and (b) the degradation products 2-chloroacetic acid and alcohol over 72 hours.

1.2 Quantification

qNMR spectroscopy is a *relative primary method* which is defined by the *Consultative Committee for Amount of Substance (CCQM)* as follows:

- A **primary method of measurement** is a method of the highest metrological quality, whose operation can be completely described and understood, and for which a complete uncertainty statement can be written in terms of the International System of Units (SI, abbreviated from the French Système international d'unités).

- A **relative primary method** measures the value of ratio of an unknown standard of the same quantity; its operation must be completely described by a measurement equation [17], [18], [19], [20].

The principle of qNMR spectroscopy is based on the measurement and subsequent signal area comparison which makes the determination of a ratio of the substances and as well as of an absolute measures possible. The different methods of determination including relative determination, absolute determination by means of standard addition as well as external and internal standards are discussed in detail in the following sections.

1.2.1 Relative Quantification Method

Thus, the determination of the substance quantity ratio n_X/n_Y of two components X and Y in a substance mixture is carried out by comparing the signal intensities I_X/I_Y with simultaneous consideration of the number of nuclei N according to equation 1.4 [11], [21].

$$\frac{n_X}{n_Y} = \frac{I_X}{I_Y} \cdot \frac{N_Y}{N_X} \tag{1.4}$$

As long as the experimental parameters are optimized, all molecules underlie the same experimental conditions. Thus, K_s (equation 1.1) is equal for the resonances which are included in the equation 1.4 and can be cancelled. The determination of the substance quantity fraction of a component X in a substance mixture consisting of Z components is carried out according to equation 1.5 [11], [22].

$$\frac{n_X}{\sum_{i=1}^{Z} n_i} = \frac{I_X \cdot N_X}{\sum_{i=1}^{Z} \frac{I_i}{N_i}} \cdot 100\% \tag{1.5}$$

1.2.2 Absolute Quantification Method

Standard Addition Method

The standard addition method is an often used technique in cases if the analyte is very reactive or if no suitable internal standard is present. In the spiking process, a known amount of analyte is added to the sample stepwise, the sample solution is measured after each addition and the increase of the analyte signal is determined. The integral value (=y-axis) is plotted against the sample concentration (=x-axis), showing ideally a linear correlation with the function y = ax + b. The original content of the analyte is determined as the absolute value of the intersection of the straight line with the x-axis (y=0) as illustrated in figure 1.6. Although the technique belongs to the standard methods in an analytical laboratory, the disadvantages of the method are the following: (i) for each analyte of interest a reference material is needed to be purchased which is very expensive depending on the substance and the number of substances, (ii) additionally, the purity of the reference substances have to be known which makes a prior quantification of them essential, (iii) since the added amount should be in the same range as the amount of present analyte, several dilution steps can be required, (iv) and finally, the method is very time-consuming, which is not optimal for a fast routine analysis in industry [23].

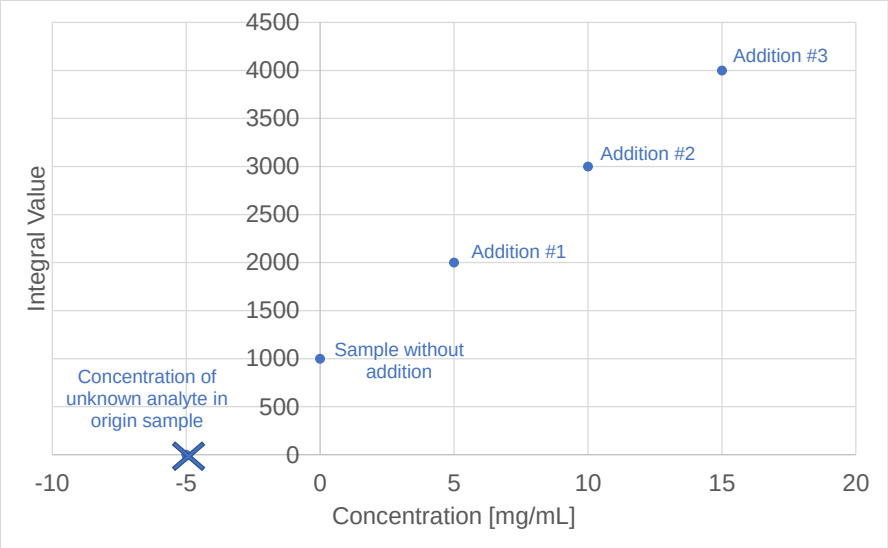

Figure 1.6: Example of a determination of an unknown concentration by standard addition.

Internal Standard

The most common qNMR method is the *internal standard method*. The content of the analyte is determined by the addition of a suitable reference material of defined purity, known as the *internal standard*. Primary standards are produced and supplied by scientific

organizations such as the European and United States Pharmacopoeia [24]. Therefore, internationally accepted primary reference material serves as an primary internal standard, ensuring SI traceability. The National Institute of Standards and Technology (NIST) offers benzoic acid as a primary reference material intended for use as a primary standard for qNMR analysis [25]. Furthermore, secondary standards are standardized against primary standard representing traceable certified reference materials [26]. Secondary standards can be purchased with a certification by e. g. Sigma Aldrich whose relative standard uncertainty, based on the uncertainty budget illustrated in figure 1.7, is determined to a typical value of 0.15% to 0.3% [27], [28], [29]. 1,2,4,5,-Tetrachloro-3-nitro-benzene; 2,4-Dichloro-benzotrifluoride and Triphenylphosphate are examples of routinely used secondary stardards for ^{1}H qNMR, ^{19}F qNMR and ^{31}P qNMR spectroscopy, respectively.

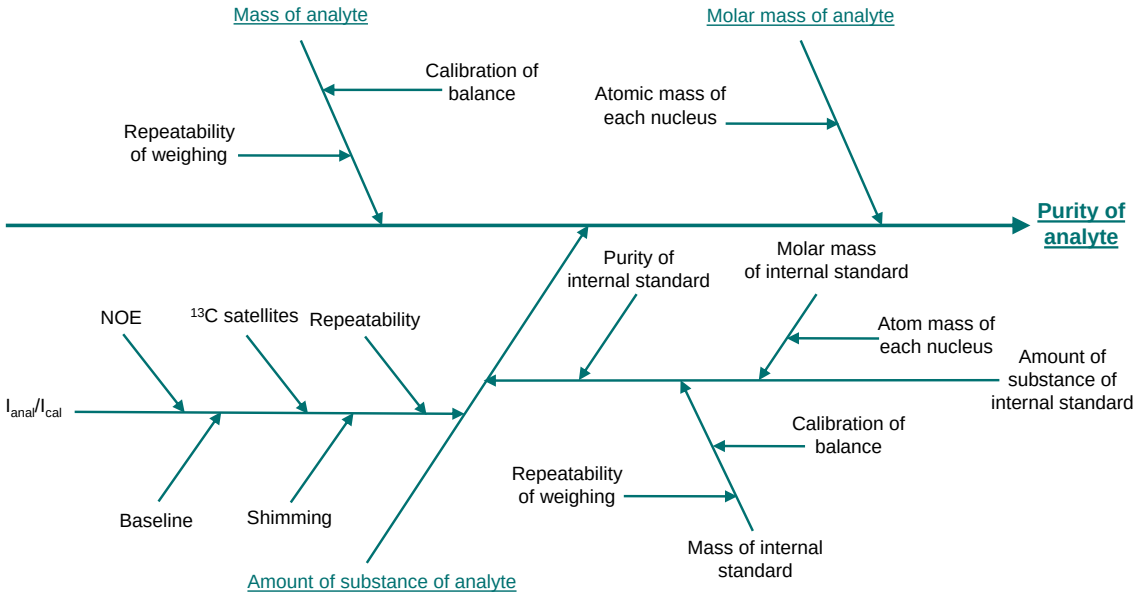

Figure 1.7: Uncertainty budget of qNMR spectroscopy [29]. [Copyright (2004) John Wiley and Sons.]

Unlike chromatography, in NMR analysis the chemical structure of the internal standard does not have to be similar to the analyte. However, the internal standard should met following conditions: presence of nucleus of interest, high purity, stable, chemical inert, non-volatile, non-hygroscopic, easy handling within the weighing process (e.g. not liquid, nonhazardous), suitable molecular weight, short *T1* time and preferably simple signal multiplicity (singlet better than multiplet) as well as cost-effective [5], [30].

The process of a qNMR analysis can be presented as follows: analyte and internal standard are weighed and dissolved, the solution is measured by NMR spectroscopy and the NMR spectrum is evaluated. One signal of analyte and reference material, respectively, is integrated. The content of the analyte (X) is determined by the weighing amount (W),

molecular weight (M), number of atoms (N), integrals (I) as well as the purity (P) for the internal standard (IS) according to equation 1.6 [11], [5]. As shown in the uncertainty budget of the qNMR measurement in figure 1.7, the measurement uncertainty of the internal standard method is determined by uncertainties of the weighing process, as well as of the spectrum evaluation and atom masses.

$$P_X = \frac{I_X}{I_{IS}} \cdot \frac{N_{IS}}{N_X} \cdot \frac{M_X}{M_{IS}} \cdot \frac{W_{IS}}{W_X} \cdot P_{IS} \tag{1.6}$$

Since the number of atoms (N) has no uncertainties, the molecular weight (M) is a well described value with a very low uncertainty and the purity of the internal standard should also show a low uncertainty, the weighing amount as well as the integration have a significant influence on the quantitative results. Thus, training and excercising in weighing and evaluating NMR spectra are essential for providing a precise and accurate qNMR result [5].

External Standard Method

If a contamination of the sample by adding standards should be avoided, the content can be determined alternatively by using the *External Standard Method* according the following two ways: (i) "tube-in-tube" method, also known as "two-tube" method or (ii) the use of two separate NMR tubes [5], [30].

The first option uses a concentric NMR tube, where a capillary, which is filled with the external standard, is placed in the NMR tube, filled with the analyte solution. The sample and reference substance are measured simultaneously, but without being mixed. The interpretation of the NMR spectrum is comparable with the internal standard method. In the second option, the sample and the reference substance are measured in two separate NMR tubes in succession. Here, it is essential that the same measuring conditions such as measurement parameters are used for both experiments. An advantage of the external standard method is that the sample is not being contaminated with other substances except the solvent. However, this procedure is more time-consuming and error-prone compared with the internal standard method [5], [30]. One source of error is the NMR tube volume and, thus, the amount of sample and standard. A research, carried out by Kristie Adams, has shown that the diameter and wall thickness of the latest precision-NMR tubes deviate, indicating a volume deviation of up to 4% (research has not been published yet). Other researchers reported uncertainties of the external standard technique of up to 2%, which is siginificantly higher than uncertainties of 0.5% which has been published for the qNMR method using internal standards [12], [28], [31]. In routine, the internal standard analysis is primarily used, but the external standard technique is considered as an alternative if the internal standard method cannot be applied [5].

1.3 Applications of qNMR Spectroscopy

NMR has found its way into European (Ph. Eur.) and United States Pharmacopoeias (USP) after numerous research articles presented NMR spectroscopy as a powerful analytical technique for the determination of identity and content of small and larger molecules. Ph. Eur. has incorporated the NMR spectroscopy in method 2.2.33 including general requirements, NMR analysis of different nuclei but mainly ^{1}H and ^{13}C, qualitative and quantitative NMR methods, parameters, fourier transform NMR as well as solid-state spectroscopy [32]. A variety of Ph. Eur. NMR methods is presented in table 1.1.

Table 1.1: NMR methods in European Pharmacopoeia (status 08/2020)

Method Title	**Identification**	**Quantification**	**Publication date & no.**
Peptide identification by nuclear magnetic resonance spectrometry	^{1}H NMR	-	07/2011:20264 [33]
Medronic acid for radio-pharmaceutical preparations	^{1}H NMR	-	07/2017:2350 [34]
Buserelin	^{1}H NMR	-	01/2016:1077 corrected 10.0 [35]
Cod-liver oil, farmed	^{13}C NMR	-	07/2012:2398 [36]
Gonadorelin acetate	^{1}H NMR	-	04/2018:0827 corrected 10.0 [37]
Goserelin	^{1}H NMR	-	01/2013:1636 corrected 9.6 [38]
Heparin calcium	^{1}H NMR	-	01/2020:0332 [39]
Heparin sodium	^{1}H NMR	-	01/2020:0333 [40]
Heparins, low-molecular-mass	^{13}C NMR	-	07/2019:0828 corrected 10.0 [41]
Hydroxypropylbetadex	-	^{1}H NMR	01/2017:1804 [42]
Lauromacrogol 400	-	^{13}C NMR	01/2020:2046 [43]
Octreotide	^{1}H NMR	-	01/2020:2414 [44]
Pemetrexed disodium heptahydrate	^{1}H NMR	-	01/2017:2637 corrected 10.0 [45]
Salmon oil, farmed	^{13}C NMR	^{13}C NMR	07/2012:1910 [46]
Starch, hydroxypropyl	^{13}C NMR	^{1}H NMR	01/2013:2165 corrected 10.0 [47]
Starch, hydroxypropyl, pregelatinised	^{13}C NMR	^{1}H NMR	07/2013:2645 corrected 10.0 [48]
Sulfobutylbetadex sodium	^{13}C NMR	^{1}H NMR	07/2019:2804 corrected 10.0 [49]
Terlipressin	^{1}H NMR	-	07/2027:2414 [50]

In the USP, NMR spectroscopy including qualification (installation, operational and performance), validation and verification is explained in the general chapter <761>, whereby chapter <1761> presents the various applications of NMR spectroscopy [51], [52].

As shown by the number of official NMR methods, the study of pharmaceutical products belongs to the most important applications of qNMR spectroscopy. Here, within only one analysis run active ingredients, by- and degradation products, excipients, as well as solvent residues in the starting, intermediate and finished products can be examined which are required for drug acceptance or storage stability. The development of qNMR methods for analyzing various pharmaceutical formulations is increasing continuously. Five applications are introduced in this chapter to present the wide range of applications of qNMR spectroscopy.

1.3.1 Quality Control of Heparin

One of the examples which demonstrates the power of NMR spectroscopy in the quality control of pharmaceutical products is the analysis of heparin sodium. Heparin is a linear sulfated polysaccharide with repeating $1 \rightarrow 4$ glycosidically linked residues of hexuronic acid and glucosamine, which represents one of the most widely used anticoagulant drugs (figure 1.8) [53], [54], [55]. In 2008, a significant high number of negative effects was associated with heparin sodium, even death of patients have been reported. After a short while, the Food & Drug Administration (FDA) and the European Directorate for the Quality of Medicines and Healthcare (EDQM) have published a ^{1}H NMR method for the quality control of sodium heparin by screening the products for contaminations and conspicuities [56], [57]. A contamination was detected in some heparin batches at a chemical shift of $\delta = 2.15$ ppm, which was identified as oversulfated chondroitin sulfate (OSCS). Since this discovery, heparin sodium monographs have been updated promptly and hormonized within the following years by the Ph. Eur., USP and Japanese Pharmacopoeia obligating the manufacturers to perform identity (and purity) testings by ^{1}H NMR spectroscopy [58], [59], [60]. By the dissolution of an appropriate amount of the heparin sample in D_2O containing 3-(trimethylsilyl)propionic acid-d_4 sodium salt (TMSP) as reference standard, the analysis of identity of heparin as well as the control of potentially existing contaminations or fraud substances can be performed [61]. This case shows that NMR spectroscopy can be used as a powerful analytical technique for the qualitative and quantitative study of the active ingredient as well as contaminations.

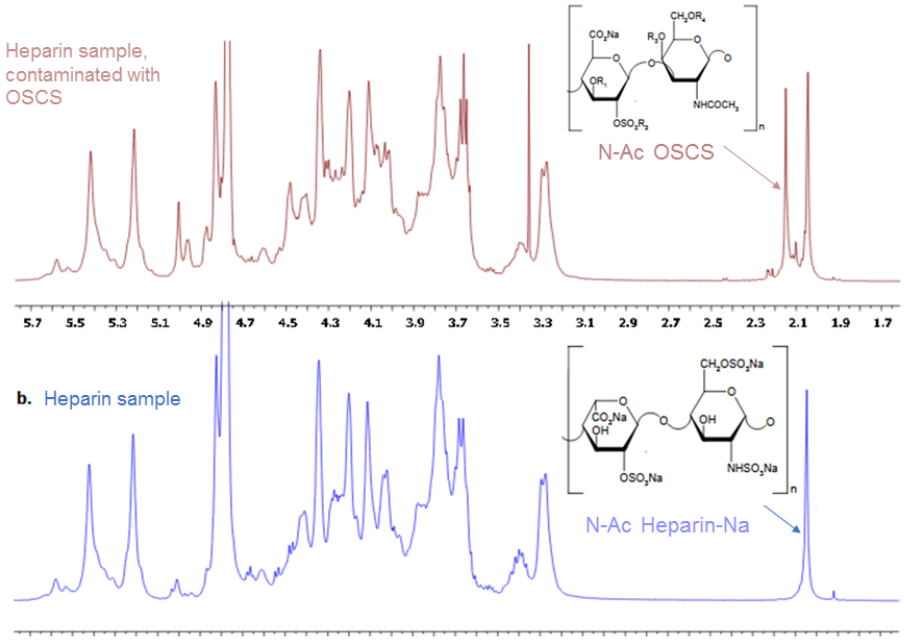

Figure 1.8: ^{1}H NMR spectrum of heparin sample (blue) and of heparin system suitability sample spiked with OSCS (red), based on [62]. [Copyright (2012) Dr. Francisco Cardenas.]

1.3.2 Quality Control of Infant Milk

Authentication is an important part of the quality control which has come even more into focus after several fraud scandals. One of the best-known food scandal was the epidemic caused by melamine poisoning in infant milk products in China in 2008. Melamine (2,4,6-triamino-1,3,5-triazine, figure 1.9) is commonly used in several industrial sectors, especially in the production of plastics [63]. However, in 2008, Chinese manufacturers of infant milk benefited from the high nitrogen content in melamine of about 67 mass-% to increase artificially the nitrogen amount in their products by adding melamine. The addition of only 1% resulted in a 4% higher nitrogen concentration, which represented the protein amount and, thus, a quality parameter of milk products. The analysis of nitrogen was performed at that time by using the Kjedahl technique [64]. However, since the Kjedahl technique is an unspecific method, melamine was not identified in the contaminated products and the infant milk products passed the quality control and entered the market. Several thousand infants fell ill suffering from a formation of urinary stones, inflammatory reactions and hyperplasia in the urinary bladder, and even some of them died [65], [66].

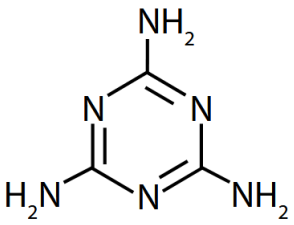

Figure 1.9: Chemical structure of melamine.

Since the reason of the epidemic was unknown at that time, alternative analytical techniques were looked for to find the background of the cases of illness and death. A ^{1}H NMR spectroscopic method was developed by Lachenmeier et al. Here, in some batches of infant milk samples an additional singlet was detected at $\delta = 5.93$ ppm, which was identified as melamine. An ^{1}H NMR spectrum of non-contaminated and contaminated infant milk products is presented in figure 1.10. This NH_2 signal was quantified by an external calibration [67]. Based on the research results, in the years between 2008 and 2012, the United Nations Food and Agriculture Organization (FAO) and the World Health Organization (WHO) set a maximum melamine level of 1 mg/kg and 0.15 mg/kg for powdered and liquid infant milk products, respectively, as well as 2.5 mg/kg for other foods and animal feed [68], [69]. This example demonstrated that the NMR spectroscopy is a powerful tool for the analysis of adulterations and contaminations, especially in infant milk products.

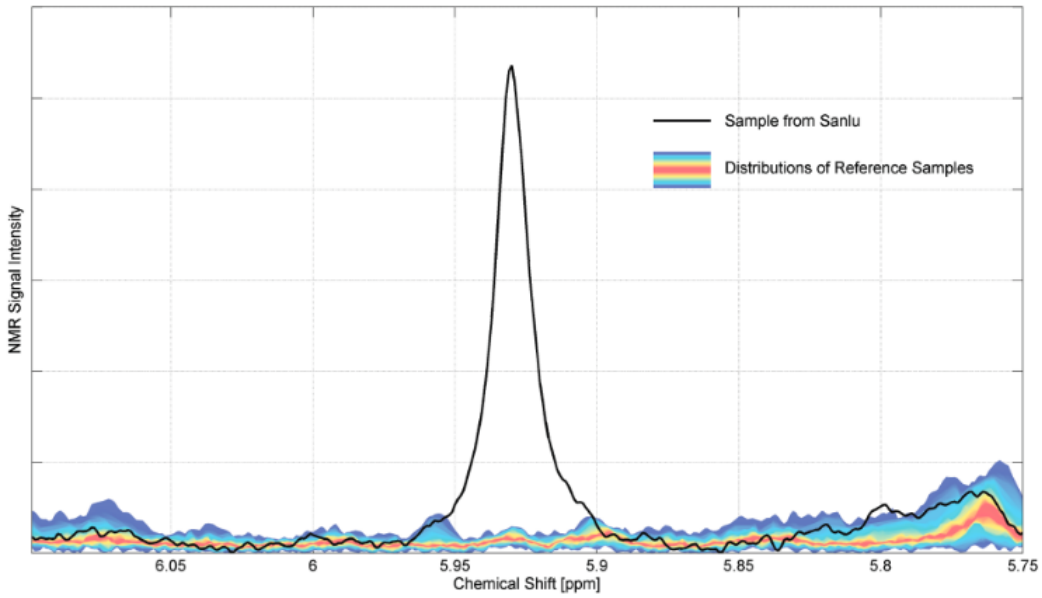

Figure 1.10: Comparison of a collection of non-contaminated infant milk samples (colored) with a melamine-contaminated sample (black) [67]. [Copyright (2009) ACS.]

1.3.3 Quality Control of Oxidation in Edible Oils

Edible oils play an important role in our daily food nutrition [70]. As a food product, oil must pass several quality control tests. A major cause of oil quality deterioration is lipid oxidation where lipids undergo oxidative processes in the presence of catalysts such as light, heat, enzymes and metals. Dependent on the condition, the oxidation processes can be divided into autoxidation, photo-oxidation, thermal oxidation, and enzymatic oxidation, whereby autoxidation is the most common lipid deterioration process forming lipid hydroperoxides as primary oxidation products [71], [72], [73], [74]. During the oxidation, saturated fatty acids show higher dissociation energies between hydrogens and carbons than unsaturated do. Thus, unsaturated fatty acids are prone to being oxidized because of their lower bond dissociation energy. As an example, the hydrogens and carbon in the C18 position of linoleic acid show a dissociation energy of 418 kJ/mol, whereby only 314 kJ/mol are required to break the bond between hydrogen and C14, and even less, namely 209 kJ/mol, are required for the breakage of the bond between hydrogen and C11 (figure 1.11) [75]. The relative rate of lipid peroxidation is given as $1 : 100 : 1200 : 2500$ for stearic acid, oleic acid, linoleic acid and linolenic acid [76].

Numerous analytical methods are used for the quality control of lipid batches. The peroxide value (PV), one of the quality parameter, is usually measured by iodometric titration, infrared (IR), high-performance liquid chromatography (HPLC), fourier transform-near infrared (FT-NIR) and NMR spectroscopy. In this chapter, FT-NIR and NMR spectroscopy are discussed in detail.

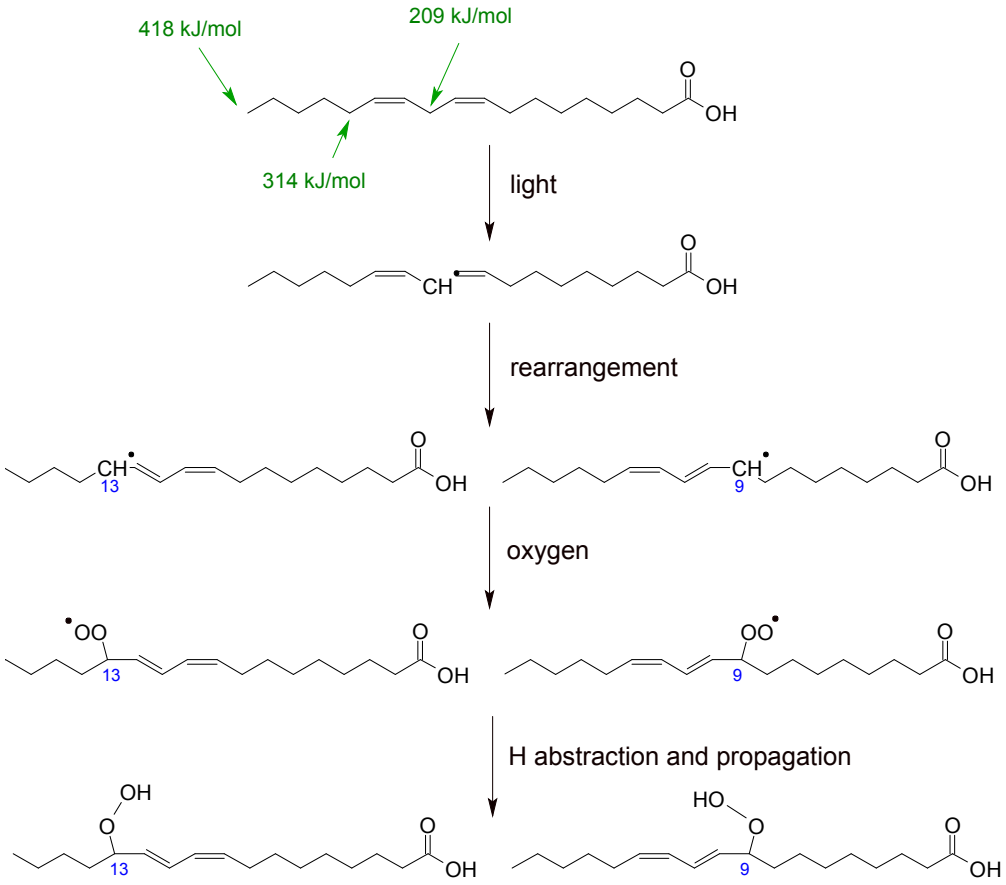

Figure 1.11: Oxidation process of linoleic acid; dissociation energies in green [75], [77], [78].

Determination of Peroxide Value by FT-NIR Spectroscopy

A FT-NIR spectroscopic method has been developed by van de Voort et al. to determine the PV in oils at levels between 10 to 100 meq/kg [79]. This FT-NIR method was improved to enable the quantitative determination of PV less than 10 meq/kg, which is a range of high interest for the edible oil industry. Therefore, a derivatization was implemented, where the reaction of triphenylphosphine (TPP) with hydroperoxides forming triphenylphosphine oxide (TPPO) was examined. TPP and TPPO showed bands between 4800 and 4500 cm^{-1} (figure 1.12). The derivatization of an oxidized oil led to a simultaneous presence of TPP and TPPO whose bands are overlapped in the spectrum. Thus, a quantification was performed by using calibration curves and chemometric techniques. The method was validated showing an applicability for edible oils with a PV over a range of 1 to 10 meq/kg with a reproducibility of $\pm$ 1.0 meq/kg. [80]

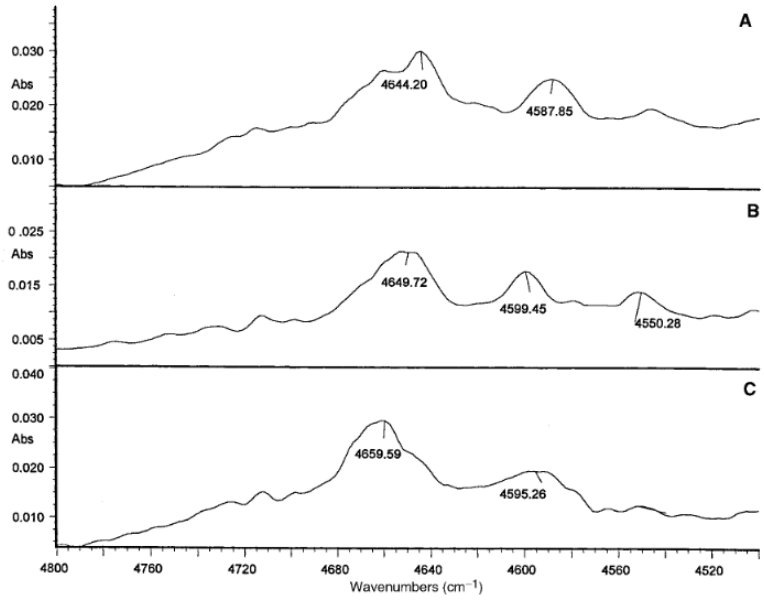

Figure 1.12: Differential spectra of (A) TPP, (B) TPPO, and (C) TPP and TPPO in canola oil [80]. [Copyright (2000) John Wiley and Sons.]

NMR Spectroscopic Method for Measuring Lipid Oxidation

NMR spectroscopy plays an important role in the analysis of fats and lipids concerning the structural determination of fatty acid profiles. ^{1}H and ^{13}C NMR experiments provide insights of the natural composition of the fatty acid profile as well as the different classes of lipid oxidation products [81], [82], [83], [84], [85]. In the last two decades, the relevance of NMR spectroscopy as a non-destructive analytical tool for the study of lipid oxidation has increased, especially due its advantages of minor sample preparation, small solvent and sample volumes as well as short experimental times. Several NMR studies on oxidative deterioration of edible oils has been published by Guillén and her research groups [86], [87], [88], [89], [90]. Primary and secondary oxidation products have also been studied by Skiera et al. Skiera developed a ^{1}H NMR assay to determine the hydroperoxide amount in edible oils without the addition of an internal standard [91], [92]. A typical ^{1}H NMR spectrum of an oxidized sunflower oil solved in $CDCl_3$/DMSO-d_6 (4:1) is presented in figure 1.13. As shown, hydroperoxides are detectable at a chemical shift of δ = 10.8 - 11.2 ppm. Skiera et al. established an equation which determined the linear relationship between the PV and the peroxide amount determined by NMR spectroscopy. This equation was used to compare the analytical results of 290 edible oil samples including black seed oils, corn oils, nut oils, olive oils, pumpkin seed oils, rapeseed oils and sunflower oils and thistle oils which have been analyzed by ^{1}H NMR spectroscopy and by titration according to Wheeler [91], [93]. The NMR data of corn oils, nut oils, rapeseed oils, sunflower oils and thistle oils were in good agreement with the titration results. However, black seed oils, pumpkin

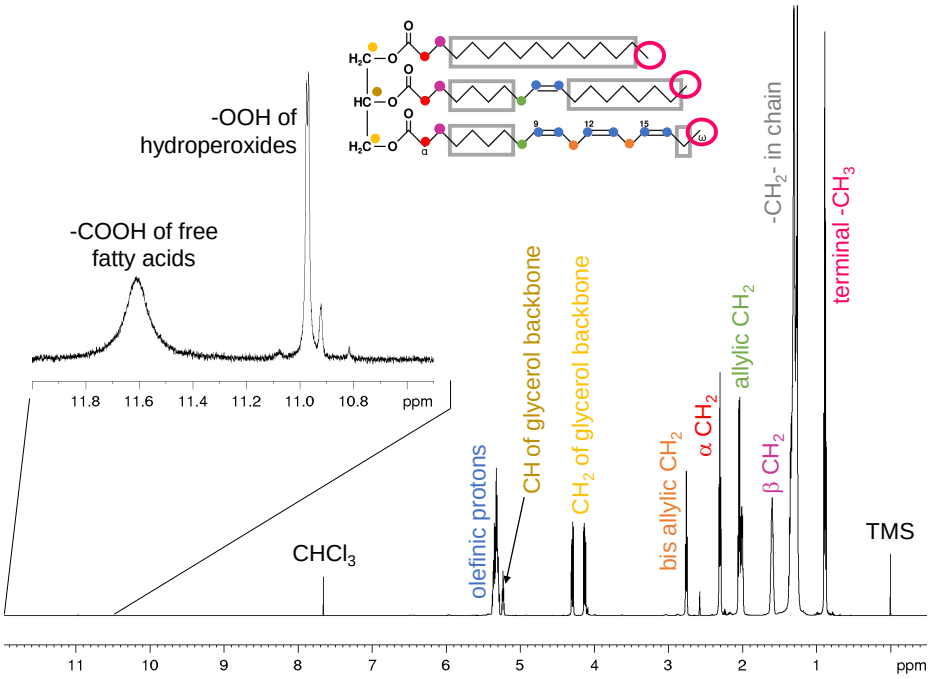

Figure 1.13: ^{1}H NMR spectrum of oxidized sunflower oil with the chemical structure of a fatty triglyceride which contains palmitic acid, oleic acid, α-linolenic acid (from top to bottom), used for signal assignment.

seed oils and olive oils exhibited significantly deviations: while the PV of black seed oils, analyzed by NMR, was too high, the PV of the olive oils and pumpkin seed oils was too low. Further investigations showed that natural oxidizing or reducing compounds such as thymochinone in black seed oils or hydroxytyrosol in olive oils have an impact on the PV results according to Wheeler. However, because cross-reactions could not be excluded in titration, it is recommended to re-evaluate the titration method as the official technique and to find a method where only peroxides are determined to represent the primary oxidation state of the oil as a quality parameter. Therefore, Skiera et al. presented the ^{1}H NMR spectroscopy as a powerful alternative technique for the quantitative determination of peroxides in edible oils [91].

1.3.4 Quality Control of Inorganic Divalent Metal Ions

The wide range of magnetically active nuclei makes NMR spectroscopy attractive for the chemical analysis of organic and inorganic substances in different kinds of matrices [94]. Some divalent cations such as Mg^{2+} and Ca^{2+} can be measured indirectly after being complexed with ethylenediaminetetraacetic acid (EDTA), whereby other nuclei are attractive for a direct measurement [95]. In this chapter a focus is set on the direct NMR analysis of cadmium, tin, lead and mercury, because $^{111/113}$Cd,$^{117/119}$Sn, ^{207}Pb and ^{199}Hg, are predestinated for the direct NMR analysis because of their spin of I=1/2.

Cadmium and tin are elements which have each two NMR active, spin 1/2 nuclei. ^{111}Cd shows a natural abundance of 12.8%, 0.6% higher than ^{113}Cd does. The narrow singlet in the cadmium NMR spectrum is shifted between -650 ppm and 0 ppm, showing couplings to other nuclei such as protons, carbons and phosphorous. In the ^{13}C NMR spectrum two set of couplings around 500 Hz are identified, whereby the ^{13}C-^{111}Cd coupling is slightly smaller than the ^{13}C-^{113}Cd coupling. In the ^{1}H NMR spectrum, the ^{1}H-$^{111/113}$Cd coupling constants are typically in the region of 50 Hz, having such a small difference that both coupling signals appear as being merged in the ^{1}H NMR spectrum [96]. $^{111/113}$Cd NMR is applied for the examination of organocadmium compounds, cadmium complexes, inorganic cadmium and cadmium binding to proteins and other molecules of biological interest [97], [98], [99].

Tin has three NMR active spin 1/2 nuclei, ^{115}Sn, ^{117}Sn and ^{119}Sn. Due to favorable nuclear magnetic properties and fairly high natural abundances of 8.6% and 7.7%, respectively, ^{119}Sn and ^{117}Sn are attractive for NMR analysis. Since ^{115}Sn has a low natural abundance of only 0.3%, ^{119}Sn and ^{117}Sn are therefore usually the nuclei of choice. Tin results in narrow signals over a chemical shift range of 6500 ppm, from +4000 ppm to -2500 ppm with $\delta^{119}\mathrm{Sn}_{SnMe_4}$=0 ppm. Because the chemical shift of tin signals is influenced by the temperature gradient in the sample, a constant temperature is essential to ensure that the chemical shift and signal width are only influenced by the substance and not by the experimental conditions [100], [101]. Tin NMR is often applied for the structure study of organic and inorganic tin compounds [102], [103]. However, by now a quantitative tin NMR method has not been published yet.

In lead chemistry, solid-state and liquid-state NMR spectroscopy has become an important analysis tool. Lead is an NMR spin 1/2 nucleus with a natural abundance of 22.1%, that yields signals over a chemical shift range of about 20,000 ppm. ^{207}Pb NMR spectroscopy is used for structure determination of organo lead compounds, where also ^{1}H-^{207}Pb and ^{13}C-^{207}Pb coupling constants have structural uses. However, ^{207}Pb NMR spectroscopy is not applied as a quantitative method so far [94], [104], [105].

^{199}Hg and ^{201}Hg are the two NMR active nuclei of mercury, whereby ^{199}Hg is a spin 1/2 nucleus with a natural abundance of 16.9% yielding sharp signals in the NMR spectrum between -3000 ppm and 500 ppm. ^{201}Hg has a spin of I=3/2. NMR active nuclei with spin $> 1/2$, which are called *quadrupole nuclei*, have a lower symmetry and thus, an electric quadrupole moment. The rapid relaxation time of quadrupole nuclei leads to broadened signals observed in the NMR spectra, which can be identified and confirmed in ^{201}Hg NMR spectra [94]. Consequently, ^{199}Hg is the mercury nucleus of choice. ^{199}Hg couples with many nuclei such as protons whose ^{1}H-^{199}Hg coupling contants are between 100 Hz and 270 Hz, and with carbon whose ^{13}C-^{199}Hg couplings are between 70 Hz and 3000 Hz depending on the bond [106].

Mercury NMR is applied in the structure and dynamics study of mercury compounds [107], [108]. However, to the best of my knowledge, there is no quantitative mercury NMR method published.

As shown, several cations can be measured directly by NMR spectroscopy because of their NMR active nuclei. Even though these methods are powerful techniques applied for structure elucidation, they are not used routinely for quantitative determinations. The literature search indicated that there are only few published qNMR methods that has been used for determination of cations in authentic samples. Monakhova et al. developed a quantitative ^{1}H NMR method to analyze Mg^{2+} and Ca^{2+} in mineral water with a limit of detection below 0.5 mg/L by using EDTA as complexation reagent [95]. A comparable method with EDTA was also applied for the quality control of aloe vera by quantifying the inorganic cations Mg^{2+} and Ca^{2+} as an additional criterion of authenticity of aloe vera [109]. Consequently, as presented, NMR spectroscopy shows various applications for the direct and indirect analysis of divalent metal ions.

1.3.5 Quality Control of Enantiomeric Products

Chirality influences significantly the biological and pharmacological properties of a pharmaceutical product regarding the interaction of the substance and the human or animal body [110]. Stereoselective methods have been developed to enable an investigation of enantioselective metabolic profiling of active substances [111]. Chiral drugs make up 40% to 50% of the market over the last years. In racemic drugs, one enantiomer often exerts the beneficial effect, whereas the other enantiomer has less, another or no effect, resulting in an effectiveness of only about 50% of the pharmaceutical product [112], [113], [114], [115]. Furthermore, different effects in the body regarding pharmacokinetics, bioavailability, protein binding, elimination half-life, pharmacodynamics, and toxicity are detectable [116]. Thus, several guidelines have been published by the United States Food and Drug Administration (FDA) and European Medicines Agency (EMA) concerning the investigation of stereoisomeric drugs [117], [118]. Based on these guidelines, most pharmaceutical companies and research institutes have been focusing on manufacturing single enantiomers in new drugs. For those pharmaceutical products, which can be already purchased as racemates, manufacturers work on alternative products containing only the active enantiomer [114]. Consequently, the analysis of the enantiomeric purity and enantiomeric excess presents an important part of the quality control of chiral drugs in the development, discovery, development and marketing of new drugs [112], [113], [114], [115].

Enantiomeric excess (ee) is a measurement of the purity of chiral molecules reflecting the degree of the enantiomeric composition where one enantiomer (R or S) exists in the product in a higher amount than the other one (S or R) [119]. The enantiomeric composition was traditionally examined by determining the optical purity which is the *"ratio of the observed optical rotation of a sample consisting of a mixture of enantiomers to the optical rotation of one pure enantiomer"* [120]. Ideally, the composition of the enantiomeric mixture is

directly proportional to the optical purity. However, since the optical purity cannot be measured in all substances [121], further analytical methods using chromatography [122], [123] and NMR spectroscopy [119], [124], [125] have been developed. Here, enantiomeric excess is determined by comparing the amount of both enantiomers. The enantiomeric excess is calculated according to equation 1.7 [120]. For example, since a racemic mixture consists of 50% R and 50% S, the enantiomeric excess is determined with 0%, while a pure enantiomer has an enantiomeric excess of 100% [119].

$$ee[\%] = \frac{|R - S|}{R + S} \cdot 100 \tag{1.7}$$

Even though numerous analytical techniques have been developed for the analysis of enantiomeric composition, the focus in this work is placed on the NMR spectroscopy.

Chiral Derivatization Agents (CDA) in NMR Spectroscopy

Enantiomeric molecules show identical NMR spectra because the corresponding nuclei have the same electronic surrounding. Upon derivatization of the enantiomers R and S with CDA, diastereomers are formed, which show different chemical and physical properties. Since diastereotopic hydrogens are non-equivalent, they appear at different chemical shifts in the ^{1}H NMR spectra which enables the determination of the enantiomeric excess according to equation 1.7 by using the respective integrals [119]. In the case of performing derivatization reactions, a quantitative conversion of the enantiomers to diastereomers without any chiral discrimination originating from kinetic resolution is required. In the NMR spectroscopy, one of the most used derivatization reagents for alcohols and amines is α-methoxy-α-trifluormethyl-phenylacetic acid, known as *Mosher's reagent* or *MTPA*.

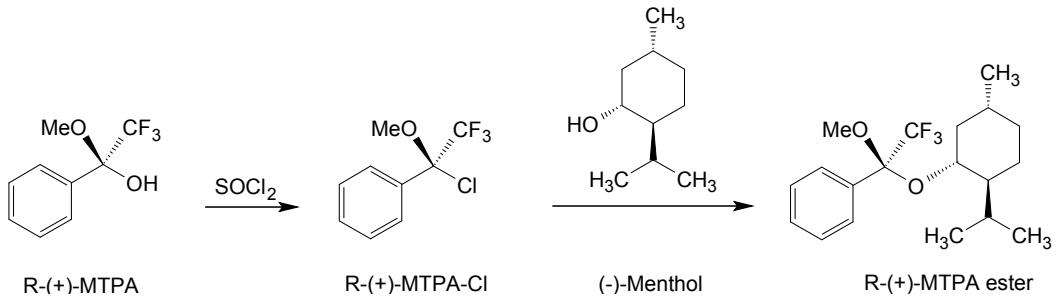

Figure 1.14: MTPA reacts with thionyl chloride forming MTPA-Cl which is used for the derivatization reaction of (-)-Menthol forming MTPA-ester.

The reaction of MTPA and the substance of interest is commonly activated by a carboxylic acid-activating agent such as N,N'-dicyclohexylcarbodiimide (DCC). Alternatively, Mosher-Chloride (MTPA-Cl), which can be formed by the reaction of MTPA and thionyl

chloride, can be used directly for derivatization reactions as active acylating agent (figure 1.14) [126], [127]. The derivatization reaction of primary and secondary alcohols or amines with Mosher-Chloride was developed in 1969. The advantage of the use of Mosher-Chloride is the impossible racemization during derivatization due to the lack of α-hydrogen at the carboxy group [126]. However, the purity of MTPA-Cl of 99.0% with an enantiomeric ratio of $\geq 99.5 : 0.5$ % declared by the distributer leads to a limitation of the determination of the enantiomeric excess.

Chiral Lanthanide Shift Reagents (CSR) and Chiral Solvating Agents (CSA) in NMR Spectroscopy

Chiral lanthanide shift reagents (CSR), such as tris(((heptafluoropropyl) hydroxy methylene)-d-camphorato)europium (*Eu(hfc)*$_3$, figure 1.15 a), which is often used for NMR spectrometer with a lower field strength, or tris[3-(tri fluoro methyl hydroxy methylene)-d-camphorato]ytterbium (*Yb(tfc)*$_3$, figure 1.15 b) are widely used for chiral discrimination. By the complexation of analytes by CSR, diastereomeric complexes are formed whose signals are shifted in the NMR spectrum. These separated signals are used to determine the enantiomeric excess [119], [128].

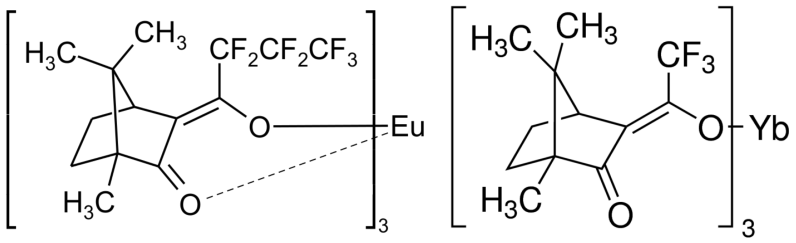

a) $Eu(hfc)_3$ b) $Yb(tfc)_3$

Figure 1.15: Examples of chiral lanthanide shift reagents (CSR).

Another option are chiral solvating agents (CSA), in which the enantiomeric analyte is exposed to a chiral environment without the formation of a covalent bond. This can be performed by running the analysis in chiral solvents or by the formation of adducts of the substrate at a chiral, enantiomerically pure complex. Hence, CSA and the analyte should contain common features of functional groups such as carboxylic, hydroxy or amine group. In figure 1.16 (S)-(-)-1-(1-Naphthyl)ethylamine and (-)-(18-crown-6)-2,3,11,12-tetracarboxylic acid are presented as two examples representing a small selection of CSA [119].

In routine ^{1}H NMR ,^{19}F NMR and ^{13}C NMR techniques are used to discriminate chiral compounds, to determine the enantiomeric excess and to assign absolute configuration by usind CSA, CSR and CDA.

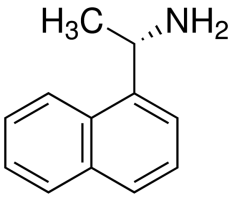

a) (S)-(-)-1-(1-Naphthyl)ethylamine

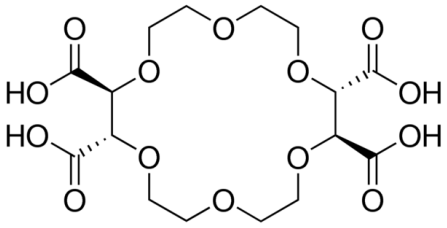

b) (-)-(18-Crown-6)-2,3,11,12-tetracarboxylic acid

Figure 1.16: Examples of chiral solvating agents (CSA).

1.4 Tagging

In information systems, tags are keywords associated to information which helps to describe and to find items [129]. In medicine, tagging or labelling is the introduction of e.g. radioactive isotopes or fluorescent groups into a molecule in order to distinguish the tagged molecule from other molecules without that tag [130]. In this thesis, *tagging* respresents the collective term of making the substances of analytical interest visible by performing reactions such as derivatizations, complexations and isotope labellings.

Chapter 2

Aims of the study

The aim of the present thesis is to solve analytical issues by developing new quantitative NMR methods using tagging reagents. The developed methods are applied to chemical, pharmaceutical and food applications.

Issue #1: The titration method, which belongs to the official methods for the determination of peroxide values, show several disadvantages: high sample and solvent amount needed, not applicable for phospholipid-containing oils like krill oil, not robust. Hence, Skiera et al. developed a new ^{1}H NMR method to determine peroxides in edible oils [91].

> **Aim #1.1:** Test the NMR method, developed by Skiera et al. [91], concerning its applicability for low-oxidized edible oils.
>
> > **Solution #1.1:** Organization and evaluation of an interlaboratory comparison test to examine the applicability of the ^{1}H NMR method as a technique for the quality analysis of edible oils with a focus on peroxides.
>
> **Aim #1.2:** Develop a ^{1}H NMR method for a fast, accurate, precise, robust and simple determination of peroxides in oils, independent of the level of oxidation, color or the presence of phospholipids.
>
> > **Solution #1.2:** Development of an ^{1}H NMR method to determine the peroxide value in vegetable and krill oil by using triphenylphosphine as tagging reagent.

Issue #2: Divalent cations such as Mg^{2+}, Ca^{2+}, Sr^{2+}, Zn^{2+}, Cd^{2+}, Hg^{2+}, Sn^{2+}, and Pb^{2+} have been commonly analyzed with complexometric titration, flame atomic absorption spectrometry, ion chromatography, inductively coupled plasma atomic absorption or mass spectrometry. Most of the methods require time-consuming separations via extraction or precipitations, high amounts of chemicals, solvents and calibration curves.

> **Aim #2**: Develop a fast and simple NMR method for the qualitative and quantitative determination of inorganic divalent cations.

Solution #2: Development of a qualitative and quantitative ^{1}H NMR method to determine divalent metal cations in model salt solutions, food supplements and pharmaceutical products by using EDTA as tagging reagent.

Issue #3: In industry, Mosher's reagent is the most used derivatization substance for the determination of enantiomeric excess of alcohols and amines by using NMR spectroscopy. However, since Mosher's reagent cannot be produced with an enantiomeric ratio of higher than 99.5%, the determination of the enantiomeric ratio of the analyte is limited to these values making the determination of enantiomeric ratios between 99.5 - 100% impossible.

Aim #3: Develop a NMR method which is applicable for the determination of enantiomeric ratios of $\geq$ 99.50% as an alternative to Mosher's reagent.

Solution #3: Development of a ^{13}C NMR method to determine the enantiomeric excess of chiral alcohols by using phosgene as tagging reagent.

Chapter 3

Interlaboratory Comparison Test

Original title: Interlaboratory Comparison Test as an Evaluation of Applicability of an Alternative Edible Oil Analysis by ^{1}H NMR Spectroscopy [131] [Copyright (2017) J. AOAC Int.]

Elina Zailer, Ulrike Holzgrabe, Bernd Diehl; J. AOAC Int., 100: 1819-1830, 2017.

3.1 Abstract

A proton (^{1}H) NMR spectroscopic method was established for the quality assessment of vegetable oils. To date, several research studies have been published demonstrating the high potential of the NMR technique in lipid analysis. An interlaboratory comparison was organized with the following main objectives: (1) to evaluate an alternative analysis of edible oils by using ^{1}H NMR spectroscopy; and (2) to determine the robustness and reproducibility of the method. Five different edible oil samples were analyzed by evaluating 15 signals (free fatty acids, peroxides, aldehydes, double bonds, and linoleic and linolenic acids) in each spectrum. A total of 21 NMR data sets were obtained from 17 international participant laboratories. The performance of each laboratory was assessed by their z-scores. The test was successfully passed by 90.5% of the participants. Results showed that NMR spectroscopy is a robust alternative method for edible oil analysis.

3.2 Introduction

Over the last few years, an increasing awareness of the demand for more effective quality assessment and authenticity control of edible oils, especially olive oil, has led to technological advances in the analysis of fats and oils [132], [133]. Assessment of the quality and authenticity of edible oils has traditionally been performed by several official analytical methods, including the evaluation of acid, peroxide, anisidine, and iodine values; di- and triglycerides; total polar compounds; tocopherols; and other parameters, such as color index, phosphorus, copper, and iron. Requirements for these indices are issued by

the European Pharmacopoeia (8th Ed.), the Council of Europe, Deutsche Gesellschaft für Fettwissenschaft, and the American Oil Chemists' Society (AOCS). Acid value is an important indicator of the quality of edible oil, which determines the amount of carboxylic acid groups in free fatty acids (FFAs). Most national and international standards for acid value assessment in edible oils are based on an acid–base titration technique in nonaqueous solvents expressing the amount of potassium hydroxide necessary to neutralize FFAs [134], [135], [136]. Peroxide value (PV) is analyzed by titration methods according to Wheeler [DGF-C-VI 2(05) Part 1] or Sully [DGF-C-VI 2(05) Part 2] that were adopted and approved with small differences by the AOCS as Cd 8-53 (using chloroform) and Cd 8b-90 (11) (using isooctane). The International Organization for Standardization (ISO) has published two titration methods, ISO 3960:2007 [visual (iodometric) endpoint] and ISO 27107:2008 (potentiometric endpoint), and publishes the European Pharmacopoeia for the determination of the PV of oils [137]. Furthermore, near-infrared methods have been designed to determine PVs in triglycerides at levels from 0 to 100 [8], [80]. Aldehydes are analyzed as an anisidine value, which is measured by AOCS Official Method Cd 18-90(11) using a spectrophotometric analysis that takes 10 min to measure absorbance at 350 nm after reaction including p-anisidine and aldehydic compounds. Iodine value, another important quality parameter, determines the amount of unsaturation in FAs analyzed by titration with iodine-based compounds [138], [139], [140], [141]. All of these techniques have several drawbacks, such as the use of high amounts of toxic solvents, lengthy times, and subsequent high costs.

In this paper, a proton (^{1}H) NMR spectroscopic method was developed for the targeted control, quality assessment, and characterization of vegetable oils by ^{1}H NMR spectroscopy. Quality parameters, such as FFAs, PV, and aldehydes, as well as the characterization of FAs in lipids and the grade of saturation, were determined in only one ^{1}H NMR analysis run, providing a rapid alternative to classical oil analyses. The presented method can be applied to a wide range of different vegetable oils. To evaluate the applicability of the alternative oil analysis by ^{1}H NMR spectroscopy and determine the robustness and reproducibility of the method, an international interlaboratory comparison was organized as an external laboratory-based quality assurance method to demonstrate individual performance. Here, we report on an interlaboratory comparison of the analysis of five edible oil samples by ^{1}H NMR NMR spectroscopy utilizing instruments with different probes and magnetic field frequencies (400, 500, and 600 MHz). Comparison between the 21 data sets that were obtained from the 17 participants is discussed in terms of mean value, SDs, and z-scores, which can be considered a performance index. Operator and instrument influence, as well as reasons for erroneous integration values are discussed.

3.3 Method

3.3.1 Materials

Five edible oils —safflower (oil 1), peanut (oil 2), walnut (oil 4), and olive (oils 3 and 5) - were purchased from local supermarkets and oil mills and sent to the participants. National participants used tetramethylsilane (TMS; Sigma-Aldrich Chemie GmbH, Steinheim, Germany) for NMR calibration, chloroform-d1 ($CDCl_3$; degree of deuteration 99.8%; Euriso-Top, Saarbrücken, Germany), and dimethyl sulfoxide-d_6 (DMSO-d_6; degree of deuteration 99.8%; Euriso-Top) as solvents dried over molecular sieve (4 Å;AppliChem, Darmstadt, Germany). International participants used calibration materials, solvents, and molecular sieves of comparable quality.

3.3.2 Sample Preparation

$CDCl_3$ and DMSO-d_6 were mixed in a ratio of 4:1. A small amount of TMS was added to calibrate the chemical shift. Five milliliters of solvent were dried over a layer of the molecular sieve. This solvent was named "$CDCl_3$-DMSO (4 + 1)." Approximately 200 ± 10 mg oil sample were accurately weighed (with a weighing accuracy of ± 0.1 mg) into individual 4 mL sample vials. One milliliter of dry $CDCl_3$-DMSO-d_6 (4 + 1) solution was added and carefully mixed. About 1 mL of solution was transferred to the NMR tubes. The samples were analyzed within 24 h after sample preparation. The prepared samples had been stable for at least 1 week. For oxidation parameters, prepared samples should be analyzed within 24 h after sample preparation.

3.3.3 Experimental NMR Analysis Procedures

Experiments were performed at a temperature of 298 ± 5 K. For all experiments, a zg30 program with 64–128 scans was used to achieve an adequate S/N of 40,000 for α-CH_2-triplet at δ 52.3 ppm. The spectral widthwas set to 24 ppm with an O1P of 8 ppm. The D1 was set to 1.00 s, the TD to 128k, and the SI to 64k. Adjustment of D1 and AQ was not necessary due to the rapid relaxation of all sample components. Rotation was optional; a non-spinning analysis was found to be optimal. Chemical shifts were referenced to TMS at δ 0.00 ppm.

3.3.4 Experimental Data Procedures

The identification and quantification of 15 signals was performed according to the signals listed in table 3.1. The chemical shifts shown in table 3.1 may have differed by ± 0.1 ppm. The signal at $\delta = 2.3$ ppm was calibrated to 2000. Participants individually decided how to integrate peroxide and aldehyde signals (i.e., either separately or all together). Furthermore, baseline correction and integration could be manually or automatically performed.

Table 3.1: Signal assignment in the ^{1}H NMR spectrum

Signal No.	Chemical shift δ, ppm	Multiplicity	Component/ structural element
1	12.0–11.4	Multiplet	FFA/–COO**H**
2	10.6–11.1	Multiplet	Peroxides/–CHOO**H**
3	9.8–9.4	Multiplet	Aldehydes/–C**HO**
4	5.32	Multiplet	Double bonds
5	5.23	Multiplet	Glycerine backbone, –C**H**–
6	4.3	Multiplet	Glycerine backbone, –C$\mathbf{H}_2$–
7	4.1	Multiplet	Glycerine backbone, –C$\mathbf{H}_2$–
8	2.79	Triplet	Bisallyl in C18:3 –CH=CH–C$\mathbf{H}_2$–CH=CH–C$\mathbf{H}_2$–CH=CH–
9	2.75	Triplet	Bisallyl in C18:2 –CH=CH–C$\mathbf{H}_2$–CH=CH–
10	2.3	Triplet	α-C$\mathbf{H}_2$
11	2.23	Triplet	FFA α-C$\mathbf{H}_2$
12	2.1–1.92	Multiplet	Allyl –C$\mathbf{H}_2$–CH=CH–C$\mathbf{H}_2$–
13	1.6	Multiplet	β-C$\mathbf{H}_2$
14	1.53–1.05	Multiplet	–C$\mathbf{H}_2$– long chain
15	0.99–0.84	Multiplet	Terminal –C$\mathbf{H}_3$

3.3.5 NMR Data Collection

Seventeen NMR laboratories took part in the interlaboratory trial (see table 3.2). In total, 21 data sets were submitted for each sample and included different operators and different spectrometers. The participants' identities were kept anonymous. Therefore, the laboratorieswere randomly numbered. The laboratory numbers listed in table 3.2 equate to the data set number, not the laboratory number. Six laboratories participated with a at 400 MHz spectrometer, eight with a 500 MHz, and seven with a 600 MHz. Double-resonance broadband probes and cryoprobes [broadband inverse (BBI), Prodigy nitrogen-cooled broadband (CPPBBO), CPQNO, PABBO BB, and CPMNP] were used.

3.3.6 Statistical Data Analysis

Integrals of the 15 signals from all the samples measured by all the participants were evaluated using Excel XLSTAT (Version 2016.05.33324). The number of outliers is presented in table 3.3 (page 32). The integrals collected from each sample underwent a two-sided Grubbs' test, with a significance level of $\alpha = 0.05$, to identify possible outliers. Outliers were not considered in the successive evaluation process. After outliers were removed, integral values were run through a proficiency test to elaborate the data and determine the mean integral value ("mean"), the corresponding absolute SDs and RSDs, and z-scores.

Table 3.2: Affiliations of the participants in the interlaboratory comparison study

Company	**City**	**Country**
Sigma-Aldrich Production GmbH	Buchs	Switzerland
Crop Science Division Bayer CropScience Aktiengesellschaft	Monheim	Germany
Roche Diagnostics GmbH	Penzberg	Germany
DSM Nutritional Products	Columbia, MD	United States
Department of Chemistry, University of Cologne	Cologne	Germany
Bruker BioSpin GmbH	Rheinstetten	Germany
Dupont Nutritional Biosciences Aps	Brabrand	Denmark
Institute of Pharmacy, University of Würzburg	Würzburg	Germany
Pennsylvania State University	University Park, PA	United States
Bayerisches Landesamt für Gesundheit und Lebensmittelsicherheit	Würzburg	Germany
Bundeskriminalamt	Wiesbaden	Germany
Bundesanstalt für Materialforschung und -prüfung	Berlin-Adlershof	Germany
SYNLAB Umweltinstitut GmbH	Hürth	Germany
Chemisches und Veterinäruntersuchungsamt	Karlsruhe	Germany
SINTEF Fiskeri og havbruk	Trondheim	Norway
BASF SE	Ludwigshafen/Rhein	Germany
Spectral Service AG	Cologne	Germany

z-Scores were calculated by the "standardization" command. Results of $|z| \leq 2.0$ were considered to be acceptable, $2.0 < |z| < 3.0$ considered questionable, and $|z| \geq 3.0$ considered unacceptable. Participation in the interlaboratory comparison was deemed successful if 80% of all required results exhibited a score of $|z| < 3.0$.

To examine the influence of the three different frequencies (400, 500, and 600 MHz) on the shape and thus integral values of the ^{1}H-NMR signals for linoleic acid (C18:2) and linolenic acid (C18:3), an analysis of variance (ANOVA) was used to determine statistical significance. A confidence interval of 95% and a tolerance of 0.0001 were used for the statistical evaluation. A posthoc Tukey's honest significant difference (HSD) test was also performed to determine individual means that were significantly different from each other.

Table 3.3: Number of integral outliers in samples safflower, peanut, walnut, and two olive oils.

Signal No.	Safflower oil oil 1	Peanut oil oil 2	Olive oil oil 3	Walnut oil oil 4	Olive oil oil 5
1	1	2	3	1	2
2	1	1	1	1	1
3	1	1	1	1	2
4	2	2	1	1	1
5	2	1	1	2	1
6	2	1	1	1	1
7	1	1	1	2	1
8	0	0	1	1	1
9	1	0	1	1	1
11	0	0	1	1	1
12	1	1	2	2	2
13	1	1	0	1	1
14	2	1	2	1	2
15	1	1	1	0	2

3.4 Results and Discussion

3.4.1 Vegetable Oil Analysis by ^{1}H-NMR Spectroscopy

A 500 MHz ^{1}H-NMR spectrum of a representative vegetable oil (walnut) in $CDCl_3$/DMSO-d_6 (4 + 1) is presented in figure 3.1; the corresponding signal assignment appears in table 3.1. The structures of the major triacylglycerides (TAGs) that are present in vegetable oil showed signals for each hydrogen inthe ^{1}H NMR spectra (figure 3.2, page 34). Glycerine backbone signals resonate at δ = 5.23, 4.3, and 4.1 ppm in a ratio of 1:2:2. Vinylic hydrogen (H_v) has a characteristic signal at δ = 5.32 ppm, which represents the number of double bonds and thus the degree of lipid unsaturation. Allylic hydrogen (H_a) at δ = 2.1–1.92 ppm and bisallylic hydrogen (H_b) at δ = 2.79 and 2.75 ppm are used to characterize unsaturated FAs, such as C18:3 and C18:2. The COOH proton in FFAs resonates as a singlet in the ^{1}H NMR spectrum at δ = 12.0–11.4 ppm when a $CDCl_3$–DMSO mixture is used as the solvent. For quantification, COOH and the α-CH_2 signals (δ = 2.23 ppm) were integrated. Quantification of the α-CH_2 group in FFAs was difficult, due to the group's low intensity and overlap with the α-CH_2 group present in other FAs (of which the oils were primarily comprised) at δ = 2.30 ppm. Skiera et al. [142] had similar results, though they used a different solvent ratio.

PV is another important quality parameter. Hydroperoxides are formed during autoxidation processes, having a typical pattern in the ^{1}H NMR spectrum at δ = 11.1–10.6 ppm

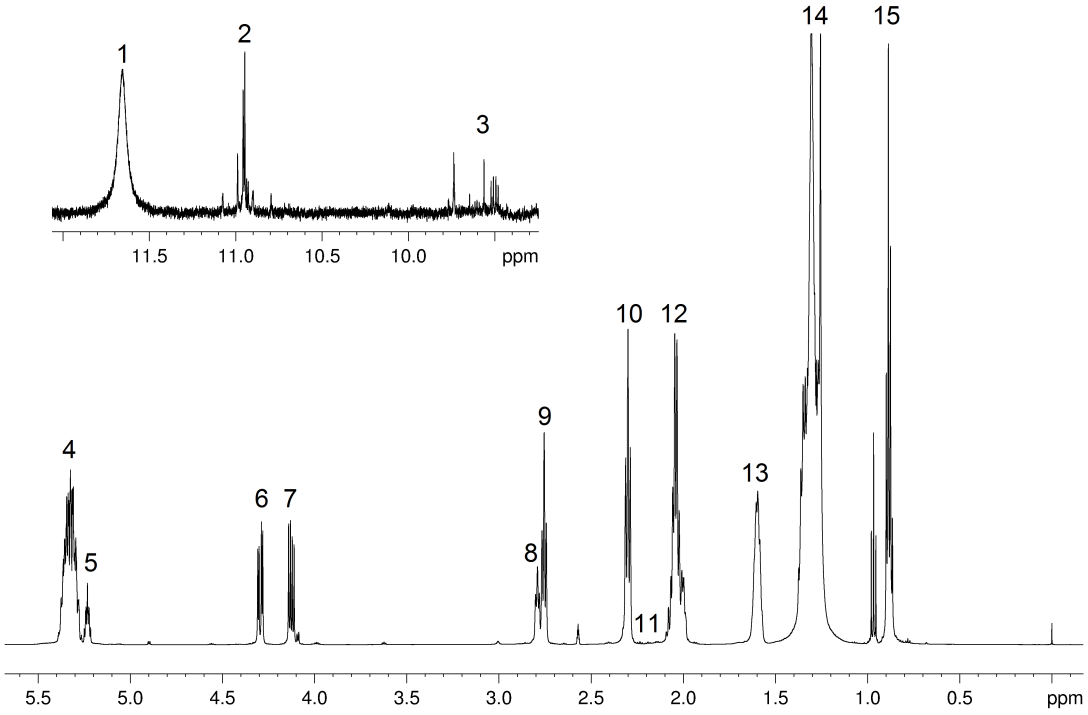

Figure 3.1: ^{1}H-NMR spectrum of a representative edible oil [walnut; oil 4, $CDCl_3$–DMSO-d_6 (4 + 1), 500 MHz].

[132], [142], [143], [144]. The three main FAs of edible oils are oleic (C18:1), C18:2, and C18:3. Due to the varying compositions of these FAs, the number and pattern of hydroperoxide signals varies. Each fatty acid (FA) reacts to several FA peroxide types, thus there can be several low-intensity peroxide signals. Direct quantification of peroxides with ^{1}H NMR spectroscopy in low-oxidized edible oils, however, is a challenge due to low S/N. Aldehydes, which are secondary oxidation products, are generated from the degradation processes of hydroperoxides and are associated with the rancidity of oils and fats [145]. Signals from the proton bonded to the carbonyl center of aldehydes can typically be found at δ = 9.8-9.4 ppm. Different aldehydes form based on the FA composition of an edible oil and the oxidation conditions present. Skiera et al. presented an ^{1}H NMR approach as an alternative to the classical p-anisidin value method [92]. By recalculating the integrals from signals 1-15, various edible oil parameters – such as FFAs, peroxides, aldehydes, and C18:1, C18:2, and C18:3 - can be determined in mol-% and mol‰. The integral for the double bonds can be recalculated as the degree of saturation with amean double-bond number per FA.

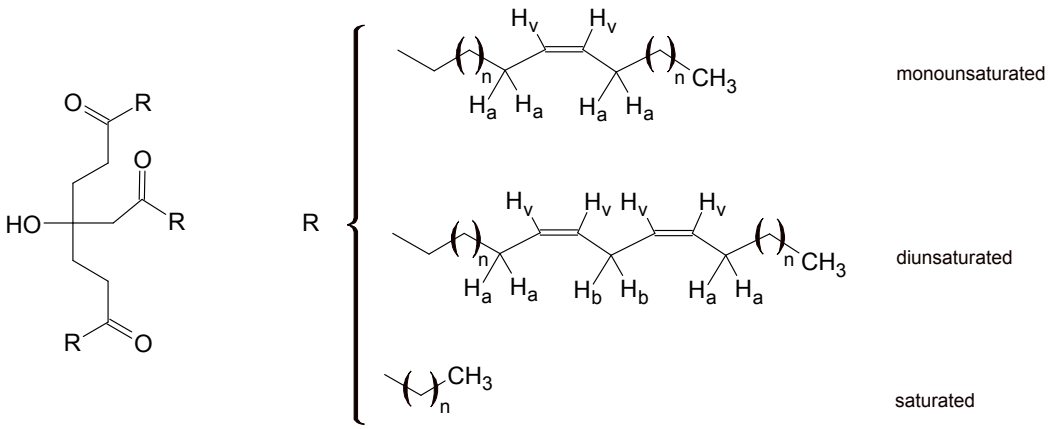

Figure 3.2: Chemical structure of the main TAGs in vegetable oils.

3.4.2 Statistical Analysis and Performance Assessment

Several national and international laboratorieswere invited in 2016 to participate in the interlaboratory comparison test for the evaluation of applicability of an alternative edible oil analysis by ^{1}H NMR spectroscopy (see table 3.2). Twenty laboratories joined the trial. Of the 20 laboratories, 17 using different operators and different spectrometers, returned a total 21 data sets; the 21 data sets were identified as "Labs 1-21." (Multiple participating laboratories from Germany, Switzerland, the United States, and Nordic countries reflected international interest in determining the quality of edible oils by alternative techniques.) Prior to the interlaboratory comparison, detailed information on chemicals, sample preparation, NMR analysis parameters, and evaluation (see section 3.3) were sent to the participants to ensure comparable conditions for all instruments. Data were collected using a standard ^{1}H NMR pulse program (zg30) across a sweep width of 24 ppm in all cases. The number of scans varied depending on probe type and magnetic field strength. Safflower, peanut, walnut, and two olive oil samples with unknown compositions and quality were analyzed and evaluated by the participating laboratories (table 3.2, page 31). For each sample, participants integrated 15 signals (listed in table 3.1, page 30), leading to a total number of available theoretical data of 1575. Some signals - such as FFAs, peroxides, and aldehydes - were not integrated because of their low intensity. Therefore, in total, 1362 data were submitted. Before computing, outliers were detected by a two-sided Grubbs test, with a significance level of $\alpha = 0.05$, and eliminated from any further statistical evaluation. Figure 3.3 (page 41) displays the total number of integral outliers in all five samples. The mean, SD, and RSD were computed from data according to ISO 13528:2015 and are presented in tables 3.4 - 3.9, (pages 35 - 40).

Table 3.4: Summary of statistical results; [a]RSD > 4 %

Signal	Oil 1			Oil 2			Oil 3			Oil 4			Oil 5		
	Mean	SD	RSD, %	Mean	SD	RSD, %	Mean	SD	RSD, %	Mean	SD	RSD, %	Mean	SD	RSD, %
1	0.46	0.30	64.79[a]	0.53	0.21	40.15[a]	6.29	0.81	12.89[a]	4.16	0.72	17.53[a]	8.85	1.31	14.85[a]
2	4.55	0.71	15.56[a]	2.66	0.60	22.66[a]	3.71	0.80	21.43[a]	1.21	0.44	36.13[a]	2.56	0.77	30.11[a]
3	0.18	0.36	199.37[a]	0.22	0.22	100.78[a]	0.24	0.62	257.97[a]	0.57	0.33	58.31[a]	0.33	0.55	167.08[a]
4	2083.67	14.15	0.68	2037.93	12.26	0.60	1852.76	15.60	0.84	3458.88	47.96	1.39	1863.41	19.82	1.06
5	331.88	6.44	1.94	333.57	7.00	2.10	331.45	7.40	2.23	351.92	14.06	4.00	329.54	6.79	2.06
6	658.89	5.66	0.86	654.94	6.70	1.02	655.83	6.04	0.92	647.84	7.30	1.13	649.28	7.22	1.11
7	677.44	5.01	0.74	679.27	7.21	41.51[a]	680.45	8.72	1.28	692.45	8.15	1.18	690.47	9.82	1.42
8	9.95	4.45	44.71[a]	14.38	5.97	2.03	30.53	3.61	11.81[a]	491.89	55.75	11.33[a]	28.38	2.93	10.34[a]
9	281.31	6.39	2.27	441.60	8.98	122.70[a]	174.89	4.40	2.52	1219.84	48.49	3.98	148.83	5.84	3.92
11	7.64	7.84	102.63[a]	4.33	5.32	0.49	13.61	10.50	77.14[a]	10.82	9.72	89.87[a]	16.73	8.87	53.02[a]
12	3636.91	47.25	1.30	3219.33	15.75	0.49	3413.26	30.32	0.89	3561.95	33.13	0.93	3447.97	35.86	1.04
13	2043.03	31.79	1.56	2031.33	27.66	1.36	2144.30	46.82	2.18	2042.56	32.33	1.58	2105.28	44.77	2.13
14	19821.21	178.47	0.90	20213.31	153.63	0.76	20473.03	229.91	1.12	15496.69	208.45	1.35	20544.84	257.54	1.25
15	3043.69	45.71	1.50	3015.72	44.09	1.46	3029.44	63.70	2.10	2839.21	233.63	8.23	3025.00	60.67	2.01

Table 3.5: Statistical results for safflower oil (oil 1)

	Signal													
Lab. No.	**1**	**2**	**3**	**4**	**5**	**6**	**7**	**8**	**9**	**11**	**12**	**13**	**14**	**15**
1	0.08	3.89	-0.69	2068.18	335.02	662.42	679.43	13.94	278.76	-	3604.35	2049.81	19789.77	3028.65
2	0.69	4.43	0.33	2082.31	317.34	662.02	677.62	5.95	280.89	-	3601.57	2007.4	19823.45	3005.21
3	-	3.96	-0.06	2090.90	336.29	658.34	680.69	3.72	290.89	17.01	3604.44	2032.95	19807.40	3111.35
4	0.31	4.56	0.04	2069.43	330.71	651.90	670.32	12.18	265.96[a]	-	3611.35	2072.64	19725.85	3043.27
5	0.40	4.71	0.17	2102.07	333.29	660.20	681.39	12.61	283.77	-	3646.43	2099.48	19947.88	3095.95
6	0.48	4.89	0.45	2089.72	336.88	666.20	679.95	12.82	271.09	2.07	3618.88	2080.86	19673.11	3151.89
7	1.12	5.10	0.88	2076.65	322.69	667.39	686.15	1.62	288.60	15.41	3657.17	2022.00	19984.84	3029.20
8	0.05	3.98	0.02	2090.65	336.52	664.85	681.45	11.00	272.90	-	3655.03	2091.24	19895.88	3033.95
9	0.62	5.18	0.83	2068.13	333.79	652.95	668.98	-	-	-	3582.42	2044.61	19466.90	3074.11
10	2.52[a]	9.06[a]	3.24[a]	2211.18[a]	358.64[a]	679.56[a]	682.40	6.22	278.66	-	3898.64[a]	2131.52[a]	20895.66[a]	3076.71
11	0.76	4.54	-	2087.05	331.14	664.71	681.62	-	290.82	-	3615.40	2038.18	19930.08	3047.19
12	-	6.67	0.19	2176.26[a]	352.90[a]	682.62[a]	679.24	9.41	287.28	2.00	3788.66	2090.72	20876.78[a]	3305.47[a]
13	0.25	3.73	0.12	2081.52	330.24	647.87	665.09[a]	16.36	273.55	-	3618.87	2015.77	19700.07	2999.79
14	0.29	3.68	0.13	2091.11	329.82	652.41	669.86	11.45	273.38	-	3622.36	2017.40	19814.45	2977.57
15	0.22	3.63	0.20	2073.14	336.91	651.33	668.97	15.29	277.90	1.72	3614.94	2026.11	19474.78	3002.00
16	-	4.62	-	2121.20	321.57	664.15	679.92	-	268.06	-	3632.80	1979.10	20071.00	3050.90
17	0.61	4.72	0.02	2080.89	332.58	655.21	676.17	6.79	281.76	-	3629.23	-	19928.07	2987.56
18	0.98	5.36	0.12	2100.71	342.37	660.42	679.39	-	279.40	-	3709.38	2031.01	20189.70	3091.49
19	0.24	4.26	0.13	2078.67	330.91	656.73	674.51	-	286.51	-	3693.18	2050.15	19849.42	3046.91
20	0.38	4.59	-	2072.54	326.44	658.69	671.93	-	-	-	3602.01	2040.66	19720.97	3030.77
21	0.35	4.43	-	2064.80	341.27	661.06	678.84	-	-	-	3629.80	2027.40	19809.35	2989.40
MEAN	0.46	4.55	0.18	2083.67	331.88	658.89	677.44	9.95	281.31	7.64	3636.91	2043.03	19821.21	3043.69
SD	0.30	0.71	0.36	14.15	6.44	5.66	5.01	4.45	6.39	7.84	47.25	31.97	178.47	45.71
RSD [%]	64.79	15.56	199.37	0.68	1.94	0.86	0.74	44.71	2.27	102.63	1.30	1.56	0.90	1.50

Table 3.6: Statistical results for peanut oil (oil 2)

	Signal													
Lab. No.	**1**	**2**	**3**	**4**	**5**	**6**	**7**	**8**	**9**	**11**	**12**	**13**	**14**	**15**
1	-0.21[a]	1.36	-1.56[a]	2023.95	332.61	656.88	681.99	15.38	440.07	-	3201.75	2044.88	20101.33	2995.79
2	0.74	2.61	0.29	2041.11	317.67[a]	658.40	681.15	6.87	445.25	-	3195.68	1996.82	20218.47	2986.65
3	-	3.11	0.38	2046.95	345.02	653.55	681.92	6.63	451.64	14.35	3232.47	2036.38	20105.69	3059.10
4	0.34	2.57	0.17	2030.71	332.31	648.65	676.02	16.02	424.23	-	3213.54	2066.40	20166.79	3032.88
5	0.43	2.91	0.12	2069.53	339.58	661.89	698.04	15.49	448.19	-	3249.53	2088.18	20412.18	3086.55
6	0.58	2.96	0.62	2049.01	339.41	662.84	685.40	15.90	428.87	2.98	3219.16	2074.59	20082.61	3134.30
7	0.78	2.76	0.43	2018.27	319.68	659.44	684.88	4.52	452.13	5.96	3235.09	1991.00	20201.23	2979.19
8	-	2.02	0.07	2049.15	336.01	660.38	685.37	22.07	428.36	-	3245.42	2102.61[a]	20269.51	2993.42
9	0.53	3.41	0.18	2029.62	327.50	644.83	670.90	-	-	-	3180.02	2049.94	19901.71	3058.71
10	0.72	3.44	0.03	2033.03	335.58	633.67[a]	642.25[a]	-	442.90	-	3225.94	2037.93	20432.17	3031.67
11	0.67	2.69	0.04	2044.44	328.72	660.47	685.95	-	450.71	-	3214.23	2029.82	20320.58	3016.97
12	-	4.55[a]	0.47	2077.62[a]	345.80	665.72	663.36	-	444.64	1.00	3292.12[a]	2041.00	20684.67[a]	3207.78[a]
13	0.27	1.92	0.20	2041.03	327.95	643.56	668.09	22.03	431.47	0.01	3216.97	2010.95	20158.49	2978.73
14	0.31	1.92	0.23	2046.35	329.39	647.13	673.15	14.72	434.49	-	3219.47	2016.47	20215.83	2959.76
15	0.44	1.95	0.20	2038.21	335.72	649.01	674.29	18.57	436.81	1.71	3220.82	2022.82	19934.19	2996.19
16	-	2.33	-	2077.70[a]	324.56	657.78	681.63	-	451.05	-	3227.70	1974.10	20456.00	3044.60
17	0.64	2.94	-	2023.96	332.26	643.55	674.50	-	447.85	-	3217.74	2020.16	20335.19	2993.81
18	0.88	3.55	0.04	2044.24	345.39	654.94	685.24	-	440.68	-	3222.10	2018.05	20419.51	3023.87
19	0.11	2.47	0.18	2037.60	329.19	653.54	677.51	-	449.44	-	3213.13	2045.94	20221.61	2994.85
20	1.28[a]	3.44	0.51	2030.71	329.57	657.36	677.65	-	-	-	3212.70	2040.56	20125.20	2985.17
21	0.58	2.72	-0.30	2022.84	335.14	658.81	682.42	-	-	-	3223.22	2020.71	20187.86	2962.13
MEAN	0.53	2.66	0.22	2037.93	33.57	654.94	679.27	14.38	441.60	4.33	3219.33	2031.33	20213.31	3015.72
SD	0.21	0.60	0.22	12.26	7.00	6.70	7.21	5.97	8.98	5.32	15.75	27.66	153.63	44.09
RSD [%]	40.15	22.66	100.78	0.60	2.10	1.02	1.06	41.51	2.03	122.70	0.49	1.36	0.76	1.46

Table 3.7: Statistical results for olive oil (oil 3)

	Signal													
Lab. No.	**1**	**2**	**3**	**4**	**5**	**6**	**7**	**8**	**9**	**11**	**12**	**13**	**14**	**15**
1	5.88	2.96	-1.21	1835.31	330.10	655.16	682.43	31.57	181.06	-	3388.66	2159.77	20229.99	3004.08
2	6.13	5.61	0.37	1840.67	317.68	658.86	684.99	29.59	172.17	11.30	3387.13	2122.73	20445.29	2983.06
3	3.86	2.47	-	1814.75[a]	336.66	658.15	683.13	34.35	167.52	20.26	3352.12	2098.95	20172.27	3023.01
4	6.47	3.81	0.25	1863.01	334.22	656.36	685.78	28.89	175.85	5.98	3446.46	2219.43	20630.16	3080.93
5	6.23	4.11	0.13	1879.85	339.02	662.26	696.12	25.99	185.81	4.97	3449.78	2210.26	20709.59	3129.74
6	6.45	3.66	0.65	1848.23	332.68	663.00	685.41	25.86	177.48	8.09	3388.61	2190.43	20287.81	3166.67
7	6.78	3.63	0.62	1844.22	319.78	664.45	690.00	1.13[a]	205.08[a]	14.70	332.34	2112.38	20585.44	2998.20
8	0.13[a]	2.69	0.13	1857.51	336.48	661.03	687.88	30.50	171.67	8.34	3442.85	2216.22	20496.71	3031.62
9	6.23	3.28	-	1847:35	293:44[a]	643.15	655.27[a]	32.58	176.96	-	3307.45[a]	2150.09	19764.70[a]	2950.57
10	8.03	4.67	0.26	1883.07	343.17	672.39[a]	663.29	29.91	171.79	35.65	3562.17[a]	2230.32	21273.40[a]	3166.26
11	6.74	4.62	0.07	1858.78	330.90	663.35	691.02	31.81	171.42	8.03	3418.31	2116.61	20655.27	3037.83
12	5.60	4.20	1.92	1870.01	342.01	667.98	661.55	34.02	177.67	7.92	3452.37	2092.72	20846.43	3207.92[a]
13	6.28	2.85	0.16	1858.01	329.42	648.22	672.66	34.31	173.17	10.03	3425.34	2119.14	20482.17	3016.30
14	6.22	2.86	0.13	1853.09	327.51	647.99	673.39	32.00	173.64	9.75	3427.40	2124.93	20445.00	2985.21
15	6.30	3.29	0.19	1835.65	332.91	647.54	672.49	35.54	175.13	10.18	3401.09	2112.25	20072.88	3002.49
16	5.97	3.35	-	1868.30	319.41	652.69	677.34	22.03	175.87	9.04	3405.60	2088.10	20583.00	3056.60
17	6.69	4.45	0.11	1867.29	337.63	654.95	681.42	-	-	42.75[a]	3469.22	2124.25	20946.67	3014.13
1 8	14.76[a]	17.54[a]	10.73[a]	1843.31	339.09	656.68	683.26	29.44	171.09	39.88	3388.35	2086.09	20515.12	3008.31
19	5.59	3.36	0.15	1833.71	329.99	650.78	678.05	-	-	-	3387.71	2155.98	20355.65	3027.89
20	7.45	4.10	0.74	1833.39	324.65	654.09	677.90	-	-	-	3393.20	2186.69	20268.29	2972.08
21	6.28	4.28	-0.55	1834.39	325.65	655.92	680.88	-	-	-	3395.32	2112.97	20259.83	2933.74
MEAN	6.29	3.71	0.24	1852.76	331.45	655.83	680.45	30.53	174.89	13.61	3413.26	2144.30	20473.03	3029.44
SD	0.81	0.80	0.62	15.60	7.40	6.04	8.72	3.61	4.40	10.50	30.32	46.85	229.91	63.70
RSD [%]	12.89	21.43	257.97	0.84	2.23	0.92	1.28	11.81	2.52	77.14	0.89	2.18	1.12	2.10

Table 3.8: Statistical results for walnut oil (oil 4)

	Signal													
Lab. No.	**1**	**2**	**3**	**4**	**5**	**6**	**7**	**8**	**9**	**11**	**12**	**13**	**14**	**15**
1	4.00	0.29	-0.96[a]	3406.19	349.66	648.35	692.91	465.20	1244.03	-	3521.10	2033.60	15375.46	2613.92
2	3.74	1.20	0.55	3460.55	311.31[a]	651.46	693.11	526.09	1197.50	8.01	3523.00	1998.68	15451.50	2996.05
3	3.15	0.63	1.24	3447.11	338.40	637.52	687.88	528.71	1161.83	18.51	3529.97	2001.21	15329.88	2572.51
4	4.28	1.10	0.37	3457.44	360.29	648.56	695.48	501.91	1254.61	2.91	3591.42	2075.48	15682.50	2771.15
5	3.92	1.34	0.46	3485.21	356.95	648.44	699.68	407.21	1305.96	5.45	3592.46	2093.02	15597.89	3072.17
6	4.06	1.12	0.62	3464.06	379.27	657.63	702.23	379.38	1305.77	5.35	3578.19	2055.37	15515.86	3150.05
7	4.15	1.46	0.80	3459.62	319.91	660.02	706.03	10.93[a]	1756.05[a]	6.81	3590.26	2027.17	15675.77	2633.77
8	0.09[a]	0.96	0.33	3454.82	353.12	652.37	696.40	538.15	1179.38	4.83	3579.13	2092.76	15479.03	3001.31
9	3.95	1.59	0.84	3379.47	367.93	630.08[a]	683.44	428.94	1273.26	38.47[a]	3561.99	2061.72	15161.07	2578.51
10	5.63	2.09	0.10	3524.80	389.33[a]	647.05	657.84[a]	529.22	1208.20	34.37	3689.61[a]	2107.66	15942.00	3108.40
11	4.73	1.84	0.25	3483.80	340.84	654.98	702.13	525.29	1180.57	5.42	3588.44	2040.51	15613.85	2638.50
12	5.39	2.79[a]	1.28	3554.23	359.85	657.93	663.61[a]	524.79	1211.54	5.26	3684.64[a]	2055.78	16024.46[a]	3208.65
13	3.77	0.85	0.36	3461.29	350.51	637.96	681.02	528.38	1191.18	6.20	3568.68	2019.83	15564.03	2975.98
14	3.88	0.83	0.44	3453.57	344.58	639.68	684.15	509.19	1211.21	6.41	3567.90	2026.35	15463.24	2936.58
15	4.05	0.88	0.47	3424.39	351.06	640.45	684.79	541.29	1172.51	7.28	3538.22	2011.59	15291.06	2977.18
16	2.48	0.91	-	3478.20	331.63	642.56	683.53	386.66	1284.00	5.94	3542.80	1951.80[a]	15398.00	2554.00
17	4.60	1.49	0.27	3543.66	346.06	657.96	706.28	516.04	1186.79	31.24	3651.49	2069.33	15955.28	2620.28
1 8	4.47	1.67	0.67	3464.57	347.42	642.69	694.51	525.68	1169.00	19.06	3531.59	2020.77	15397.35	3063.18
19	3.71	0.98	0.41	3808.65[a]	373.41	642.00	687.38	-	-	-	3544.34	2035.47	15422.58	3013.62
20	5.27	1.58	1.01	3369.51	359.46	640.03	683.30	-	-	-	3526.27	2010.85	15197.25	2549.82
21	4.07	1.39	0.30	3405.22	356.20	649.18	692.27	-	-	-	3549.74	2013.97	15420.32	2587.87
Mean	4.16	1.21	0.57	3458.88	351.92	647.84	692.45	491.89	1219.84	10.82	3561.95	2042.56	15496.69	2839.21
SD	0.73	0.44	0.33	47.96	14.06	7.30	8.15	55.75	48.49	9.72	33.13	32.33	208.45	233.63
RSD [%]	17.53	36.13	58.31	1.39	4.00	1.13	1.18	11.33	3.98	89.87	0.93	1.58	1.35	8.23

Table 3.9: Statistical results for olive oil (oil 5)

	Signal													
Lab. No.	**1**	**2**	**3**	**4**	**5**	**6**	**7**	**8**	**9**	**11**	**12**	**13**	**14**	**15**
1	8.58	1.81	–1.15	1835.96	326.03	646.74	689.08	31.11	150.90	—	3410.72	2155.63	20305.89	3000.50
2	8.31	4.18	0.49	1843.59	309.82[a]	646.67	686.50	29.03	145.09	15.54	3402.42	2068.86	20360.59	2973.56
3	8.38	1.93	—	1863.36	327.37	641.29	688.90	32.40	145.06	24.76	3453.93	2059.53	20468.66	3011.96
4	9.23	2.61	0.28	1870.32	327.65	648.21	692.06	27.64	150.04	10.09	3468.02	2170.64	20609.47	3073.49
5	9.30	2.78	0.33	1894.56	337.36	656.26	707.41	26.32	161.38	11.44	3499.55	2186.45	20884.09	3144.67
6	9.68	3.66	1.09	1857.03	330.63	653.00	693.18	24.56	153.32	11.99	3434.33	2155.27	20293.22	3154.39
7	9.24	2.83	0.55	1876.29	324.71	662.90	707.40	1.60a	179.54a	15.24	3495.71	2101.26	20833.23	3033.15
8	13.07	1.81	—	1866.63	329.58	654.09	695.61	—	144.91	13.07	3479.95	2177.09	20589.88	3035.47
9	7.97	2.19	—	1777.75[a]	335.00	620.78[a]	670.19	32.02	164.20	—	3351.76a	2122.37	19593.70a	2891.92
10	1.59a	1.11	3.13[a]	1891.63	343.64	664.39	707.48	26.32	143.02	48.81a	3562.70a	2212.71a	21469.40[a]	3213.10[a]
11	9.63	3.31	0.05	1874.44	324.51	657.28	698.94	30.97	149.37	13.11	3461.51	2095.65	20784.24	3052.54
12	8.45	3.36	1.43	1886.58	337.01	651.14	650.24[a]	29.85	148.40	—	3473.71	2052.69	20900.03	3210.39[a]
13	8.44	1.94	0.29	1883.73	327.77	644.01	683.92	31.29	143.09	11.48	3460.22	2088.38	20769.50	3062.09
14	7.14	2.01	0.36	1862.19	324.33	642.85	684.48	28.36	146.64	15.16	3444.44	2086.82	20441.73	2993.95
15	8.72	2.65	0.26	1859.30	334.29	644.81	687.73	30.78	145.82	14.05	3435.86	2059.44	20304.93	3006.32
16	6.37	1.71	—	1856.60	318.80	636.44	676.66	21.19	148.00	8.12	3397.20	2030.50	20415.00	3022.00
17	13.86[a]	5.23[a]	3.16[a]	1889.36	328.09	653.87	695.04	28.30	145.60	40.06	3521.62	2115.98	21095.98	3055.53
18	9.33	3.54	0.27	1847.97	341.54	646.65	691.39	28.56	142.22	30.05	3415.72	2063.75	20264.14	2963.26
19	8.33	2.46	0.30	1839.48	322.97	643.35	683.81	—	—	—	3418.38	2113.36	20393.38	3022.33
20	9.34	2.70	0.32	1833.95	319.47	644.48	681.44	26.07	152.48	—	3405.68	2110.54	20281.68	3008.17
21	8.71	2.67	0.06	1835.20	330.16	647.14	688.25	26.09	148.22	—	3432.40	2091.41	20356.24	2969.76
Mean	8.85	2.56	0.33	1863.41	329.54	649.28	690.47	28.38	148.83	16.73	3447.97	2105.28	20544.84	3025.00
SD	1.31	0.77	0.55	19.82	6.79	7.22	9.82	2.93	5.84	8.87	35.86	44.77	257.54	60.67
RSD [%]	14.85	30.11	167.08	1.06	2.06	1.11	1.42	10.34	3.92	53.02	1.04	2.13	1.25	2.01

The results of the proficiency tests were assessed with the help of z-scores. Classical z-scores were calculated according to ISO 13528:2015:

$$z_i = \frac{(x_i - x_{pt})}{\sigma_{pt}}$$

where x_i = proficiency test result; x_{pt} = assigned value; and σ_{pt} = SD. A z-score was assigned to each participant laboratory for its performance. To simplify the interpretation of z-scores, the following agreements were established (an example is presented in figure 3.3):

$|z| \leq 2.0$, satisfactory participation (figure 3.3; light-gray bars)

$2.0 < |z| < 3.0$, questionable result (figure 3.3; medium-gray bars)

$|z| \geq 3.0$, unsatisfactory participation (figure 3.3; dark-gray bars)

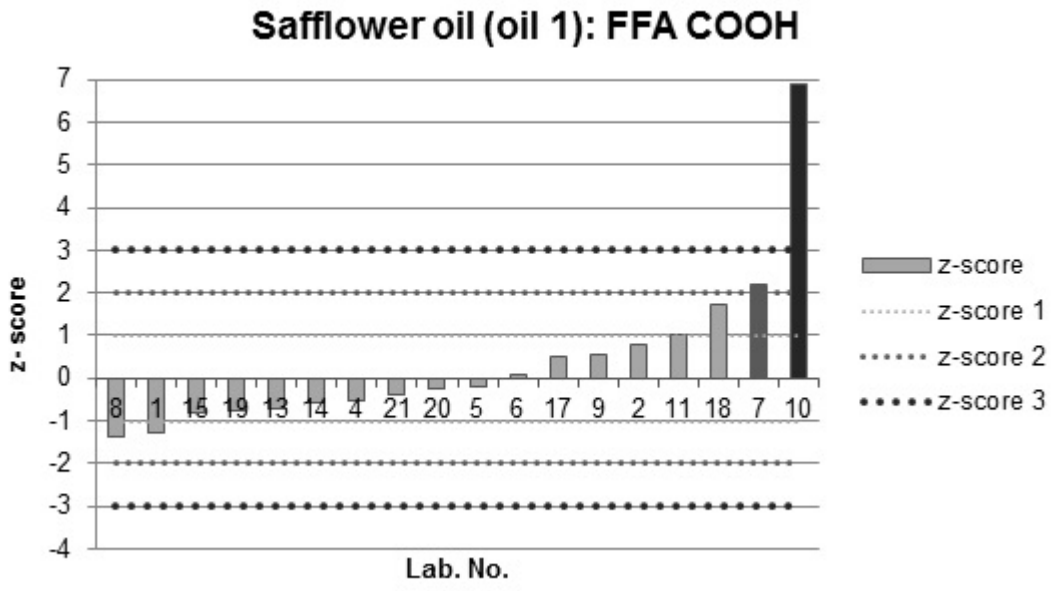

Figure 3.3: Statistical evaluation of z-scores presented in an example of the integration FFAs (COOH) signals in safflower oil.

Participation in an interlaboratory comparison was deemed successful if 80% of all required results exhibited a value of $|z| < 3$. In the present interlaboratory comparison, 89.5% of all submitted data showed $|z| \leq 2.0$, 5.9% showed $2.0 < |z| < 3.0$, and 4.6% showed $|z| \geq 3.0$. Figure 3.4 presents the percentages of z-scores the participants achieved, with a limit of $|z| < 3$. Nineteen of the 21 laboratories successfully passed the test (figure 3.4, light gray bars). Ten laboratories provided excellent results, passing the interlaboratory

comparison at 100%. Two laboratories did not pass the interlaboratory comparison (figure 3.4, black bars). Laboratory 12 had integrated additional signals to the determined range of $\delta = 11.1$–10.6 ppm, which resulted in increased values for the PV (signal 2). Results of laboratory 10 showed several evaluation deviations.

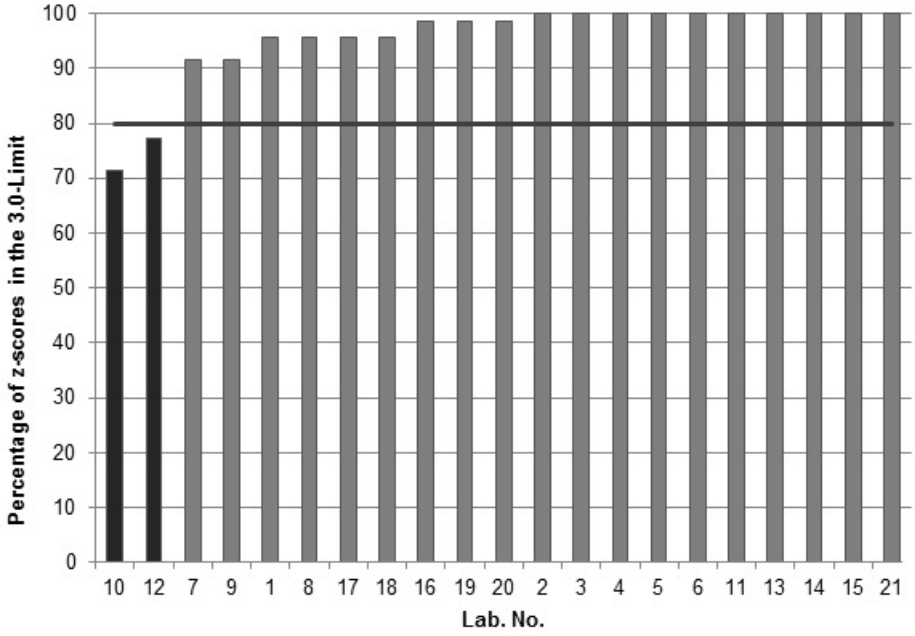

Figure 3.4: Performance assessment based on z-scores, with light grey bars as successful participation and dark grey bars as non-successful participation.

3.4.3 Challenging Signals

It is well known that operator error commonly affects quantitative NMR (qNMR) results. To obtain accurate results, phase and baseline corrections, as well as integration, had to be precisely performed [144], [145], [146], [147]. To cover 99% of the total signal intensity (the signal being a Lorentzian line), integration would need to be extended to 64 times the full width at half maximum [1], [5], [22], [148]. In these NMR spectra, such large-scale integration was not possible because of the high number of signals. Nevertheless, a broad enough integration range had to be chosen to cover a maximum percentage of the total area (figure 3.5b). One of the most ubiquitous issues with qNMR is baseline correction, which significantly affects the integrated area under a signal. Usually the baseline is automatically corrected, but some additional minor baseline correction may be needed to achieve optimal integration values. In this study, automated and manual baseline corrections were performed. Phase correction has been found to be one of the most challenging aspects in evaluating NMR spectra; an incorrectly phased spectrum cannot correctly be evaluated. de Brouwer [149] showed that a group of six experienced NMR operators who performed

a manual phase correction had an average difference up to 1% for a set of 14 integrals, with individual integrals deviating up to 2.5%. Because not all of the operators included in our study were experienced in evaluating oil, the deviation in our study was higher. In our case, the erroneous phase highly influenced signals at δ = 4.0–6.0 ppm. Because of these problems, several automatic baseline correction algorithms were already presented to replace the time-consuming manual correction, but were not applied here [150], [151].

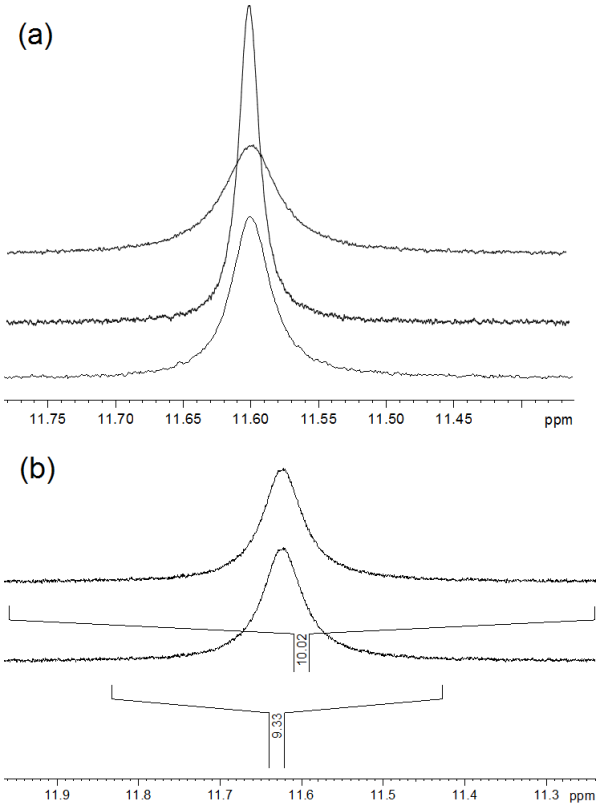

Figure 3.5: ^{1}H NMR spectra of olive oil (sample 3) with (a) different contents of protic compound H_2O in solvent and (b) different integration ranges; details: FFA COOH.

About 60% of data had an RSD of < 3%. However, a higher RSD was observed for signals 1, 2, 3, 8, and 11. Signal 1 represented the carboxyl group in FFAs. The COOH proton in all FFAs resonates as a broad singlet at δ = 12.0–11.4 ppm. It is well known that protic matrix or solvent impurities affect proton transfer processes, which results in signal broadening. Figure 3.5a demonstrates how FFA COOH signal shape is affected by the different components of the protic compound H_2O in the samples and solvent. The integration range significantly influenced the integration value (see figure 3.5b), especially when broad signals were integrated.

Signal 2 was assigned to peroxide hydrogens. As already discussed, peroxides are routinely measured as PV according to Wheeler. PV is expressed in milliequivalents of active

oxygen per kilogram, covering all compounds that oxidize potassium iodide under the defined conditions [152], [153]. The proposed method was not specific, leading to partially erroneous results because of cross-reactions, false-positives, or frauds. Skiera et al. reported a new ^{1}H NMR assay as a tool to determine the amount of hydroperoxide needed for the assessment of oxidative state in edible oils. Performance of the NMR method was compared with the Wheeler approach by relative sensitivity. The results demonstrated that the Wheeler method and NMR spectroscopy method exhibit similar analytical performance [91]. Figure 3.6 shows the peroxide signals in the spectra of all five edible oil samples. Safflower oil (sample 1) is highly oxidized with a peroxide S/N of 170 (600 MHz, 64 ns), representing a relative measurement uncertainty of about 1%. In contrast, under the same conditions, sample 5 contained a smaller peroxide concentration with an S/N of 30. Such a low S/N leads to higher relative measurement uncertainties, in this case more than 10%. Correlation between the S/N of the signals and the SD and RSD results is well known [1].

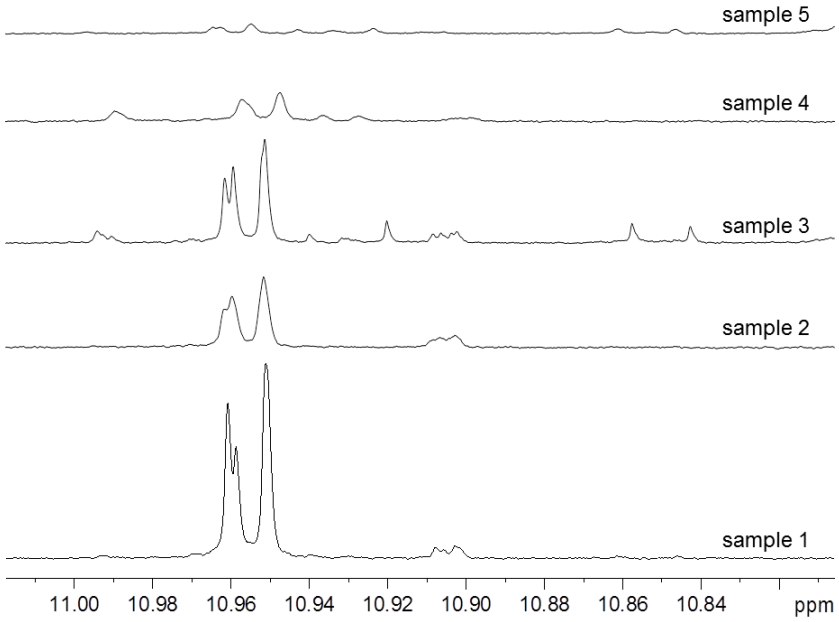

Figure 3.6: ^{1}H NMR spectra: Integration range of the peroxides in all five edible oil samples.

The quantification of signal 3 (representing aldehydes) showed the highest deviations (100–260%). The aldehyde signals had a very low S/N (2–5; 600 MHz, 64 ns; figure 3.7). Mathematically, the LOD is determined as the intensity for which the S/N equals 3. Visual evaluation of the LOD in sample 5 revealed several aldehyde signals. However, in all five samples, the S/N values were lower than the LOQ, some lower than the LOD, resulting in the very high SDs observed. Some participants provided negative signal intensities, which were the result of erroneous baseline correction (see tables 3.5-3.9, pages 36-40). Quantification of the α-CH_2-group in FFAs (signal 11, $\delta = 2.24$ ppm) was challenging due

to the low S/N of the signal and overlap with the α-CH_2 group ($\delta = 2.30$ ppm) in the FAs, which is part of a TAG. Because of that the α-CH_2-integral of the FFA is overestimated.

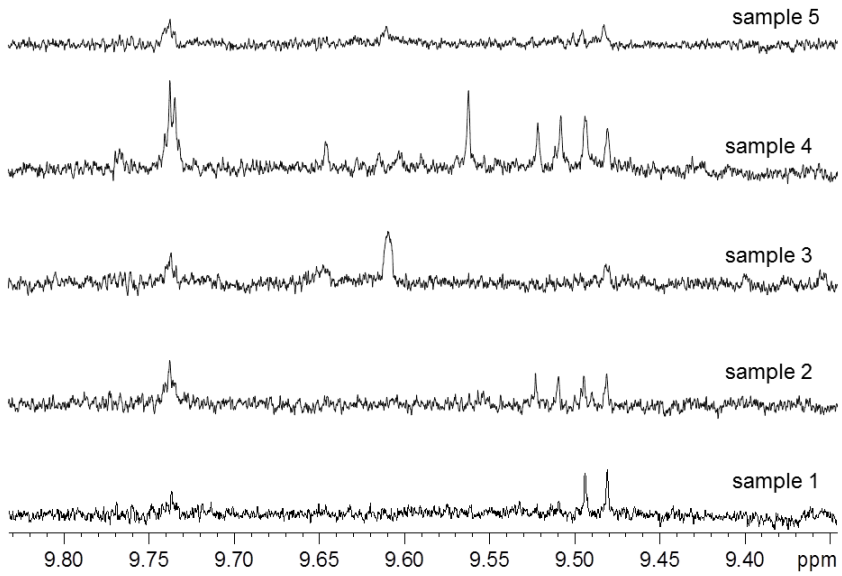

Figure 3.7: ^{1}H NMR spectra: Integration range of the aldehydes in all five edible oil samples.

3.4.4 Effect of the Instrument

The interlaboratory comparison comprised NMR instruments from different vendors and of varying frequencies (400, 500, and 600 MHz) and used a range of probe types (BBI, CPPBO, CPQNO, PABBO BB, and CPMNP). ANOVA was used to compare the three frequencies (400, 500, and 600 MHz) for statistical significance. A posthoc Tukey's HSD test was also performed to identify individual means that significantly differed from each other. The Tukey HSD test proved that the results for signals 1–7 and 9–15 recorded by the 400, 500, and 600 MHz spectrometers were comparable. Only signal 8 (18:3 FAs) was not comparable, distinguished by high deviation (RSD >> 3%). Figure 3.8 demonstrates the dependence of signal width and overlap for 18:3 and 18:2 on the strength of the magnetic field. Confirmed by Tukey's HSD test, the 18:3 signal recorded by the 400 MHz spectrometers significantly differed in shape and integral value compared with the spectra from the 500 and 600 MHz spectrometers. Because there were increased errors associated with the evaluation of the 18:3 signal in ^{1}HNMR spectra recorded by 400 MHz spectrometer, we recommend that analysis of FA distribution be conducted on NMR spectrometers with frequencies greater than 400 MHz.

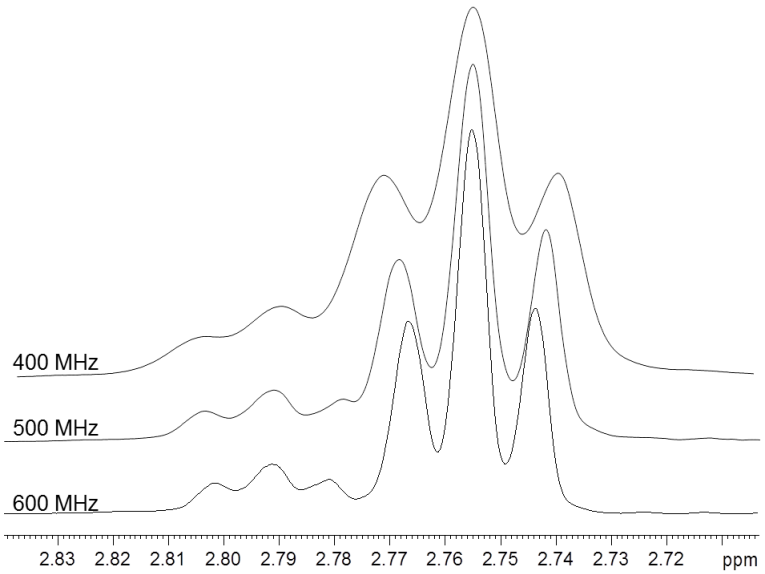

Figure 3.8: ^{1}H NMR spectra: Integration range of 18:3 and 18:2 FAs.

3.5 Conclusions

An interlaboratory comparison was carried out to evaluate the applicability of an alternative NMR analysis of edible oil. Seventeen international laboratories, using different NMR spectrometers and different operators, demonstrated their individual performance by presenting a total 21 data sets. The interlaboratory comparison was successfully completed for 19 data sets; 2 data sets did not pass the interlaboratory comparison test because those laboratories had not achieved the required success limit of 80%. The results of the presented interlaboratory test confirmed the robustness of the NMR spectroscopy method and the reproducibility of the quality parameter values from the edible oils. High-resolution NMR offered several advantages over conventional methods, providing a straightforward approach for the qualitative and quantitative analysis of oils and fats. Furthermore, this interlaboratory comparison determined that there is a need for NMR education, practice, and exercise in young and experienced NMR scientists alike. A well-founded understanding of NMR spectra evaluation is a basic learning goal for students of spectroscopy, as well as specialists of the subject area. A hands-on approach in NMR data acquisition, processing, and analysis is the most powerful and effective method of teaching. Practical experience with acquiring and processing NMR spectra to determine the correct integral values is extremely valuable for chemistry students and specialists and provides the foundation for all the results presented in this paper.

3.6 Acknowledgments

We thank all participants for providing their results for publication.

Chapter 4

Peroxide Value

Original titel: NMR Spectroscopy: Determination of Peroxide Value in Vegetable and Krill Oil by using Triphenylphosphine as Tagging Reagent [154]

Elina Hafer, Ulrike Holzgrabe, Sascha Wiedemann, Kristie M. Adams, Bernd Diehl;
European Journal of Lipid Science and Technology, 122: 1900442-1900452, 2020.

4.1 Abstract

Hydroperoxides are formed as the primary product during lipid oxidation being analyzed as the peroxide value to detect the degradation level of oils and fats. As an alternative to the classical titration method according to Wheeler, a ^{1}H-{^{31}P} decoupled NMR method was developed using triphenylphosphine as a tagging agent. Triphenylphosphine reacted with peroxides to form triphenylphosphine oxides. The quantification of the peroxide value was performed by comparing the amount of reacted triphenylphosphine oxide and non-reacted triphenylphosphine. This approach eliminated the requirement for an additional internal standard. Low-oxidized oils (peroxide value < 3 meq/kg) and high-oxidized oils with peroxide values of 150 meq/kg were precisely quantified with an RSD of 4.90 % and 0.16 %, respectively. A total number of 108 oil samples have been examined using the newly-developed ^{1}H-{^{31}P} decoupled NMR method, indicating the applicability for vegetable oils and krill oils.

Keywords
NMR spectroscopy, peroxide, triphenylphosphine, peroxide value, oxidation

Abbreviations

BHT	butylated hydroxytoluene	NMR	Nuclear Magnetic Resonance
C_6D_6	deuterated benzene	PC	phosphatidylcholine
$CDCl_3$	Deuterated chloroform	PV	peroxide value
EPA	eicosapentaenoic acid	S/N	signal-to-noise ratio
D1	relaxation delay	T1	relaxation time
DHA	docosahexaenoic acid	TAG	triacylglyceride
DMSO-d_6	deuterated Dimethyl sulfoxide	TPP	triphenylphosphine
LOD	Limit of Detection	TPPO	triphenylphosphine oxide

4.2 Introduction

Oils and fats are valuable natural products that are highly promoted for their nutrient content and contribution to the human diet, and in numerous industrial and pharmaceutical applications, therapeutic and/or cosmetic products [155], [156], [157]. Oxidation of oils and fats influences the nutritional quality, flavor and price; high levels of oxidation reduce the shelf-life and increases the toxicity of the product [158], [159]. Polyunsaturated fatty acids are especially prone to oxidative degradation by several factors such as fatty acid composition, concentration of antioxidants and pro-oxidants, type and concentration of reactive oxygen species, temperature, light and presence of metals [160]. The major processes of lipid oxidation during food processing and storage is autoxidation [77]. In autoxidation and photooxidation, hydroperoxides are formed as primary products that can degrade in further reaction processes to aldehydes, ketones, alcohols and acids (figure 4.1) [160], [161], [162].

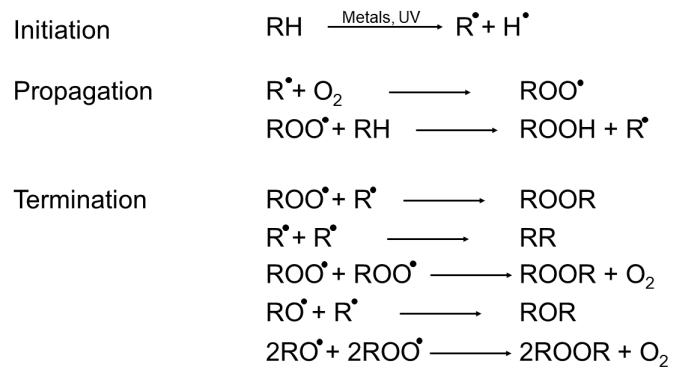

Figure 4.1: Oxidation process of fatty acid forming a hydroperoxide within three steps: initiation, propagation, termination [162].

Several analytical methods are available to determine the degree of oxidation, but none of them is optimal. One of the first successful methods was the iodometric titration developed by Lea [163] and Wheeler [93]. The method was standardized by several scientific organizations like the American Oil Chemists' Society as AOCS method Cd 8-53 [164], as a DIN norm [165], an European Pharmacopoeia method in chapter 2.5.5 [166] or as DGF method C-VI 6a Part 1 (05) by the German Society for Fat Science [167]. In the iodometric titration method, formed iodine I2 is titrated with sodium thiosulfate after the reaction of potassium iodide with the peroxide. Because the amount of formed iodine is proportional to the peroxide concentration, the peroxide value (PV) is determined by the consumption of thiosulfate. The PV states the milliequivalents of active oxygen per kilogram of oil/fat (unit: meq/kg).

Despite being the official method used routinely in industry today, the iodometric titration method has several limitations. The technique is labor-intensive, time-consuming and condition-dependent; it requires large amounts of sample (up to 10 grams) and chemicals which generate a significant amount of waste [168], [169]. A ring test has unraveled the weakness with regard to reproducibility; this is due to the problem that the titration results depend on the reaction time and sample amount [170]. Furthermore, titration methods show several limits: specificity and error susceptibility [171]. Presented by Skiera et al., titration results are significantly influenced by the matrix, the composition and concentration of secondary phytochemicals leading to false positive or false negative PV results [172], [173]. Especially olive oil, which has a high commercial value, is subject to strict food quality control, which is regulated in the European Union by the Commission Regulation No 2568/91. The official PV limits are set to 20 meq/kg for (extra) virgin olive oil, and to 5 meq/kg for refined olive oil [174]. To obtain correct PVs which are not influenced by external conditions or matrix, it is essential to find an alternative method which is fast, robust, error-free and sustainable. In contrast to the titration technique, the alternative method should be applicable for pigmented oils and phospholipid-containing products like krill oil.

Over the past decades, several alternative methods have been developed to determine the PV of oils and fats such as colorimetry, chromatography, infrared spectroscopy and Nuclear Magnetic Resonance (NMR) spectroscopy [175], [176], [177], [178], [179]. Saito, and later Shahidi and Wanasundara used ^{1}H NMR spectroscopy to determine the peroxide concentration by comparing the ratio of olefinic and aliphatic protons as well as the ratio of aliphatic and diallylmethylene protons in fatty acids [177], [178]. A further NMR method was developed by Skiera et al.; here hydroperoxides (δ = 10.5–11.5 ppm) were quantified directly [172]. The primary limitation of this NMR method is the low sensitivity. Because various triacylglycerides lead to different hydroperoxides, the signal-to-noise ratio (S/N) of each individual hydroperoxide signal is low, and thus, the uncertainty of low-oxidized oils with PV $<$ 10 meq/kg can increase to $\geq$ 10% of S/N of 30) [131]. Thus, the NMR method according to Skiera et al. was not applicable for either low-oxidized oils or phospholipid-containing samples, whereby phospholipid-containing samples also cannot

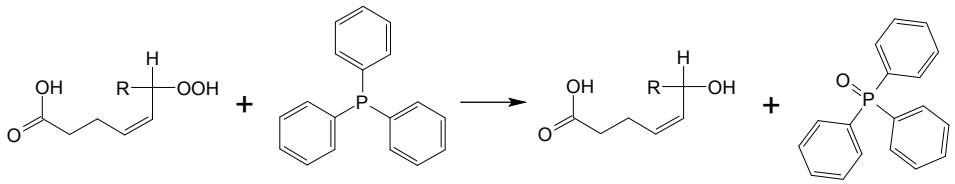

Figure 4.2: Deoxygenation reaction of hydroperoxides with TPP to form TPPO and the corresponding alcohol [180].

be examined by iodometric titration [93], [172]. To overcome this challenge, an alternative quantitative NMR method was developed to determine the peroxide amount in edible oils by using triphenylphosphine (TPP) as a derivatization agent. TPP reacts with peroxides to form triphenylphosphine oxide (TPPO; figure 4.2). By the comparison of the integrals of the signals of TPPO and non-reacted TPP, the PV could be determined quantitatively [meq/kg].

Here, ^{1}H and ^{31}P NMR analyses were investigated as potential analytical techniques. The performance of the TPP NMR method was compared with the NMR method presented by Skiera et al. [172] and the iodometric titration method [93].

4.3 Method

4.3.1 Materials

A total of 79 vegetable oil samples including olive oil, sunflower oil, rapeseed oil, nut oils, pumpkin seed oil, corn oil, linseed oil, grape seed oil, soya oil, wheat germ oil, black seed oil, 2 fish oils, 3 lecithins and 24 krill oil samples were collected from diverse German supermarkets or were provided by German oil mills.

NMR Spectroscopy: Triphenylphosphine (TPP) and benzaldehyde were purchased from Sigma Aldrich (MERCK). Deuterated chloroform ($CDCl_3$, 99.8 atom% D) + 0.3% tetramethylsilane (TMS), hexadeuteriodimethylsulfoxide (DMSO-d_6, 99.9 atom% D) + 0.3% TMS and benzene (C_6D_6, 99.50 atom% D) were purchased from Eurisotop. endo-1,4,5,6,7,8,8-Heptachloro-2,3-epoxy-4,7-methano-3a,4,7,7a-tetrahydroindane, dichloromethane and butylated hydroxytoluene (BHT) were purchased from Riedel-de Haen, LGC Promochem, TCI Europe, respectively.

Titration: Potassium iodide (Sigma-Aldrich), sodium thiosulfate solution (0.1 mol/L, AppliChem), acetic acid 100% (Roth) and isooctane (Roth) for the titration of the PV were of analytical grade. Cumene hydroperoxide (Merck) was of technical grade.

4.3.2 Sample Preparation

3.3.2.1 Holistic NMR Method

200 mg of the oil sample was dissolved in 0.8 mL of $CDCl_3$/DMSO-d_6 (v/v 4:1). After shaking, the solution was transferred into a 5-mm diameter NMR tube.

Spiking of krill oil: 4 samples were prepared using oxidized materials: (a) 200 mg sunflower phosphatidylcholine (PC), (b) a mixture of 100 mg sunflower PC and 100 mg sunflower oil (c) 200 mg krill oil, (d) a mixture of 100 mg krill oil, 50 mg of sunflower PC and 50 mg of sunflower oil. All samples were then dissolved in 1 mL of $CDCl_3$/DMSO-d_6 (v/v 4:1).

3.3.2.2 TPP ^{1}H-{^{31}P} decoupled NMR Method

Derivatization reaction with TPP: (a) 200 mg oxidized sunflower oil and (b) a mixture of 200 mg oxidized sunflower oil and 5 mg TPP were accurately weighed and dissolved in 1 mL $CDCl_3$ / DMSO-d_6 (4:1 v/v-%), respectively.

Solvent: 20 mg of TPP were dissolved in 1 mL of the following solvents: (a) $CDCl_3$, (b) $CDCl_3$ / DMSO-d_6 (4:1 v/v-%), (c) $CDCl_3$ / MeOD (2:1 v/v-%) and (d) C_6D_6, respectively. Each solution was analyzed hourly over the course of 6 hours.

TPP ^{1}H-{^{31}P} decoupled NMR Method as Routine Analysis

200 mg oil sample and 5-10 mg Triphenylphosphine (TPP) were weighed and dissolved in 1 mL C_6D_6.

S/N ratio comparison

200 mg oil sample and 5 mg TPP were weighed and dissolved in 1 mL C_6D_6. ^{1}H-{^{31}P} decoupled NMR and ^{31}P NMR analyses were performed.

Linearity

A cumene hydroperoxide solution was prepared by solving 15 μL cumene hydroperoxide in 1 mL C_6D_6. 5 separate oil/cumene hydroperoxide mixtures were prepared by spiking a 200 mg of sunflower oil with 0 μL, 5 μL, 10 μL, 15 μL and 20 μL of the cumene hydroperoxide solution. 5 mg TPP and 1 mL C_6D_6 were then added to each spiked oil sample.

Robustness

10 mg of benzaldehyde, heptachloro-endo-epoxide, dichloromethane, butylated hydroxytoluene (BHT) were weighed, mixed with 5 mg TPP and dissolved in 1 mL C_6D_6.

Astaxanthin

(a) 200 mg krill oil and 5 mg TPP and (b) 200 mg krill oil, 5 mg TPP and 0.4 μmol astaxanthin were weighed and dissolved in 1 mL C_6D_6, respectively.

Krill Oil Oxidation Test

5 krill oil / sunflower oil samples have been prepared with a total weight of 200 mg: 100% krill oil, 75% krill oil, 50% krill oil, 25% krill oil, and 0% krill oil. Each sample and 5 mg TPP were weighed and dissolved in 1 mL C_6D_6.

3.3.2.3 Titration Method according to Wheeler

The PV was analyzed according to the official DGF method C-VI 6a [167]. 5 g of the oil sample was weighed and dissolved in a mixture of isooctane and glacial acetic acid. After adding a saturated potassium iodide solution to the oil sample, the elemental iodine was titrated with a thiosulfate solution and starch was used indicator. The PV was then calculated using the amount of thiosulfate required to reach the titration endpoint.

4.3.3 Experimental NMR Analysis

NMR Methodology

All NMR spectra were recorded on an Avance III HD NMR spectrometer (Bruker, Karlsruhe, Germany, 500.41 MHz) and equipped with a BBFO^{PLUS} SmartProbe. The ^{1}H NMR spectra were recorded with the following acquisition parameters: spectral width 24 ppm, number of scans 32, relaxation delay 1 s, acquisition time 5.45 s.

For the holistic method, the relaxation time (T1) values of the hydroperoxide protons were approximately equivalent to the T1 values of the triacylglyceride protons, the integration values were influenced in the same way. Thus, a complete relaxation was not necessary.

The ^{1}H-{^{31}P} decoupled NMR spectra were recorded with the following acquisition parameters were: spectral width 24 ppm, number of scans 32, relaxation delay 2 s, acquisition time 5.45 s.

The ^{31}P NMR spectra were recorded with the following acquisition parameters: spectral width 100 ppm, number of scans 512, relaxation delay 10 s, acquisition time 6.50 s.

For a two-dimensional 1H J-resolved (JRES) experiment the sample presented in the chapter 3.3.2.2 *TPP ^{1}H-{^{31}P} decoupled NMR Method: Derivatization reaction with TPP* was used. The JRES spectrum was recorded with the following acquisition parameters: spectral width 2.5 ppm, number of scans 8, relaxation delay 2 s.

The experiments were carried out at 298 K, Data was processed by using Bruker's TOPSPIN-NMR software version 3.5 (Bruker, Rheinstetten, Germany).

4.4 Results and Discussion

4.4.1 Holistic NMR Method

The holistic NMR method was developed by Skiera et al. [172]. A typical ^{1}H NMR spectrum of an oxidized sunflower oil, acquired using the holistic approach, is presented in figure 4.3.

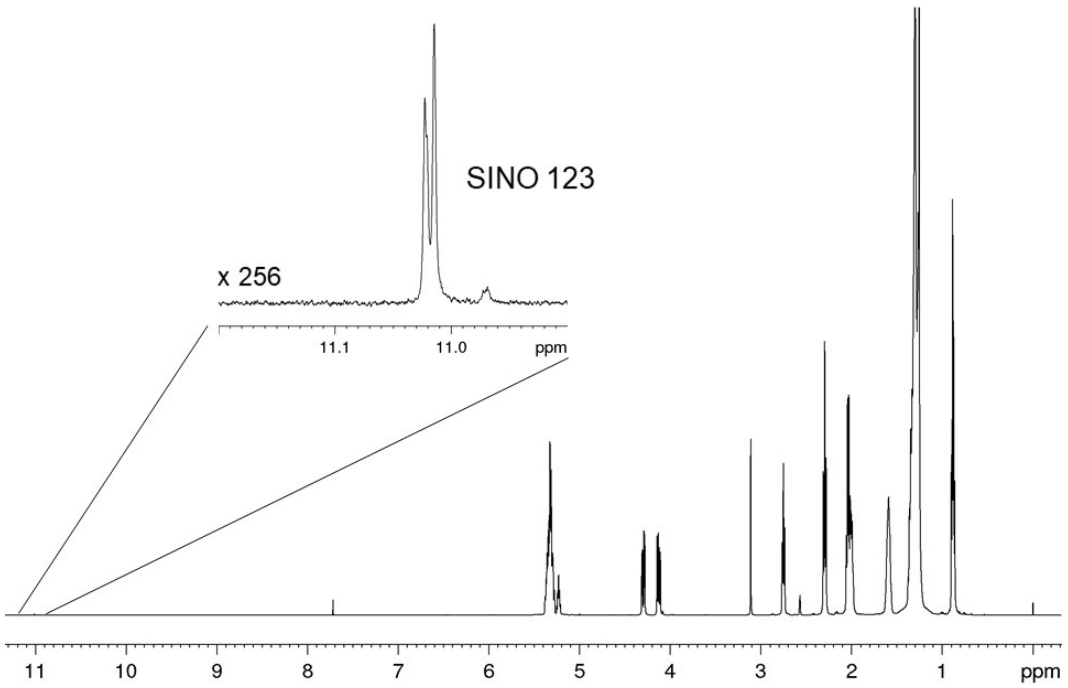

Figure 4.3: ^{1}H NMR spectrum of an oxidized sunflower oil with a PV of 38 meq/kg; in $CDCl_3$ / DMSO-d_6 (4:1 v/v-%).

The hydroperoxide signal (-OOH) of each fatty acid hydroperoxide resonates as a singlet at a chemical shift of δ = 11.0–11.3 ppm. Phosphatidylcholin (PC) hydroperoxides give observable signals in the ^{1}H NMR spectra because PC possesses a zwitterionic structure. The signals of the PC hydroperoxides are shifted to lower field (δ = 11.4–11.6) [181], [182]. Because the chemical shifts of the signals of the triacylglyceride (TAG) hydroperoxide and the PC hydroperoxide are significantly different, the molar ratio of TAG and PC hydroperoxides can be determined (figure 4.4b). This makes the NMR method applicable for the analysis of the oxidation grade of PC samples (figure 4.4a).

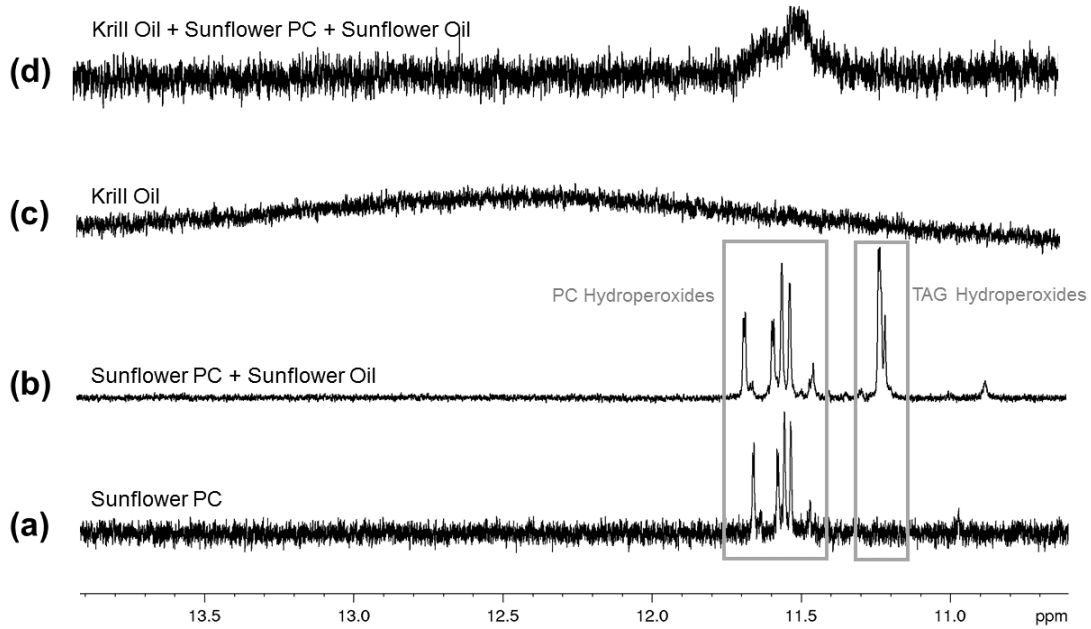

Figure 4.4: ^{1}H NMR spectra of (a) oxidized sunflower PC, (b) sunflower PC + sunflower oil, (c) krill oil, (d) krill oil + sunflower PC + sunflower oil (from bottom to top) ; in $CDCl_3$ / DMSO-d_6 (4:1 v/v-%).

The ^{1}H NMR spectrum of oxidized krill oil (figure 4.4c) shows a very broad, non-evaluable signal between $\delta = 11$ and 14 ppm. The signal broadening effect is due to the fast exchange of all exchangeable protons of the peroxide, carboxylic and phosphate groups in krill oil, which contains a mixture of TAG and a variety of phospholipids such as PC, phosphatidylinositol and phosphatidylethanolamine. Thus, the protons exchange too fast as to being measured during an NMR experiment. To prove that the krill oil as a matrix has this effect on the ^{1}H NMR spectrum, krill oil was spiked with oxidized PC and sunflower which gave individually well resolved signals. However, after being added to krill oil, well resolved signals of the peroxides have not been identified any more. However, the spiking experiment resulted in a broad signal at $\delta = 11.4$ ppm (figure 4.4d). These results confirm that the holistic NMR method, developed by Skiera et al., was applicable for analyzing the PV in oxidized PC samples, but not for other phospholipid-containing samples such as krill oil. Therefore, a new method is developed.

4.4.2 TPP ^{1}H-{^{31}P} decoupled NMR Method

Derivatization with TPP

The developed "TPP NMR" method is based on the well-characterized stoichiometric conversion of triphenylphosphine (TPP) with peroxides to form triphenylphosphine oxide

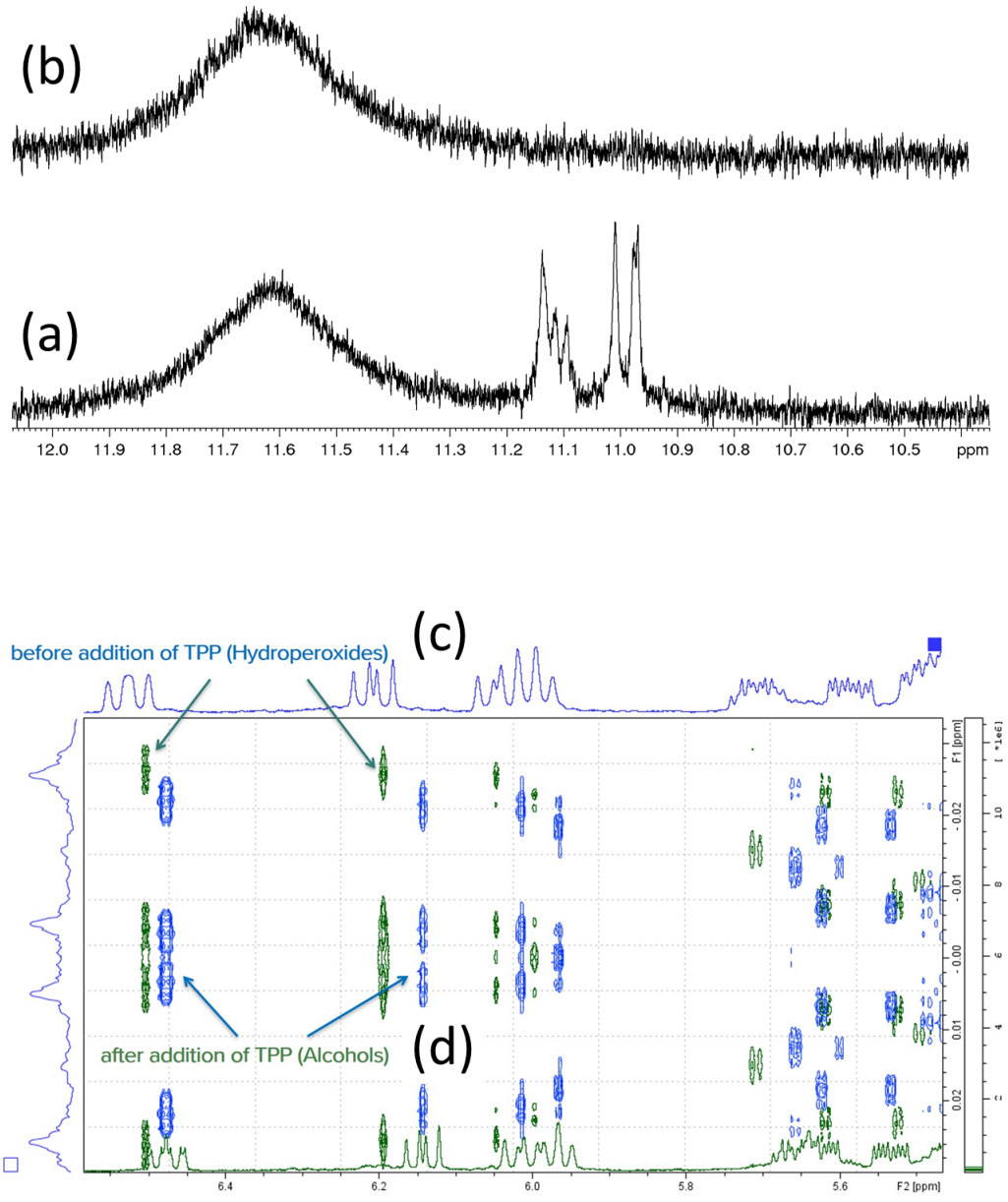

Figure 4.5: ^{1}H NMR spectra of oxidized sunflower before (a) and after the addition of TPP (b), top, with the corresponding JRES NMR spectrum of oxidized sunflower before (c) and after the addition of TPP (d), bottom.

(TPPO) and alcohols (figure 4.2, figure 4.5). The reaction occurred rapidly in non-polar solvents in less than 2 minutes [31]. Using an excess of TPP ensures that all peroxides present are converted to TPPO. The ^{1}H NMR spectra (solvent: $CDCl_3$/DMSO-d_6, 4:1) are compared before and after the addition of TPP. After the addition of TPP, the hydroperoxide signals disappear and alcohol signals increase (figure 4.5 top: before (a) and after the addition of TPP (b)). Other deviations are not identified. Thus, the observable substances do not influence the tagging reaction and as shown in the JRES NMR spectrum, TPP reacts only with the present peroxides (figure 4.5 bottom: before (c) and after the additiona of TPP (d)). Based on the stoichiometric conversion of TPP to TPPO [180], the oxidation degree [meq/kg] can be calculated by the ratio of the integrals of the non-reacted TPP and the reacted TPPO, where TPP serves as a reductant and also as an internal standard, which obviates the need for an additional internal standard.

Solvent

The influence of the solvent was studied using ^{1}H NMR spectroscopy. A mixture of $CDCl_3$ and DMSO-d_6 is commonly used for the quality analysis of lipids by NMR spectroscopy [20]. For the TPP NMR method, the effect of the following solvents was investigated: $CDCl_3$, $CDCl_3$ / DMSO-d_6 (4:1 v/v-%), $CDCl_3$ / MeOD (2:1 v/v-%) and C_6D_6. To quantify the degree of autooxidation, and thus assess the stability of TPP after sample preparation, an amount of TPP was dissolved in the appropriate solvent. The TPPO amount was analyzed quantitatively every hour and compared with the starting TPPO amount. In $CDCl_3$, the amount of TPPO increased by 8.5% after six hours, indicating that $CDCl_3$ is not a suitable solvent. Furthermore, the TPPO signal overlapped with the CHCl3 residual in $CDCl_3$, thus complicating accurate integration of the TPPO signal. The amount of TPPO in $CDCl_3$ / MeOD (2:1 v/v-%) and $CDCl_3$ / DMSO-d_6 (4:1 v/v-%) increased 1.5% after six hours. C_6D_6 showed the lowest level of autooxidation; the amount of TPPO increased only 0.7% after 6 hours. Based on the very low autoxidation rate of TPP in C_6D_6, C_6D_6 was selected as an appropriate solvent for the TPP NMR method.

TPP NMR Experiment

Because TPP and TPPO contain both protons and phosphorus nuclei, these substances can be measured using both ^{1}H and ^{31}P NMR spectroscopy. A ^{1}H NMR spectrum was compared with a ^{1}H-{^{31}P} decoupled NMR spectrum. Application of ^{31}P decoupling led to a less complex multiplet, thus increasing the S/N and the precision of integration. Thus, the following investigations were performed as ^{1}H-{^{31}P} decoupled NMR experiments.

To check which method is more appropriate for PV analysis, the S/N and relaxation time (T1) were compared for a sunflower oil with a PV of 38 meq/kg using the alternative TPP NMR method (^{1}H-{^{31}P} decoupled NMR spectroscopy) and the traditional ^{31}P NMR spectroscopic method developed by Skiera et al. [172]. Typical ^{1}H-{^{31}P} decoupled NMR and ^{31}P NMR spectra of an oxidized sunflower oil are displayed in figure 4.6, respectively.

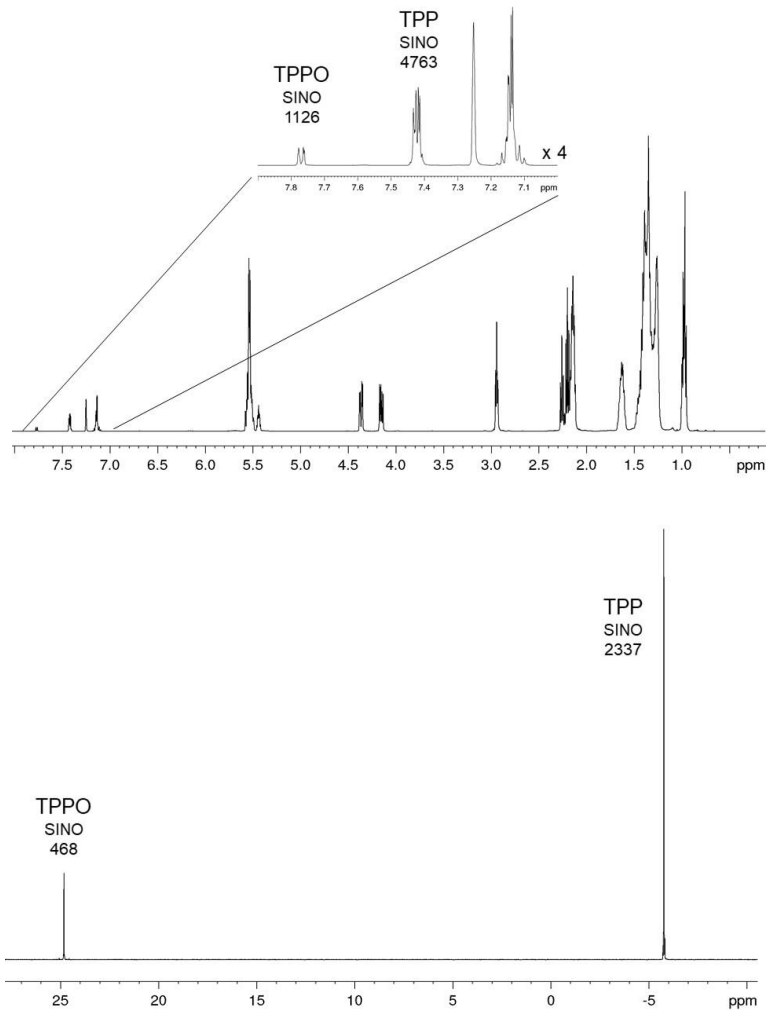

Figure 4.6: ^{1}H-{^{31}P} decoupled NMR spectrum (top) and 31P NMR spectrum (bottom) of an oxidized sunflower oil with a PV of 38 meq/kg (TPP NMR method); in C_6D_6.

The advantages and drawbacks of both ^{1}H-{^{31}P} decoupled NMR and ^{31}P NMR spectroscopic techniques were compared. The advantage of ^{31}P NMR spectroscopy was the low number of singlets: TPP was shifted to δ = -5.7 ppm and TPPO to δ = 24.8 ppm, without any signal overlapping (figure 4.6). However, ^{31}P NMR spectroscopy had two drawbacks: the low S/N compared to ^{1}H-{^{31}P} decoupled NMR spectra and the high D1 and, thus high T1 values of TPP and TPPO (table 4.1). As presented in table 4.1 in the ^{31}P NMR measurement, the T1 of TPP was very long and considerably different compared to the T1 of TPPO, which renders the ^{31}P NMR analysis unsuitable as a fast routine method. In the ^{1}H-{^{31}P} decoupled NMR spectra, the T1 values of the TPP protons and the TPPO protons were in the same order of magnitude, leading to a required relaxation delay (D1) of 20 seconds to achieve full relaxation of all protons (figure 4.6). However, because short relaxation times are advantageous for suitable routine analyses, a D1 of 2 seconds was

Table 4.1: S/N and T1 of TPP and TPPO in ^{1}H-{^{31}P} decoupled NMR and ^{31}P NMR spectra, PV = 38 meq/kg (figure 4.5).

NMR Analysis	**^{1}H-{^{31}P} decoupled NMR**	**^{31}P NMR**
Number of scans (ns)	32	512
S/N_{TPP}	4763	2337
S/N_{TPPO}	1126	468
$T1_{TPP}$ [sec]	3.5	15.1
$T1_{TPPO}$ [sec]	2.6	2.9

examined. The fully relaxed (D1 = 20 sec) and partly relaxed NMR signals (D1 = 2 sec) were integrated and compared. A D1 time of 2 sec led to a quantification error of 1%, which was deemed acceptable for this type of analysis. Decreasing the D1 value to 2 seconds shortens the experiment by 10 minutes, which makes the TPP ^{1}H-{^{31}P} decoupled NMR method ideal as a routine PV analysis technique. Based on the comparison of the ^{1}H-{^{31}P} decoupled and ^{31}P NMR methods, the ^{1}H-{^{31}P} decoupled NMR spectroscopy with D1 = 2 sec offered the best prerequisites as a technique of choice to determine the PV routinely.

Validation of the TPP ^{1}H-{^{31}P} decoupled NMR method

Selectivity
In the ^{1}H-{^{31}P} decoupled NMR spectra, the chemical shifts of TPPO and TPP were δ = 7.8 ppm and δ = 7.4 ppm, respectively. In the NMR spectrum of oxidized oil in C_6D_6, the benzene signal was detected at δ = 7.25 ppm with the ^{13}C satellites at ± 80 Hz. Thus, the TPP signal which was used for the integration was overlapped with the ^{13}C satellites of benzene. The integral of one ^{13}C satellite was calculated by integrating the benzene signal, and this value was subtracted from the TPP signal. Consequently, the TPPO amount was quantifiable. The selectivity was confirmed.

Linearity and range
The compound-specific linearity was examined. To assess the linearity and the measuring range, a sunflower oil sample was spiked with five different concentrations of cumene hydroperoxide to simulate an artificial oxidized oil. The PV was plotted against the added amount of cumene hydroperoxide resulting in a coefficient of determination of $R^2 = 0.9997$. The TPP NMR method was considered valid for the PV range of 1 meq/kg to 170 meq/kg. However, if an excess of TPP exists, the method will be linear in a range up to a concentration where either the oil or TPP cannot be dissolved completely in C_6D_6. As a recommendation for the quantitative analysis of PV, 5 mg TPP should be added to 200 mg oil with PV $\leq$ 170 meq/kg to ensure complete reaction of the hydroperoxides. In very low-oxidized oils, the amount of TPP should be decreased to obtain TPPO signals with a better S/N.

Precision
Iodometric titration measurements according to Wheeler were found to have a limit of detection (LOD) of PV > 2.0 meq/kg with an uncertainty of 2% [183]. The precision of the TPP NMR method was assessed by performing the sample preparation with a high-oxidized and a low-oxidized oil five times, respectively. The PV of the low-oxidized oil was determined to be 2.78 meq/kg with a relative standard deviation (RSD) of 4.90%. The high RSD was due to the relatively low S/N of the TPPO signal ($S/N_{TPPO} = 72$). The PV of the high-oxidized oil was determined to be 158.72 meq/kg with an RSD of 0.16% ($S/N_{TPPO} = 4020$). Previous studies demonstrated that a S/N of 30 resulted in an RSD of 10%, and a S/N of 150 of 1% [11], [184]. Though the RSD was lower in this research, the overall trend was confirmed: the higher the PV, the higher the S/N, and the lower the RSD. To further decrease the RSD, the S/N of the TPPO signal should be increased by examining the following options: use less TPP, use more sample amount, or increase the number of scans.

Limits of Detection (LOD) and Quantification (LOQ)
The main purpose in this study was the quantitative determination of the PV in low-oxidized oils. LOQ was determined in a routine sample (200 mg oil sample, 5 mg TPP, ns = 32). In this case, a low-oxidized oil with a PV of 2.78 meq/kg resulted in a TPPO signal with a S/N of 72 (figure 4.7). Based on the presented parameters, the LOD is 0.1 meq/kg and the LOQ 0.4 meq/kg.

Robustness
The validation of robustness included the examination of possible influencing substances. Because oils are a complex mixture of more or less bioactive non-nutrient compounds with oxidative or antioxidative properties such as tri- and diacyglycerides, free fatty acids, tannins, flavones, triterpenoids, steroids, saponins, alkaloids, and aldehydes, the following chemicals were investigated as potential cross-reaction partners of TPP: n-oxides, aldehydes, phenols and epoxides [185]. TPP was mixed with a definite amount of n-oxides, benzaldehyde, phenols and epoxides. The TPPO signals were compared with pure TPP sample. The respective ^{1}H-$\{^{31}P\}$ decoupled NMR spectra showed that n-oxides, aldehydes, phenols and epoxides did not influence the formation of TPPO. Furthermore, to prevent oil oxidation, several kinds of natural and synthetic antioxidants are often used. One of the most used synthetic antioxidants is butylated hydroxytoluene (BHT, E321) [186]. No antioxidant signals were identified in the ^{1}H-$\{^{31}P\}$ decoupled NMR spectrum, due to the high number of signals of the TAG and the low S/N. To examine whether TPP would react with the antioxidant BHT, pure BHT and TPP were dissolved in $CDCl_3$/DMSO-d_6 (4:1). The respective ^{1}H NMR spectrum showed signals of the reactants BHT and TPP, but no signals of a reaction product were identified. Thus, BHT does not react with TPP.

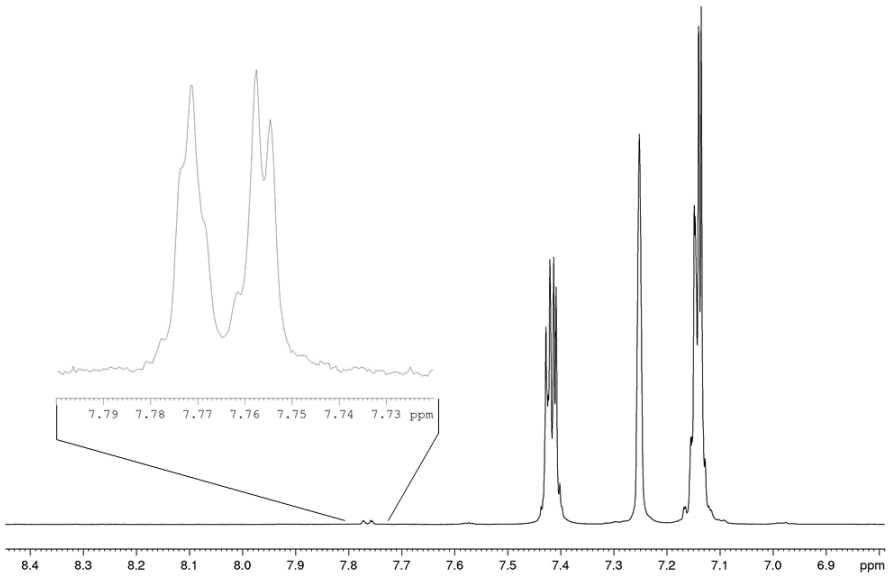

Figure 4.7: ^{1}H-{^{31}P} decoupled NMR spectrum of a low-oxidized sunflower oil (PV = 2.78 meq/kg) after the reaction with TPP; $S/N_{TPPO} = 72$; in C_6D_6.

4.4.3 Comparison of titration and NMR methods

Iodometric titration with thiosulfate according to Wheeler is considered as one of the most used method to evaluate the content of hydroperoxides [93]. Here, the PV represents the amount of iodine which is formed during the reaction of present lipid peroxides and iodide, and then titrated with sodium thiosulfate:

$$LOOH + 2\,I^- + 2\,H^+ \longrightarrow I_2 + LOH + H_2O$$

$$2\,Na_2S_2O_3 + I_2 \longrightarrow 2\,NaI + Na_2S_4O_6$$

To compare the iodometric assay and the NMR methods, 20 fresh and autoxidized oil samples were analyzed using the titration method according to Wheeler, the holistic NMR method by Skiera et al. and the TPP NMR method [93], [172]. 44 vegetable oil samples were analyzed NMR spectroscopically according to Skiera et al. [172] and by using TPP as a derivatization agent. 13 oils have been examined by the TPP NMR method and by titration according to Wheeler [93]. For the oils, the PV extended over a range of 0.78 meq/kg and 191.4 meq/kg. Because the aim of the new method was the quantitative determination of PV in oils, especially in low-oxidized samples, a high number of fresh oils was examined. 54% of the analyzed oils showed PV < 50 meq/kg. The results of the analyses were presented in table 4.2. The mean deviation between the results obtained by

the TPP NMR and the NMR holistic control methods was 5% with higher deviations at PV < 10. However, the PV results were stated as comparable. Paired sample t-tests found no significant differences between the peroxide results examined by the TPP ^{1}H-{^{31}P} decoupled NMR method and the holistic NMR method (t = 0.0061).

Table 4.2: PV results of 79 vegetable and fish oils and lecithins being examined by titration, holistic NMR method and TPP NMR method [meq/kg].

	PV [meq/kg]		
	Holistic NMR	**TPP NMR**	**Titration**
10 % Olive + 90 % Sunflower Oil	-	23.32	23.71
25 % Olive + 75 % Sunflower Oil	-	28.39	29.19
50 % Olive + 50 % Sunflower Oil	-	39.90	32.96
75 % Olive + 25 % Sunflower Oil	-	44.82	42.83
90 % Olive + 10 % Sunflower Oil	-	50.29	45.48
Almond Oil	119.80	104.72	-
Camelina Oil	12.15	16.87	23.74
Camelina Oil	< LOD	9.63	11.55
Camelina Oil	12.15	16.87	-
Crude Fish Oil	11.60	10.54	13.81
Crude Fish Oil	< LOD	6.02	2.99
Lecithin	< LOD	4.50	-
Linseed Oil	< LOD	1.63	4.28
Linseed Oil	26.04	29.07	-
Olive Oil	83.70	76.36	57.75
Olive Oil	119.44	110.94	96.05
Olive Oil	141.47	134.91	96.00
Olive Oil	86.40	85.89	73.30
Olive Oil	64.37	64.70	51.01
Olive Oil	108.54	102.44	74.57
Olive Oil	190.97	190.35	148.19
Olive Oil	174.44	176.85	141.63
Olive Oil	163.41	163.29	129.70
Olive Oil	58.86	61.58	53.00
Olive Oil	171.12	158.72	-
Olive Oil	9.90	12.80	-
Olive Oil	119.44	110.94	-
Olive Oil	141.47	134.91	-
Olive Oil	86.40	85.89	-
Olive Oil	64.37	64.70	-
Olive Oil	108.54	102.44	-
Olive Oil	190.97	190.35	-

Olive Oil	122.18	119.97	-
Olive Oil	174.44	176.85	-
Olive Oil	163.41	163.29	-
Olive Oil	58.86	61.58	-
Peanut Oil	-	18.28	23.74
Peanut Oil	32.53	31.80	-
Pistachio Oil	-	15.40	19.92
Poppy-seed Oil	109.15	166.10	-
Pumpkin Seed Oil	-	32.86	49.71
Pumpkin Seed Oil	170.31	191.4	-
Pumpkin Seed Oil	61.16	54.70	-
Pumpkin Seed Oil	137.56	174.13	-
Rapeseed Oil	12.07	12.42	11.14
Rapeseed Oil	-	9.81	11.04
Rapeseed Oil	59.13	53.47	-
Rapeseed Oil	21.56	22.56	-
Rapeseed Oil	1.10	1.27	-
Rapeseed Oil	12.07	12.42	-
Rapeseed oil	32.15	33.50	-
Refined Sunflower Oil	113.69	98.10	-
Rice germ Oil	8.26	9.94	-
Safflower Oil	146.37	140.62	119.01
Safflower Oil	-	113.27	109.01
Safflower Oil	31.64	27.21	-
Safflower Oil	23.71	24.08	-
Safflower Oil	2.99	3.12	-
Safflower Oil	146.37	140.62	-
Sesame Oil	16.68	15.03	-
Sesame Oil	14.36	15.22	-
Soybean Lecithin	$<$ LOD	2.46	-
Soybean Oil	-	15.70	18.18
Soybean Oil	14.05	12.80	-
Soybean Oil	87.58	85.10	-
Soybean Oil	8.71	11.41	-
Sunflower Oil	17.60	16.44	19.96
Sunflower Oil	37.02	33.57	25.42
Sunflower Oil	-	19.79	25.42
Sunflower Oil	42.15	47.81	-
Sunflower Oil	2.76	2.78	-
Sunflower Lecithin	37.02	33.57	-

Sunflower Oil, refined	107.72	100.08	-
Unknown Oil	< LOD	0.78	0.82
Unknown Oil	144.42	144.30	-
Walnut Oil	-	11.88	18.74
Walnut Oil	127.68	123.10	-
Walnut Oil	4.59	4.48	-
Walnut Oil	146.86	144.98	-

Comment: Methods which have not been used for the analysis of an oil are marked with "-".

The mean deviation between the TPP NMR and, classical titration methods was 20%. These results confirmed the study outcome performed by Skiera et al. [172]. Using the paired t-test, a significant difference between the NMR methods and the titration (TPP-titration: t = 2.7979; holistic-titration: t = 4.2496) was detected. Regarding the TPP NMR method, small variations of the PV can be explained by the purity of TPP and the balance uncertainty. However, these parameters cause only small approximations which are estimated to around 1%. The widely used iodometric titration appears to have more limits. For instance, even minor modifications of the experiment conditions in temperature, solvent grade or analyst can influence the titration results significantly. Thus, the standard operating procedure must be carefully attended to receive reproducible results [166]. Furthermore, the visual determination of the end point is difficult due to the subjective assessment of the color change from dark blue to clear, which is even more challenging in pigmented oil samples like krill oil with its natural red color. In addition, the reaction itself shows some limitations. Iodine can also be formed by oxygen, which liberates iodine from the potassium iodine, and by being absorbed by unsaturated fatty acid bonds [171], [187]. These processes lead to an overestimation of the measuring PV. Another important parameter is the reaction time. Lea recommended a storage of 1 hour in the dark, whereas recent methods recommend a reaction time of 1 minute [163], [164], [165], [166]]. Apart from these limitations, the reaction process cannot be monitored so that cross-reactions can take place without being noticed. Since oils are natural products which are composed of a high number of substances, cross-reactions are possible during the titration with several ingredients. The advantage of the NMR spectroscopy is that the reaction of TPP and hydroperoxides is visible by observing disappearing hydroperoxide signals and growing alcohol signals in the ^{1}H NMR spectra (solvent: $CDCl_3$/DMSO-d_6); the method is selective and specific. Olive oils showed significantly higher deviations in the PV examined by the three methods than other oil samples did. It was demonstrated that in olive oil, the titration method consistently resulted in lower PV compared to the NMR methods (table 4.2). The difference was attributed to the influence of phytochemicals or antioxidants on the titration reaction [172]. Furthermore, the PV results obtained by titration were influenced by substances with a high number of double bonds, such as squalene in olive oil and/or astaxanthin in krill oil. Astaxanthin is a carotenoid which is present naturally in salmon oil in a maximum concentration in a range of 26-38 mg/kg [188]. In this study, it was verified that an addition of 0.4 μmol astaxanthin to a krill oil reduced the PV from 9.97 meq/kg

to 8.72 meq/kg, a loss of about 13%. This experiment indicated that a cross-reaction with astaxanthin took place during the titration. The PV results obtained using the TPP NMR method were not influenced by the concentration of astaxanthin. This experiment was an example of possible cross-reactions, representing for several possible cross-reaction partners. The aim of the research was not to determine all substances which influenced the titration results, but the example of astaxanthin showed that the titration is an error-prone technique. Thus, there is a need for alternative methods like the NMR spectroscopy.

4.4.4 Hydroperoxides in krill oil

Five krill/sunflower oil mixtures have been prepared, mixed with TPP and measured over a time period of 43 hours. Figure 4.8 presents a typical ^{1}H-{^{31}P} decoupled NMR spectrum of krill oil after the reaction with TPP. The signal of the non-reacted TPP was identified at δ = 7.35 ppm and the signal of the reaction product TPPO at δ = 7.70 ppm. In the 100% krill oil sample, an increase of PV of 3.3% was detected after 2 hours. In the 100% sunflower oil (0% krill oil) sample, the PV increased only up to 0.3% within 2 hours. Because krill oil is a complex mixture of TAG, phospholipids and characteristic substances such as astaxanthin, the driver of the higher oxidation was not identified. Nevertheless, the goal of the presented work was to develop an alternative method for the analysis of the PV in krill oil, and this goal was achieved. To obtain the most accurate PV results, it is recommended to run the peroxide analysis within 60 minutes after finishing the sample preparation.

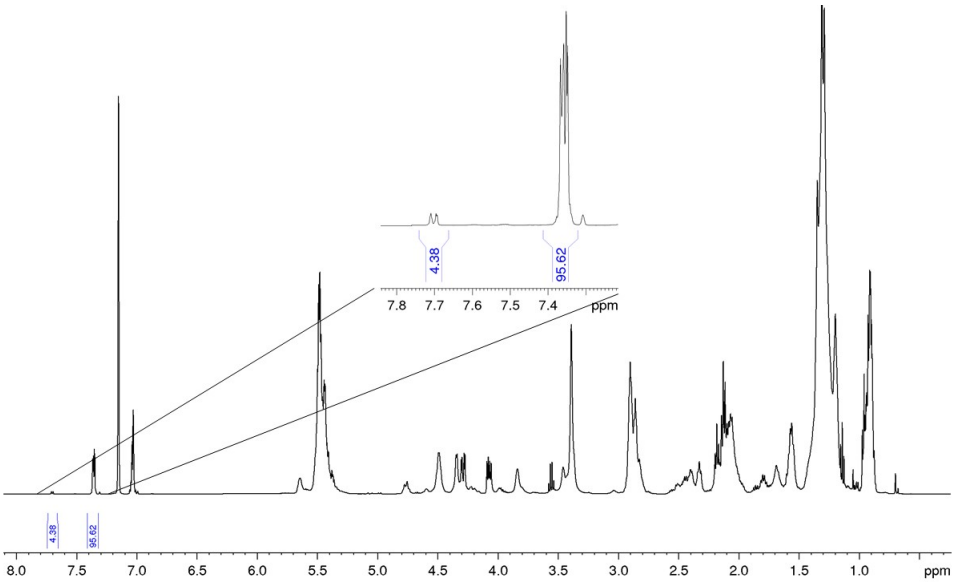

Figure 4.8: ^{1}H-{^{31}P} decoupled NMR spectrum of krill oil after reaction with TPP; in C_6D_6.

The quality of 24 individual krill oils was examined using the method parameters described herein (table 4.3). Krill oil contains a high number of phospholipids; thus, the Food and

Table 4.3: PV results of 24 krill oils determined by the TPP NMR method.

	PV [meq/kg]		**PV [meq/kg]**
Krill oil 1	8.51	Krill oil 13	1.32
Krill oil 2	2.87	Krill oil 14	10.08
Krill oil 3	5.31	Krill oil 15	7.15
Krill oil 4	9.97	Krill oil 16	10.42
Krill oil 5	3.36	Krill oil 17	8.73
Krill oil 6	5.07	Krill oil 18	9.68
Krill oil 7	4.74	Krill oil 19	7.76
Krill oil 8	3.10	Krill oil 20	1.81
Krill oil 9	4.41	Krill oil 21	1.30
Krill oil 10	5.23	Krill oil 22	2.27
Krill oil 11	1.17	Krill oil 23	1.63
Krill oil 12	3.87	Krill oil 24	1.88

Agriculture Organization of the United Nations and the World Health Organization states that the PV should be less than 5 meq/kg [**?**]. 13 of 24 krill oil samples showed PV $<$ 5 meq/kg, thus meeting the quality requirements. PV levels higher than 5 meq/kg were detected in 11 krill oils, thus failing the requirements. It should be noted that these 11 krill oil samples had been stored over a time period of 3 to 12 months at room temperature. However, previous studies showed that the PV analysis of krill oil using the AOCS method is challenging [164], [166], [189]. Furthermore, 10% to 90% of dietary supplements containing eicosapentaenoic acid (EPA) and docosahexaenoic acid (DHA) like krill oil were tested and reported to be non-compliance in the past decades [190]. Consequently, PV analysis is an essential part of quality control for krill oil.

4.5 Conclusions

NMR spectroscopy is a powerful analytical tool to determine the amount of peroxides quantitatively in vegetable and marine oils by using TPP as tagging reagent. The PV can be determined within 4 minutes with LOD and LOQ values of 0.1 meq/kg and 0.4 meq/kg, respectively. PV results obtained by the TPP NMR method and the titration method according to Wheeler showed significant differences, especially when analyzing olive oil where titration results showed consistently lower PV. During the titration, several external conditions as well as the matrix can have individual impacts on the reaction leading to wrong positive or negative PV results. Especially the composition of the analyzed oil is responsible for cross-reactions. As the matrix does not have any influence on the NMR TPP method and the validation of the method was successful, the NMR spectroscopy is stated as a reliable alternative to determine the PV in different kinds of oil products.

Chapter 5

Divalent Metal Cations

Original title: Qualitative and Quantitative ^{1}H NMR Spectroscopy for Determination of Divalent Metal Cation Concentration in Model Salt Solutions, Food Supplements and Pharmaceutical Products by Using EDTA as Chelating Agent [191] [Copyright (2020) Magnetic Resonance Chemistry]

Elina Hafer, Ulrike Holzgrabe, Katharina Kraus, Kristie Adams, James M. Hook, Bernd Diehl;
Magnetic Resonance Chemistry, 58: 653-665, 2020.

5.1 Abstract

This paper introduces an ^{1}H NMR method to identify individual divalent metal cations Be^{2+}, Mg^{2+}, Ca^{2+}, Sr^{2+}, Zn^{2+}, Cd^{2+}, Hg^{2+}, Sn^{2+}, and Pb^{2+} in aqueous salt solutions through their unique signal shift and coupling after complexation with the salt of ethylenediamine tetraacetic acid (EDTA). Furthermore, quantitative determination applied for the divalent metal cations Ca^{2+}, Mg^{2+}, Hg^{2+}, Sn^{2+}, Pb^{2+} and Zn^{2+} (LOQ: 5-22 μg/mL) can be achieved using an excess of EDTA with aqueous model salt solutions. An internal standard is not required since a known excess of EDTA is added and the remaining free EDTA can be used to recalculate the quantity of chelated metal cations. The utility of the method is demonstrated for the analysis of divalent cations in some food supplements and in pharmaceutical products.

Keywords
NMR spectroscopy, metal ions, EDTA, complexation, food supplements, pharmaceutical products

5.2 Introduction

Inorganic metal cations are essential for human health and can be found in numerous foods such as fruits and vegetables, mineral water [95], edible oils [192], and honey [193] but also in high concentrations in food supplements [194] and in pharmaceutical products for treating heartburn and stomach ailments [195]. Conversely, some metal ions have a negative impact on human health e.g., cadmium, mercury and lead. These so-called heavy metals are toxic and are known to bioaccumulate, becoming concentrated in fish and other shellfish as well as in plants (e.g. Cd from phosphate fertilisers); thus, ingesting seafoods with high concentrations of cadmium, mercury or lead should be avoided [196], [197]. For a long time, inorganic cations have been analyzed quantitatively using complexometric titration [198]. Generally, ethylenediaminetetraacetic acid (EDTA) is used as a chelating agent in a titration, where the end point is determined both visually by using an indicator such as eriochrome black T or xylenol orange and by voltammetry, using an electrode [199], [200], [201]. Because titration is sensitive to several parameters such as pH and temperature, these values usually need to be monitored and controlled continuously. In more recent decades, additional methods have been developed for flame atomic absorption spectrometry (F-AAS) [202], ion chromatography [203], and inductively coupled plasma atomic absorption or mass spectrometry (ICP-AAS/MS) [204] [205]. These techniques are advantageous due to their sensitivity, reliability and accuracy. However, there are significant drawbacks associated with these methods: they are time-consuming, require complex sample preparation, and some methods, like the titration technique, are non-specific. While nuclear magnetic resonance (NMR) spectroscopy is not as sensitive as some other analytical techniques, it is a powerful tool for providing a broad range of chemical information, including identification and quantification, within one relatively fast analytical measurement. NMR active nuclei such as magnesium, calcium, zinc, tin, mercury and lead can, in principle, be analyzed directly with ^{25}Mg NMR, ^{43}Ca NMR, ^{67}Zn NMR, $^{111/113}$Cd NMR, ^{199}Hg NMR and ^{207}Pb NMR spectroscopy. However, their sensitivities relative to ^{1}H NMR are extremely low (≤ 0.01) [206]. Consequently, the analysis by ^{1}H NMR spectroscopy, after derivatization with chelating agent, is a powerful alternative. NMR methods exploiting several nuclei have been developed with ^{1}H, ^{19}F and ^{31}P NMR spectroscopy. Intracellular calcium can be measured by ^{19}F NMR of symmetrically substituted difluoro derivatives of 1,2-bis(o-aminophenoxy)ethane-N, N, N',N'-tetra acetic acid (nFBAPTA) as chelators. Additional cations such as Mg^{2+}, K^{+}, and Zn^{2+} can also be identified in the ^{19}F NMR spectra after chelation with nFBAPTA [207]. Similarly, a quantitative ^{31}P NMR method for Mg^{2+} complexation with the four nucleoside phosphates adenosine diphosphate, guanosine diphosphate, cytidine diphosphate and uridine diphosphate, has also been reported. The binding of Mg^{2+} to the phosphate chain leads to a variation of the chemical shift δ_α of the signal of P_α the integral value of which can used to calculate the Mg^{2+}-concentration [208]. In contrast, the advantage of the ^{1}H NMR spectroscopy when compared with ^{19}F and ^{31}P NMR spectroscopy is, on the one hand, its inherently higher sensitivity, and, on the other hand, the additional information which can be extracted directly from the ^{1}H NMR spectrum such as the presence of other ingredients. Previous ^{1}H NMR methods using

EDTA for complexation of metal ions have demonstrated that, based on the chelated metal ion, the Metal-EDTA-complex showed characteristic signals with specific chemical shifts. Furthermore, the chemical shifts of free EDTA and chelated EDTA differ sufficiently make quantification possible by the addition of a known excess of EDTA [209]. This has been reported previously for quantifying Y^{3+}, Al^{3+}, Zn^{2+}, Cd^{2+} and Pb^{2+} using standard addition and calibration curves [210]. An internal standard was not needed because the amount of complexed EDTA is equal to the amount of metal ions present in the sample as presented by Somashekar who applied the simple pulse-acquire ^{1}H NMR method for the quantitative analysis of calcium and magnesium in human serum [211]. Based on this knowledge, a quantitative ^{1}H NMR spectroscopic method is now reported using EDTA for the routine determination of a wide variety of divalent metal cations (Be^{2+}, Mg^{2+}, Ca^{2+}, Sr^{2+}, Zn^{2+}, Cd^{2+}, Hg^{2+}, Sn^{2+}, Pb^{2+}) in model solutions of mineral salts, and then elaborated for application to their detection and quantification in authentic food and pharmaceutical products.

5.3 Method

5.3.1 Materials

Beryllium sulfate tetrahydrate ($BeSO4 \cdot 4\ H_2O$, assay $\geq$ 99.99 %) was purchased from Alfa Aesar, Magnesium chloride hexahydrate ($MgCl_2 \cdot 6\ H_2O$, assay $\geq$ 46.5 %) and calcium chloride ($CaCl_2$, assay $\geq$ 98.0 %) from Carl Roth, maleic acid, strontium chloride ($SrCl_2$, assay $\geq$ 99.99 %), barium chloride dihydrate ($BaCl_2 \cdot 2\ H_2O$, assay $\geq$ 99.0 %) and tin (II) chloride dihydrate ($SnCl_2 \cdot 2\ H_2O$, assay $\geq$ 99.995 %) from Sigma Aldrich (Merck), lead (II) nitrate ($Pb(NO_3)_2$, assay $\geq$ 99.999 %), cadmium chloride ($CdCl_2$, assay $\geq$ 99.99 %) and mercury (II) chloride ($HgCl_2$, assay $\geq$ 99.5 %) from Sigma-Aldrich, and zinc sulfate heptahydrate ($ZnSO_4 \cdot 7\ H_2O$, assay 99.5 – 103 %) from Fluka.

Ethylenediaminetetraacetic acid (EDTA, assay $\geq$ 99 %) from Carl Roth, cesium carbonate (Cs_2CO_3, assay $\geq$ 99.9 %) from Albemarle, deuterium oxide (D_2O, 99.90 %D) and 3-(trimethylsilyl)-propionic acid-d_4 Na-salt (TMSP) from Eurisotop were used to prepare the EDTA/D_2O stock solution.

A total of five different food supplements and two pharmaceutical products used to treat heartburn were purchased from supermarkets in Germany.

5.3.2 Sample Preparation

EDTA/D_2O Solution

The EDTA/D_2O stock solution was prepared by weighing EDTA (11 g) and dissolving in D_2O (200 mL) with 0.002% (w/v) of TMSP as a chemical shift reference. The pH of the solution was adjusted to 7.2 by addition of approximately 23 g of solid Cs_2CO_3.

Qualitative Analysis and T_1 Determination of Met-EDTA-complexes

Salts of magnesium, calcium, zinc, cadmium, mercury, tin and lead (5 to 20 mg) were dissolved separately in the EDTA/D_2O stock solution (1000.0 μL). After complete dissolution was achieved, the solution was transferred into a 5 mm NMR tube and measured by ^1H NMR spectroscopy.

Quantitative Analysis of Met-EDTA-complexes

The salts of magnesium, calcium, zinc, cadmium, mercury, tin and lead were dissolved in D_2O (10-20 mg/mL). Different quantities of the salt solutions, the stock solution EDTA/D_2O and D_2O were prepared as outlined in table 5.1 (n=3), and then transferred into 5 mm NMR tubes and measured by ^1H NMR spectroscopy.

Sample No.	**Salt solution [μL]**	**Stock EDTA/D_2O [μL]**	**D_2O [μL]**
1	400	600	0
2	200	300	500
3	100	150	750
4	100	100	800
5	50	100	850

Table 5.1: Sample Preparation for the Quantitative Analysis of Metal Ions

Water Samples

A standard solution of lead was prepared from lead nitrate (10 mg) in D_2O (2 mL). The artificial "lead-contaminated" water samples were prepared as presented in table 5.2, to which EDTA/D_2O stock solution (500.0 μL) was added.

Sample No.	**$Pb(NO_3)_2$-solution [μL]**	**H_2O [μL]**
1	500	0
2	300	200
3	100	400
4	50	450
5	10	490

Table 5.2: Preparation of Artificial "lead-contaminated" Water Samples

Food Supplements

The internal standard reference maleic acid (6 mg) and the food supplement product (10-20 mg) were dissolved in the stock EDTA/D_2O solution (1000.0 μL) and after complete dissolution, transferred into a 5 mm NMR tube measurement by ^{1}H NMR spectroscopy.

5.3.3 ^{1}H NMR Measurements

Qualitative and Quantitative Analysis of Metal Cations in Artificial Salt Solutions

The ^{1}H NMR spectra were recorded on an Avance III HD 500 NMR spectrometer (Bruker, Karlsruhe, Germany) equipped with a BBFO^{PLUS} SmartProbe, operating at 500.41 MHz, using the *"zg30"* pulse sequence. The acquisition parameters were: spectral width, 24 ppm; number of scans, 16; acquisition time, 5.45 s. The repetition delay was 1 s. The T1 was determined using the inversion recovery pulse program on all model salt solutions for the free and the complexed EDTA signals. The experiment was carried out at 298 K. Data was processed by using Bruker's TOPSPIN-NMR software version 3.5 (Bruker, Rheinstetten, Germany).

Quantitative Determination of Lead in Artificial "Lead-Contaminated" Water Samples

The ^{1}H NMR spectra were recorded using a water suppression pulse sequence (*zgcpgppr*) with the following acquisition parameters: spectral width, 24 ppm; number of scans, 16; relaxation delay, 1 s; acquisition time 5.45 s. The experiment was carried out and processed as above.

Intramolecular Exchange Processes of Met-EDTA-complexes

The ^{1}H NMR spectra were recorded using the *"zg30"* pulse sequence with the following acquisition parameters: spectral width, 24 ppm; number of scans, 16; relaxation delay; 1 s, acquisition time, 5.45 s. Spectra were measured after changing the temperature of the sample in 10 K increments from 278 K to 348 K. Data was processed as above.

5.3.4 Calculation

For the calculation of single metal ions equation 5.1 is used which is based on the well-known formula 5.2 for quantitative NMR spectroscopy (definition in table 5.3). Because of the 1:1 stoichiometry, 1 mole of the cation is chelated by 1 mole EDTA forming 1 mole EDTA-complex. Thus, the difference of the weighed and the analyzed amount of EDTA is equivalent to the amount of chelated EDTA and, thus the concentrations of cations. In equation 5.1 the amounts of chelated complexes and remaining free EDTA are compared

	Salt (Met-Salt)	**EDTA**	**Metal-EDTA Complex (Met-EDTA)**	**Internal Standard (IS)**	**Sample**
Molecular weight [g/mol]	$M_{Met-Salt}$	M_{EDTA}	$M_{Met-EDTA}$	M_{IS}	M_{Sample}
Initial Weight [mg]	$m_{Met-Salt}$	m_{EDTA}	$m_{Met-EDTA}$	m_{IS}	m_{Sample}
Content [%- by weight]	$P_{Met-Salt}$	P_{EDTA}	$P_{Met-EDTA}$	P_{IS}	P_{Sample}
Integral	$I_{Met-Salt}$	I_{EDTA}	$I_{Met-EDTA}$	I_{IS}	I_{Sample}
Number of atoms	$N_{Met-Salt}$	N_{EDTA}	$N_{Met-EDTA}$	N_{IS}	N_{Sample}

Table 5.3: Declaration of variables

by taking the integrals, number of protons, known weight of EDTA and the molecular weights into account.

$$m_{Met-salt} = \frac{\frac{m_{EDTA}}{M_{EDTA}} \cdot P_{EDTA} \cdot I_{Met-EDTA} \cdot \frac{N_{EDTA}}{N_{Met-EDTA}}}{I_{Met-EDTA} \cdot \frac{N_{EDTA}}{N_{Met-EDTA}} + I_{EDTA}} \cdot M_{Met-EDTA} \tag{5.1}$$

$$P_{Sample} = \frac{I_{Sample}}{I_{IS}} \cdot \frac{N_{IS}}{N_{Sample}} \cdot \frac{m_{IS}}{m_{Sample}} \cdot \frac{M_{Sample}}{M_{IS}} \cdot P_{IS} \tag{5.2}$$

In the cases of mixtures or spectra in which signals of the free EDTA were overlapping, the well-established qNMR equation 5.3 was used.

$$m_{Met-Salt} = \frac{N_{IS}}{N_{Met-EDTA}} \cdot \frac{I_{Met-EDTA}}{I_{IS}} \cdot \frac{M_{Met-EDTA}}{M_{IS}} \cdot \frac{P_{IS}}{P_{Met-EDTA}} \cdot m_{IS} \tag{5.3}$$

5.4 Results and Discussion

The ^{1}H NMR spectrum of free EDTA (figure 5.1, top) shows two singlets at δ =3.67 and 3.28 ppm, arising from the four acetate-methylene protons (-N-**C**$\mathbf{H_2}$-CO_2-), and the two backbone methylene groups (-N-**C**$\mathbf{H_2}$-**C**$\mathbf{H_2}$-N-), respectively. The integral ratio of these two signals is 2:1, respectively.

5.4.1 pH effect on the chemical shift of EDTA

At pH 7, EDTA is a Lewis base, with six potential binding sites: two tertiary amino groups which may donate two pairs of electrons to a metal ion, and four carboxylate groups. EDTA is a highly effective chelating agent, which complexes numerous metal cations with charges

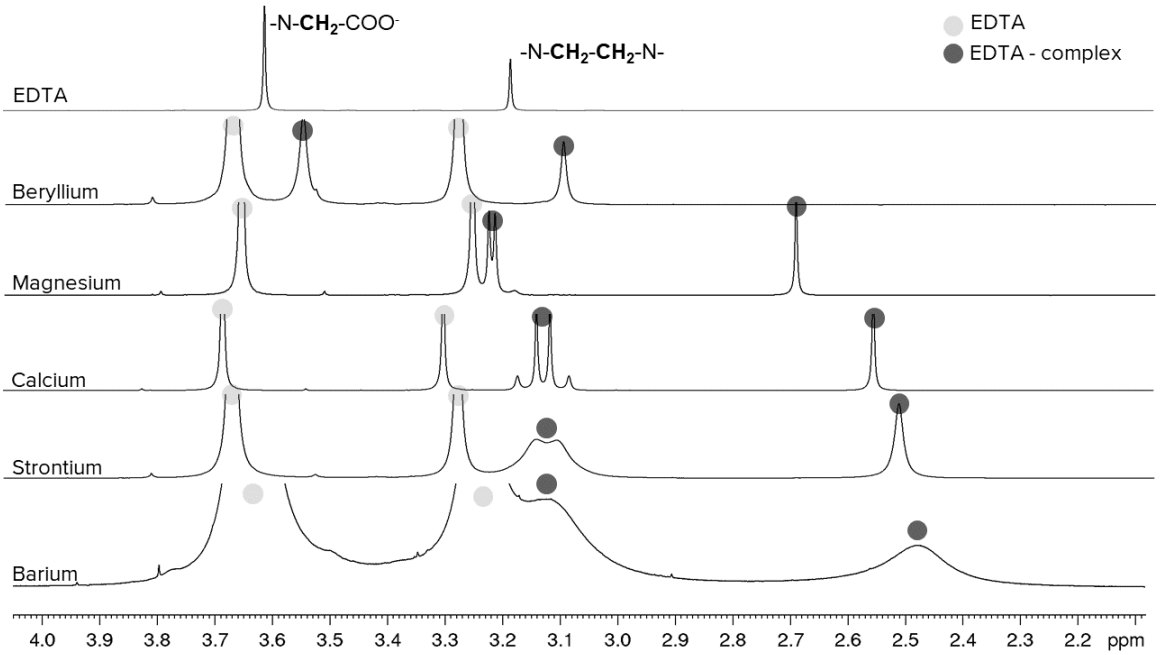

Figure 5.1: 500 MHz ^{1}H NMR spectra of EDTA (pH 7.20) and periodic group 2 metal cations after EDTA complexation.

+1 forming a cage-like structure around the metal ion with 1:1 stoichiometry (figure 5.2) [212].

Depending on the pH of the solution, EDTA can be present in six protolysis levels. The first four protolysis steps depend on the carboxylic group (pKs of 0.0, 1.5; 2.0; 2.66) and the following two levels on the amine group (pKs of 6.16, 10.24) [213], [214]. Thus, increasing the pH of the solution leads to a high field shifting of the EDTA signals in the ^{1}H NMR spectrum due to these negative charges. Once the process of protonation or deprotonation is completed, the EDTA signals do not shift further (figure 5.3).

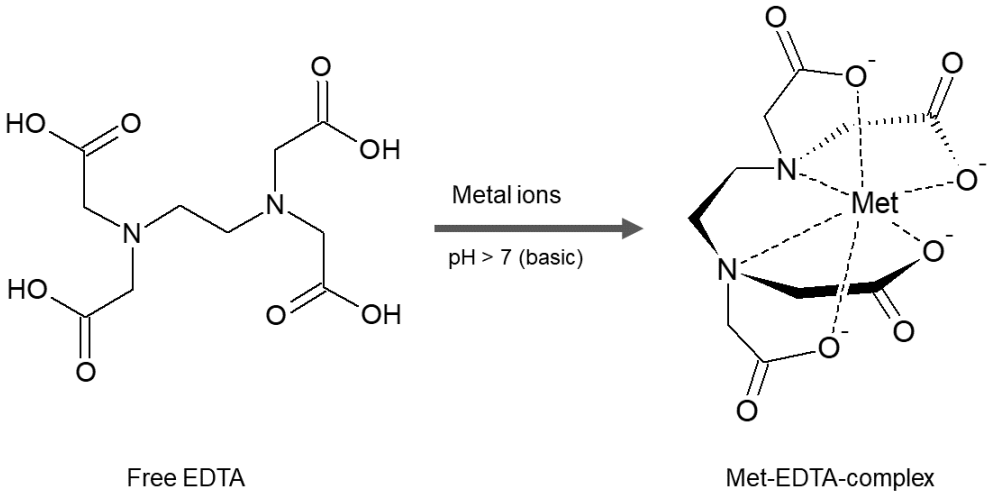

Figure 5.2: Complexation of metal ions by EDTA [206], [210].

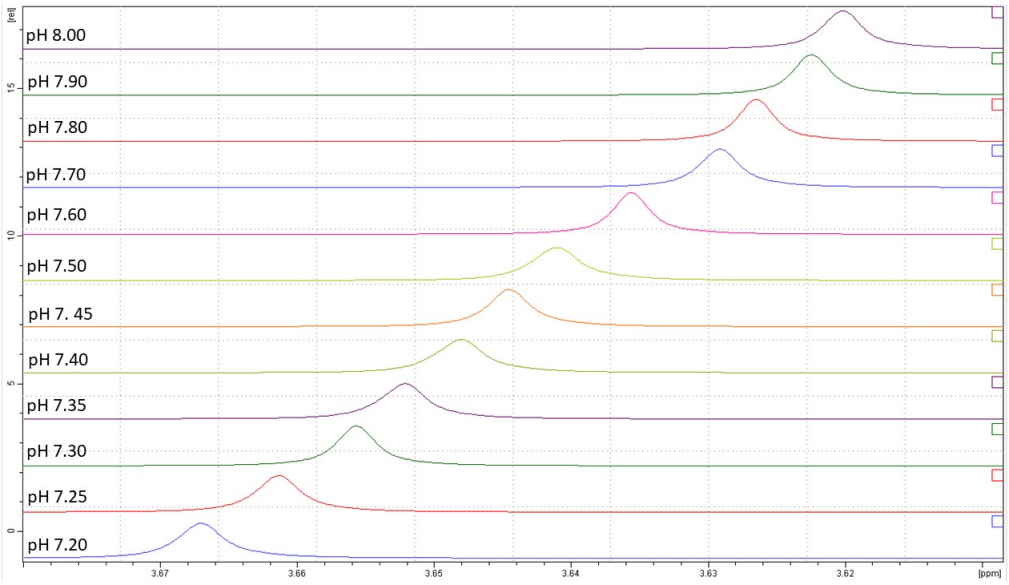

Figure 5.3: 500 MHz ^{1}H NMR spectra of EDTA in D_2O, from pH 7.20 to 8.00; edited to show the -CH_2CO_2- only.

5.4.2 Qualitative Analysis of Metal Ions and Intramolecular Exchange Processes of Met-EDTA-complexes

It is well known that EDTA forms octahedral coordination complexes with divalent cations. These water-stable metal ion EDTA complexes (abbreviated to "Met-EDTA-complex") produce specific ^{1}H NMR signal patterns, depending on the specific metal cation involved in the coordination complex [215]. The ^{1}H NMR spectra of Be-, Mg-, Ca-, Sr-, Ba-, Zn-, Cd-, Hg-, Sn-, and Pb-EDTA complexes are shown in figures 5.4, 5.5, 5.6 with the respective signal assignments collected together in table 5.4. Based on the thermodynamic stability, and therefore the dissociation constant, the complexes do not show any processes of dissociation, protonation or deprotonation under the existing conditions, so that signals of the Met-EDTA-complex do not change. Thus, in contrast to the signals of the free EDTA, the signals of the chelated EDTA are unique, as presented in figure 5.7. In each NMR spectrum, there are two signals of the free EDTA and two signals of the Met-EDTA-complex, respectively, which can be separately identified. Upon complexation, the methylene protons in the N-$\mathbf{CH_2}$-$\mathbf{CH_2}$-N-groups which appear as singlets (δ = 2.48 ppm – 3.14 ppm), and the four acetate-methylene protons (N-$\mathbf{CH_2}$-CO_2^-) appear as AB patterns or single lines, both of which are shifted to δ = 3.08 ppm – 3.55 ppm, except the four acetate-methylene protons of Pb-EDTA which are shifted to δ = 3.71 ppm. The two methylene protons each have different chemical environments due to restricted rotation of the acetate-methylene groups (N-$\mathbf{CH_2}$-CO_2^-) in most of the EDTA-complexes leading to different chemical shifts, v_A and v_B. Thus, a well resolved AB spin pattern is observed for EDTA complexes of Mg^{2+}, Ca^{2+}, Zn^{2+}, Cd^{2+}, Hg^{2+}, Sn^{2+}, and Pb^{2+}. The J-couplings of the Met-EDTA complex which contained cations of the elements with a spin of 1/2 were presented in table 5.5.

	δ (-N-$\mathbf{CH_2}$-$\mathbf{COO^-}$) [ppm]	δ (-N-$\mathbf{CH_2}$-$\mathbf{CH_2}$-N-) [ppm]
Free EDTA	3.67	3.28
Be-EDTA-complex	3.54	3.10
Mg-EDTA-complex	3.22	2.70
Ca-EDTA-complex	3.13	2.57
Sr-EDTA-complex	3.12	2.52
Ba-EDTA-complex	3.12	2.48
Zn-EDTA-complex	3.37	2.88
Cd-EDTA-complex	3.27; 3.23; 3.08; 3.05	2.71
Hg-EDTA-complex	3.18	2.68
Sn-EDTA-complex	3.55	3.02
Pb-EDTA-complex	3.71	3.14

Table 5.4: 500 MHz ^{1}H NMR signal assignment of Met-EDTA-complexes at pH=7.2

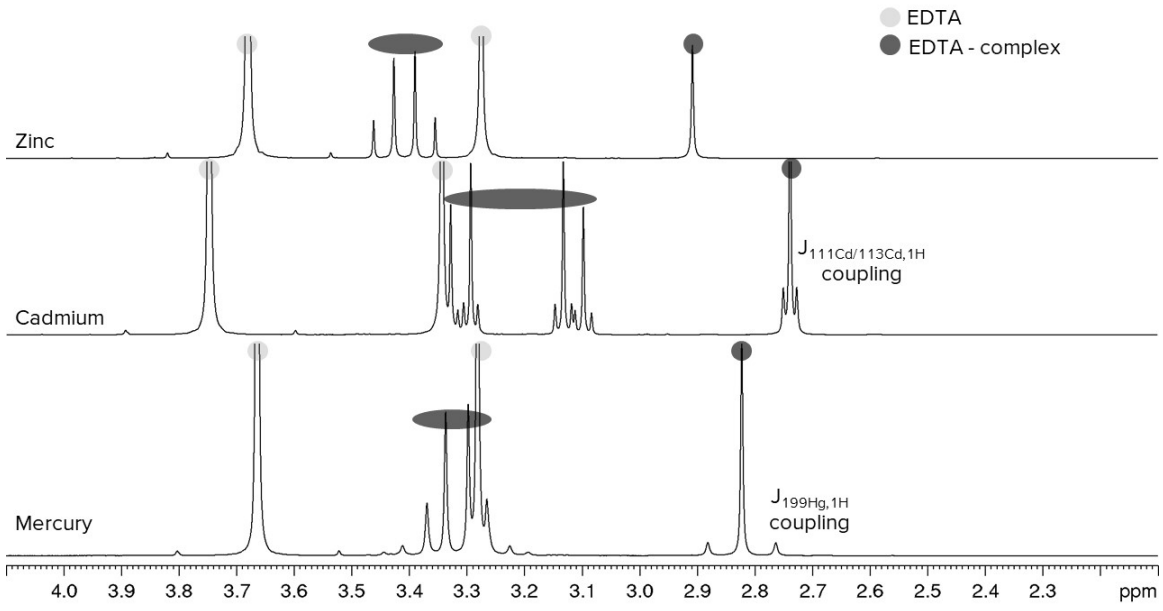

Figure 5.4: 500 MHz ^{1}H NMR spectra of periodic group 12 metal cations after EDTA complexation.

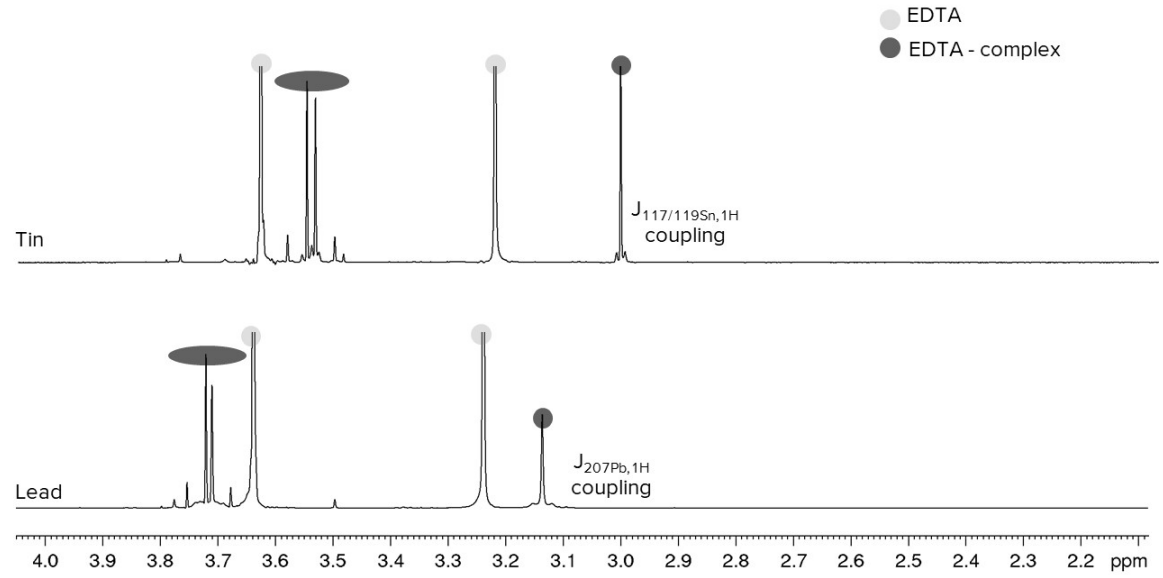

Figure 5.5: 500 MHz ^{1}H NMR spectra of periodic group 14 metal cations after EDTA complexation.

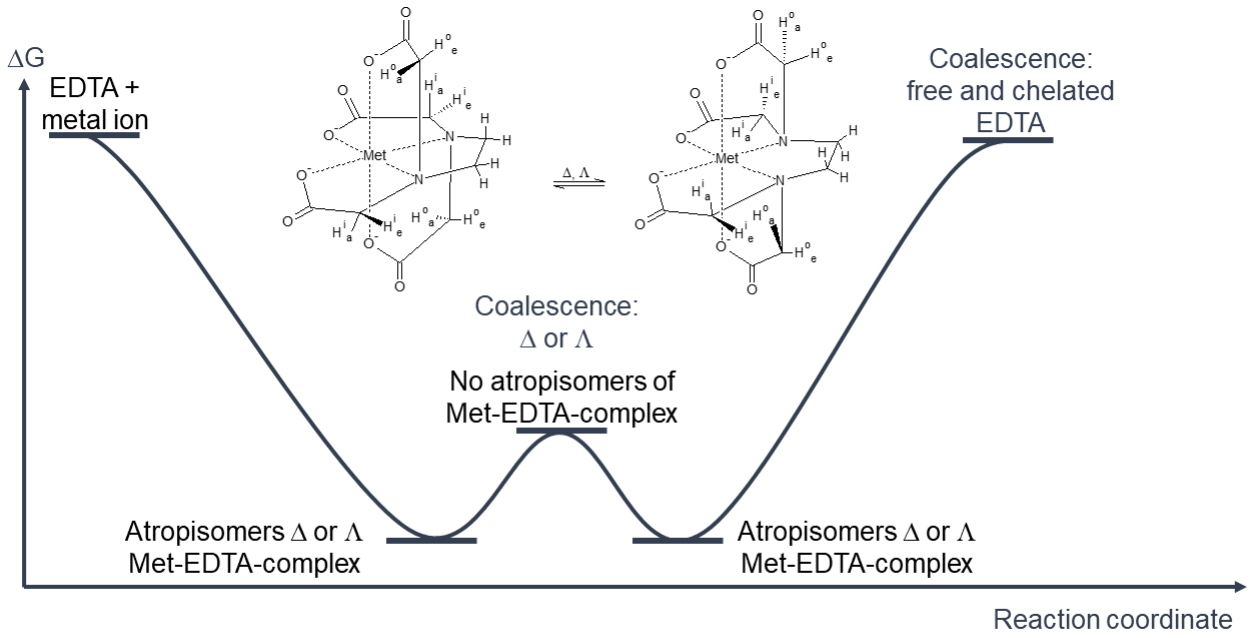

Figure 5.6: Free energy diagram of the complexation of metal ions using EDTA as chelating agent with the respective Δ and Λ configurations of the Met-EDTA-complexes [206], [210].

500 MHz	δ (^{1}H) [ppm]	$\lvert^{2}$J (^{1}H-^{1}H)$\rvert$ [Hz]	$\lvert^{3}$J (^{m}X-^{1}H)$\rvert$ [Hz]	Figure
^{113}Cd-EDTA	3.16 2.71	5.85 / 6.81 -	11.71 / 13.61 11.11	figure 5.8
^{119}Sn-EDTA	3.55 3.02	16.54 / 16.59 -	2.90 / 4.14 7.19	figure 5.5
^{199}Cd-EDTA	3.18 2.60	16.17 / 16.47 -	35.96 / 37.99 58.99	figure 5.4
^{207}Pb-EDTA	3.18 2.68	15.98 / 16.39 -	37.89 59.05	figure 5.5

Table 5.5: 500 MHz ^{1}H NMR signal assignment of Met-EDTA-complexes at pH=7.2

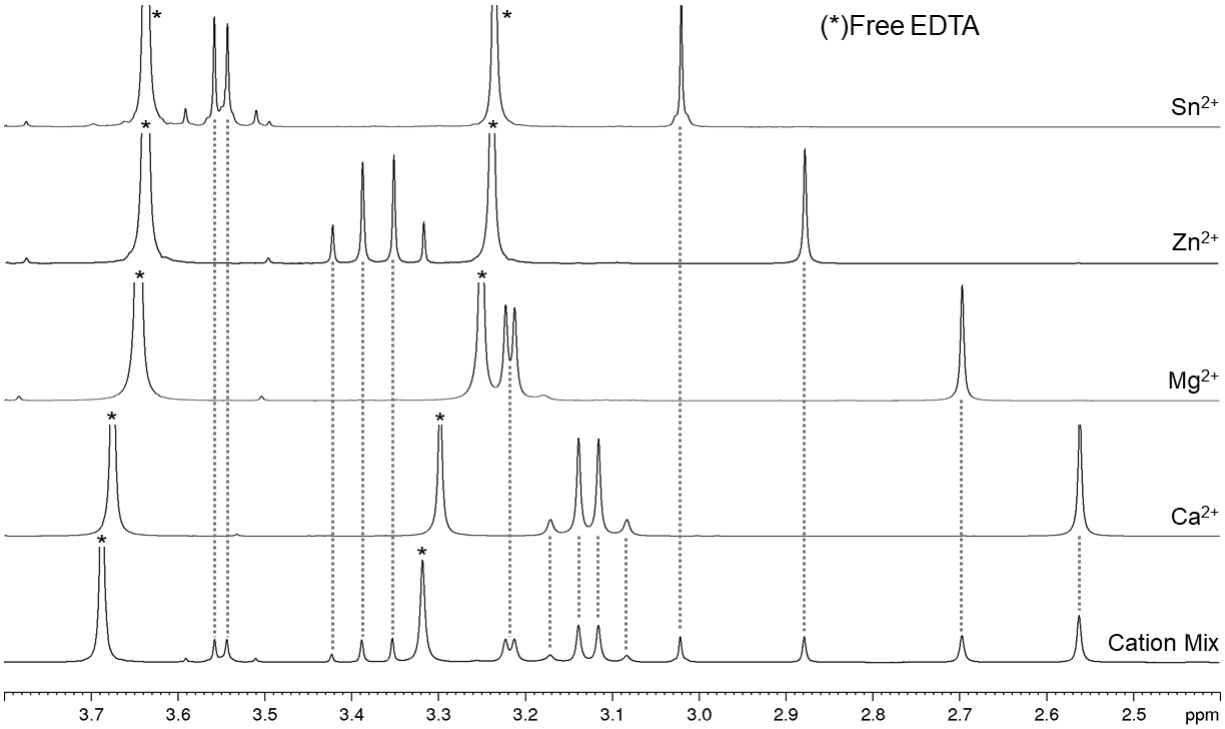

Figure 5.7: 500 MHz ^{1}H NMR spectra of a metal cation mixture after complexation with EDTA.

Because of the restricted rotation, the Met-EDTA-complex is present in two different configurations, Δ and Λ, as presented by Gennaro, Mirti and Casalino (figure 5.6) [209]. A specific definition of Δ and Λ is not made because they are enantiomers behaving as mirror and mirror images. In each confirmation, the protons are oriented in different directions: out-of-plane axial (H_o^a), out-of-plane equatorial (H_o^e), in-plane axial (H_i^a) and in-plane equatorial (H_i^e), see figure 5.6. In the absence of any intramolecular exchanges an AB quartet can be identified in the ^{1}H NMR spectrum of Met-EDTA-complex. Since enantiomers show identical signals in the NMR spectra, Δ and Λ cannot be distinguished.

When the reaction is slow on the NMR time scale, no chemical exchange occurs:

$$k << \pi \frac{\Delta v}{\sqrt{2}} \tag{5.4}$$

where k is the interconversion rate constant and Δ is the separation of the NMR signals.

By increasing the measurement temperature a faster exchange of free EDTA and chelated Met-EDTA-complexes (EXSY NMR spectrum not presented) as well as an interconversion of the two configurations Δ and Λ occur which can be identified as a signal broadening or even a collapse of the AB spin system in the ^{1}H NMR spectra (figure 5.9, page 80).

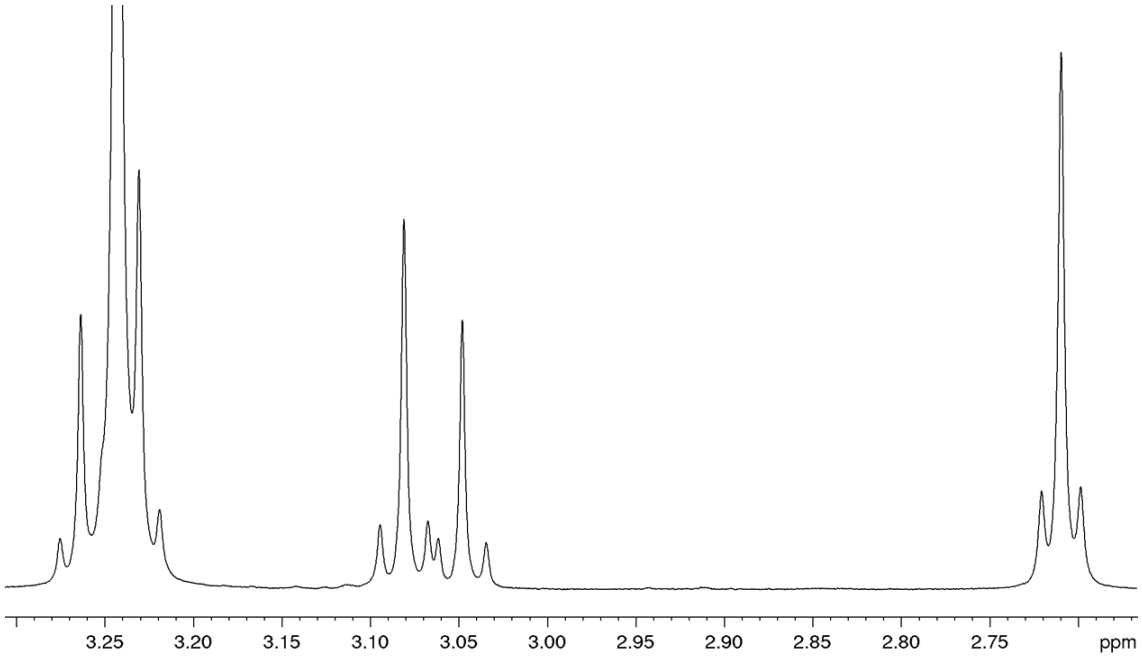

Figure 5.8: 500 MHz ^{1}H NMR spectrum of a Cd-EDTA-complex.

At high temperatures a broad singlet results at the weighted average chemical shift of the two conformers, Δ and Λ. The temperature at which this occurs, depends on the metal ion complexed. Here, the first-order interconversion rate constant can be calculated using the following equation:

$$k_{T_c} << \pi \frac{\Delta v}{\sqrt{2}} \tag{5.5}$$

where k_{T_c} is the rate constant at the coalescence temperature, T_c [26]. At even higher temperatures, coalescence of the free and chelated EDTA NMR signals occurs, resulting in one very broad singlet for the protons in the N-$\mathbf{CH_2}$-$\mathbf{CH_2}$-N-unit and another singlet for the N-$\mathbf{CH_2}$-CO_2-unit (figures 5.6, 5.9). The temperatures of the different states and rate constants depends on the chelated metal ion and, thus, the signal shapes vary for each Met-EDTA-complex at different temperatures. To explain the interconversion, we measured ^{1}H NMR spectra of the Hg-EDTA complex at several different temperatures (figure 5.9). At 278 K, the complex was "frozen", and a well-resolved AB pattern is observed with a linewidth at full width and half maximum (FWHM) of 3.4 Hz. A 30 K increase in temperature (308 K) results in a comparable FWHM linewidth. An additional 20 K increase in temperature (328 K) causes an increase of 7 Hz of the FWHM linewidth. These results clearly demonstrate the increase of the exchange rate of the complex states Δ and Λ with temperature.

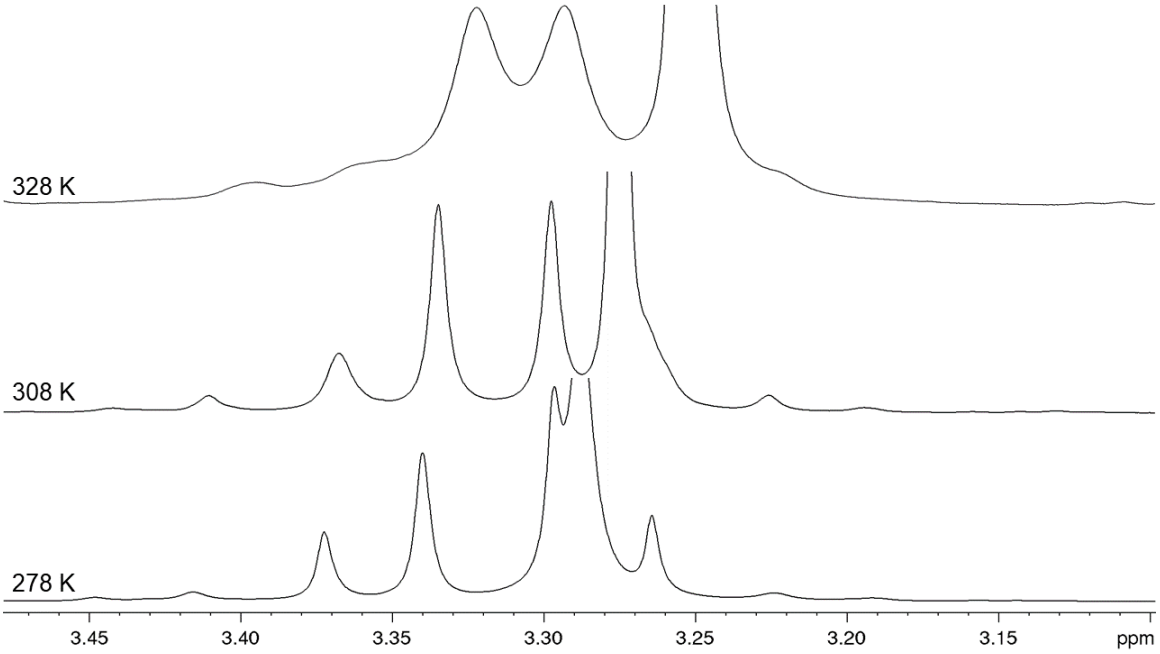

Figure 5.9: Comparison of 500 MHz ^{1}H NMR spectra of the Hg-EDTA-complex at T = 278 K, 308 K and 328 K.

As presented in figure 5.1, the Sr-EDTA-complex showed a broad signal at T = 298 K, due to exchange between the Δ and Λ states, resulting in broader signals moving towards coalescence. The Ba-EDTA-complex showed two broad singlets (figure 5.1). Here, the AB spin system collapsed completely since the exchange between the configuration Δ and Λ was too fast for being measured by ^{1}H NMR spectroscopy. The same, but less pronounced effect was detected in the Be-EDTA-complex (figure 5.1). Thus, the quantification of Sr^{2+}, Ba^{2+}, and Be^{2+} was not possible by using EDTA as a chelating agent in ^{1}H NMR spectra at room temperature. Met-EDTA-complexes which showed broadened signals at T = 298 K needed to be analyzed at lower temperatures than 298 K to slow down the exchange rate in order to "freeze" the signals. However, since the goal was to develop a quantitative method for metal ion analysis as a routine measurement at room temperature, only magnesium, calcium, zinc, cadmium, mercury, tin and lead were analyzed quantitatively in single-salt solutions and also in mixtures of divalent cations.

5.4.3 Quantitative Analysis of Metal Ions in Artificial Salt Solutions

Quantification of the metal ion concentration was performed by adding an excess of the stock EDTA solution without inclusion of an internal standard reference material. Comparing the initial amount and the non-complexed amount of EDTA results into the determination of the amount of the metal complex and, thus, the amount of the cation. For qNMR calculations of Ca^{2+}, Mg^{2+}, Hg^{2+}, Pb^{2+} and Zn^{2+}, the NMR signals of the free

EDTA and of the Met-EDTA-complex were integrated. Based on 1:1 stoichiometry, the content of the metal ion can be calculated by equation (1) [22]. In the case of mixtures of different metal ions or if the signal of the free EDTA was overlapped with other signals such as those from the matrix, the addition of an internal standard, here maleic acid, was required. Equation (2) was used to calculate the metal ion concentration. Ca^{2+}, Mg^{2+}, Hg^{2+}, Pb^{2+} and Zn^{2+} quantitatively in separate solutions, and the results are presented in table 5.5. Using the sample preparation conditions outlined in Section 2.2.3, LOQs were found to be between 5 and 22 μg/mL. These values were higher than the LOQ values obtained by another NMR method which was developed to quantify cations in mineral water with LOQs of 1.39 mg/L for Ca^{2+} and 0.87 mg/L for Mg^{2+} [95], and by flame AAS and ion chromatography [202], [216]. However, to achieve a lower LOQ, several options are possible. On the one hand, the amount of EDTA can be decreased to reduce the excess, and thus, the signal of the Met-EDTA-complex will be relatively stronger. Furthermore, by increasing the number of scans (ns) and by using more sensitive probes will lead to a lower value for LOQ.

Quantification of the metal ions required measuring the T1 values of both free EDTA and the respective Met-EDTA-complex, and these were determined to be between 350 ms to 650 ms. Thus, an acquisition time of 5.45 with a D1 time of 1 sec is sufficient for a full relaxation of all NMR signals to be quantified (D1 $>>$ 5 x T1).

The ^{1}H NMR spectra of the Met-EDTA-complexes showed linearity between 0.1 mg/L and 20 mg/L. The regression coefficients of the calibration curves were between 0.9979 and 1 for Ca^{2+}, Mg^{2+}, Hg^{2+}, Sn^{2+}, Pb^{2+} and Zn^{2+}. However, as presented by Monakhova et al. the linearity range of Ca^{2+} and Mg^{2+} was determined up to 500 mg/L, as long as EDTA is present in an excess [95]. Comparable values were obtained for nominal and measured concentrations, as shown in table 5.6. 58 % of the analyses showed a lower difference of the nominal and measured value of 3 %; 21 % differed by 1 %. All differences were observed with less than 9% deviation, which are comparable to those presented by Monakhova et al. [95].

Table 5.6: Quantification of $CaCl_2$, $HgCl_2$, $MgCl_2$, $Pb(NO_3)_2$, $ZnSO_4$ (n = 3)

Salt	Nominal value [mg/mL]	Measured value [mg/mL]	Deviation [%]	$LOQ_{ns=16}$ [μg/mL]
$CaCl_2$	8.00	8.04	0.50	6
	4.00	3.98	0.52	
	2.00	2.03	1.49	
	1.00	1.01	1.51	
	0.50	0.51	1.17	
$HgCl_2$	8.28	8.38	1.21	14
	4.06	4.21	3.53	
	2.03	2.12	4.60	
	1.02	1.02	0.27	
	0.51	0.45	-9.00	
$MgCl_2$	8.78	8.75	-0.34	5
	4.29	4.27	-0.34	
	2.14	2.17	1.46	
	1.07	1.08	1.16	
	0.54	0.55	2.67	
$Pb(NO_3)_2$	9.54	8.91	-6.60	22
	4.77	4.54	-4.82	
	2.01	2.10	4.30	
	1.01	1.09	1.99	
	0.50	0.52	8.05	
$ZnSO_4$	8.08	8.41	4.08	10
	4.04	4.20	3.96	
	2.02	2.09	3.47	
	1.01	1.08	6.90	
	0.50	0.52	4.00	
$SnCl_2 \cdot 2\ H_2O$	4.08	4.10	0.52	11
	2.04	2.03	-0.52	
	1.02	0.99	-1.76	
	0.51	0.49	-4.80	
$CdCl_2$	4.03	4.14	2.76	8
	2.02	2.07	2.66	
	1.01	1.04	3.44	
	0.50	0.51	2.19	

5.4.4 Application in Artificial Samples: Quantitative Analysis of Lead in Water

Artificial "lead-contaminated" water samples in a concentration range of 0.05 to 2.53 mg/mL Pb(NO3)2 were analyzed. A comparison of the ^{1}H NMR spectra of a 0.31 μM and 15.25 μM aqueous lead solutions is presented in figure 5.10. The quantitative nominal and real values are presented in figure 5.11. As observed, the values were comparable, showing higher deviations at lower concentrations. In 2013, the concentration limit of lead in potable water was set to 0.010 mg/L (= 0.000010 mg/mL) in Germany [217]. These low concentration levels of lead in potable water have been recommended also by the World Health Organization (WHO) [218]. Because of the LOQ of Hg of 0.05 mg/mL, this NMR method as detailed here is not sensitive enough for quantifying lead in solution at concentrations considered unsafe for human consumption.

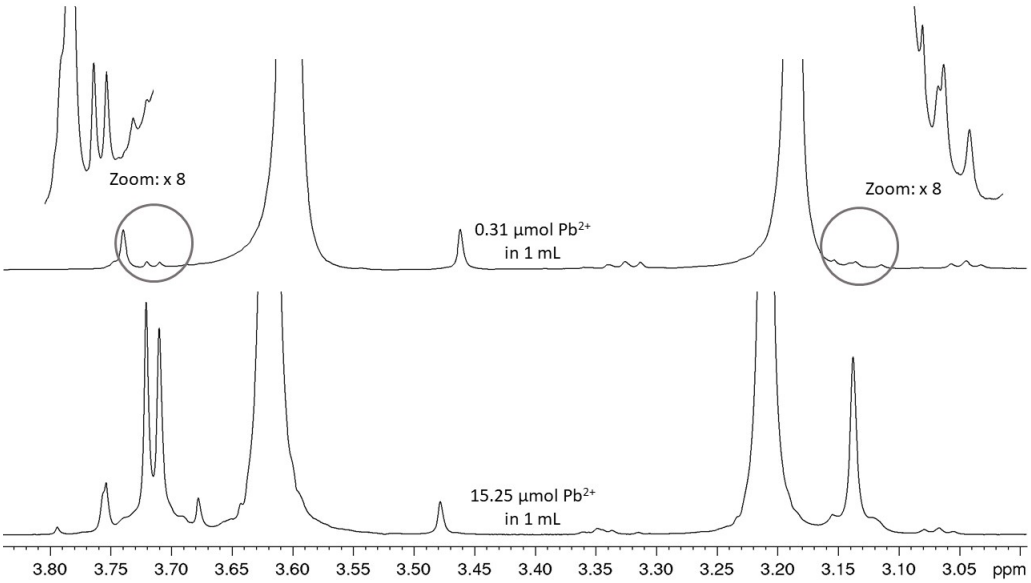

Figure 5.10: 500 MHz ^{1}H NMR spectrum of 15.25 μM (bottom) and 0.31 μM Pb^{2+} in 1 mL water (top), with a water suppression sequence.

5.4.5 Application to Commercial samples: Quantitative Analysis of Metal Ions in Food Supplements and Pharmaceutical Products

The qNMR results for determining the Ca^{2+}, Mg^{2+} and Zn^{2+} concentrations in five food supplements and two pharmaceutical products against heartburn are summarized in table 5.7. The ^{1}H NMR spectrum of the heartburn sample, after complexation with EDTA is shown in figure 5.12, and are clearly arising from the Ca (major) and Mg (minor) chelates.

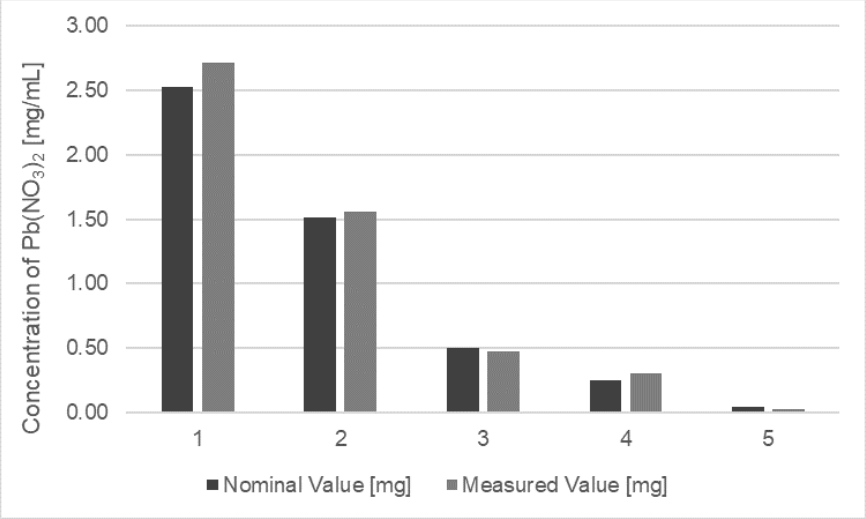

Figure 5.11: Quantification of $Pb(NO_3)_2$ in artificial "lead-contaminated" water.

The chemical shifts of the signals of the Met-EDTA-complexes did not differ from those presented in table 5.7. However, based on the high amount of carbonate in the product, the solution showed a higher pH value, and thus, the signal of the free EDTA shifted to 3.17 ppm. The quantitative results showed a broad variation in metal cation content ranging from 3.63 w/w-% to 57.51 w/w-% for Ca^{2+}, from 1.43 w/w-% to 5.64 w/w-% for Mg^{2+}, and from 0.03 w/w-% to 5.09 w/w-% for Zn^{2+}. Thus, the application of this ^{1}H qNMR method can be justified for products containing wide-ranging amounts of calcium, magnesium and zinc. The higher deviations can be explained to a large extent by the labelled amount of Ca^{2+}, Mg^{2+} and Zn^{2+}. Because the concentrations of these metal cations were labelled as "amount per tablet", the variation of the tablet weight leads to a higher deviation of the nominal and measured values. Furthermore, using this ^{1}H qNMR method, the total cation amount, e.g. Mg^{2+}, was determined. However, some products contained more than one magnesium-containing ingredient such as combined with citrate, or in the form of the oxide. Due to the different molecular weights of these two forms of magnesium and the unknown ratio of these substances, the calculation of the real value contained a higher deviation. Samples which contained only one substance with the respective metal cation showed lower deviations between the nominal and the real value. Taking these uncertainties into account, the nominal and real values were present in a comparable concentration range.

Sample	Metal ion	Nominal value [w/w-%]	Measured value [w/w-%]
Granulate with minerals	Ca^{2+}	5.43	5.04
	Mg^{2+}	1.31	1.94
Multivitamins (Peach)	Ca^{2+}	2.79	3.63
Multivitamins (Sport)	Ca^{2+}	5.80	7.38
	Mg^{2+}	5.80	3.82
	Zn^{2+}	0.07	0.03
Stomach pastilles	Ca^{2+}	41.67	44.62
Heartburn product	Ca^{2+}	51.22	57.51
	Mg^{2+}	3.77	1.43
Multivitamins (Mg)	Mg^{2+}	4.29	5.64
Granulate with Zinc	Zn^{2+}	4.09	5.09

Table 5.7: Quantification results of calcium, magnesium and zinc content by ^{1}H qNMR [w/w-%]

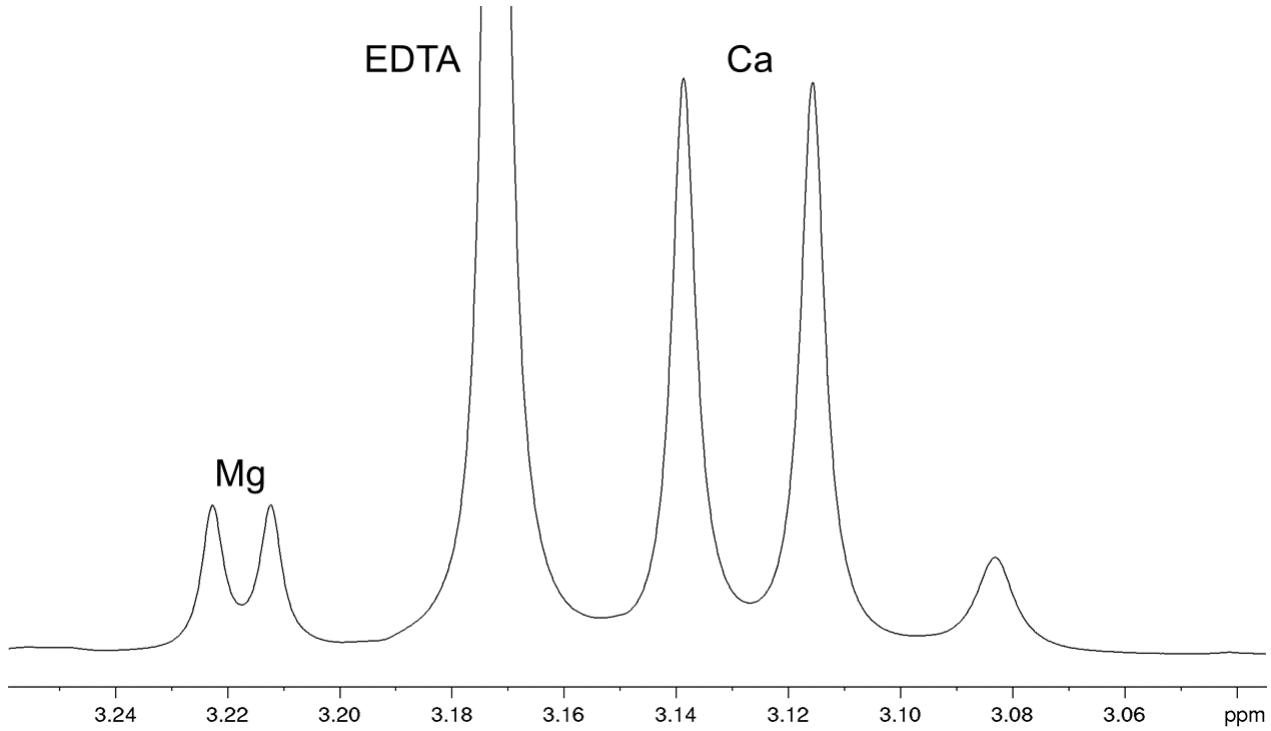

Figure 5.12: 500 MHz ^{1}H NMR spectrum of heartburn product in D_2O after complexation with EDTA.

5.5 Conclusions

It is well-known that EDTA forms octahedral coordinated complexes with divalent metal cations which can be distinguished by their individual fingerprint in the ^{1}H NMR spectra. In this study, ^{1}H NMR spectroscopy was presented as a powerful tool for the qualitative analysis of Be^{2+}, Mg^{2+}, Ca^{2+}, Sr^{2+}, Ba^{2+}, Zn^{2+}, Cd^{2+}, Hg^{2+}, Sn^{2+}, and Pb^{2+} and the quantitative determination of Ca^{2+}, Mg^{2+}, Hg^{2+}, Sn^{2+}, Pb^{2+} and Zn^{2+} (LOQ: 5-22 μg/mL) by using an excess of EDTA. Since EDTA serves as the complexation agent and simultaneously as the internal standard, an additional internal standard is not required. By the addition of a known amount of EDTA, salts of Be^{2+}, Mg^{2+}, Ca^{2+}, Sr^{2+}, Ba^{2+}, Zn^{2+}, Cd^{2+}, Hg^{2+}, Sn^{2+}, and Pb^{2+} can be identified in all aqueous samples. As an application, the quantitative analysis of Ca^{2+}, Mg^{2+}, and Zn^{2+} in food supplements and pharmaceutical products was chosen. The concentrations of Ca^{2+}, Mg^{2+}, and Zn^{2+} analyzed were in a comparable concentration range to that which was claimed on the label of the product. This application is just one of a broad range of possible applications for the quantification of divalent charged cations by ^{1}H NMR spectroscopy, in chemicals, food and pharmaceutical products. The presented EDTA derivatization is a method which could be adopted for benchtop NMR spectrometer in future. The titration by EDTA to examine metal ions is a technique which is often taught in universities where the titration end point is determined visually by indicators or voltammetry by electrodes [199], [200], [201]. The use of NMR spectroscopy in this respect has an educational-didactical reason purpose because it also enables the analysis of the reaction and the dynamics of the Met-EDTA-complexes.

Chapter 6

Enantiomeric Excess

A Rapid ^{13}C NMR Assay for Enantiomeric Excess of Alcohols by using Phosgene as Tagging Agent

Elina Hafer, Ulrike Holzgrabe, Bernd Diehl; unpublished

6.1 Abstract

A ^{13}C NMR technique for the quantitative determination of the enantiomeric excess of menthol, borneol, 1-phenylethanol and linalool by use of ^{13}C-labelled phosgene as derivatization reagent was described. The derivatization formed RR/SS and meso carbonate diesters whose carbon signals were separated, whereby in the presented study the carbonyl signals were used for quantification. Discrimination was studied by analyzing artificial mixtures of the enantiomers of the tested chiral alcohol menthol. The developed method was used for the quality control of further alcohols such as borneol, 1-phenylethanol and linalool. The ^{13}C NMR method is quantitative in the determination of enantiomeric excess with LOQ $> 99.5\%$.

6.2 Introduction

Stereoisomers are substances with the same molecular formula and connectivity but a different spatial arrangement of atoms [219]. Enantiomers are chiral molecules which are mirror images of each other, so they represent non-superimposable stereoisomers with identical chemical and physical properties in an achiral environment. Because living organisms are themselves chiral, the behavior of each of the enantiomers of a chiral drug can vary in vivo. In other words, the R-enantiomer of a drug can behave differently than the S-enantiomer of the same chiral drug in human body [220], [221]. Thalidomid is a well-known example where the S-enantiomer shows teratogenic properties in contrast to the R-enantiomer which is sedetive and harmless [222]. This drug disaster demonstrates the need of discrimination

and quantification of enantiomers in the asymmetric synthesis and pharmaceutical industry. Following the global trend of producing primary eutomers instead of racemates has brought the need of the analysis of the enantiomeric excess (ee) [223], [224]. Over the years several analytical methods have been developed to distinguish between the enantiomers: liquid chromatography (LC), gas chromatography (GC) and capillary electrophoresis (CE) [225], [226], [227], [228], [229]. Among the stereodiscrimination methods, nuclear magnetic resonance (NMR) spectroscopy represented a powerful tool for the analysis of the enantiomeric purity. Chiral derivatizing agents (CDAs), and chiral shift reagents (CSRs) with chiral solvating agents (CSAs) as subset are the most frequently used approaches for the determination of the enantiomeric ratios by NMR spectroscopy [230]. CSAs associate with the enantiomers through non-covalent interactions between the CSA and the compound of interest leading to chiral recognition via the formation of diastereomers or via different association constants. Since CSAs generally undergo fast exchanges with the analyte, there are numerous methods where CSAs are used in routine analysis [230]. To outline just one example, Wolf et al. presented an enantioselective ^{1}H NMR method by using 3,5-dinitrobenzoyl-derived amide as a CSA for the analysis of tertiary alcohols exhibiting proximate amide, nitro, and amino functions [231]. CSRs, as subset of CSA, are complexes of a lanthanide metal and a chiral ligand, whereby lanthanides induce large chemical shifts without excessive broadening of the lines [232], [233]. Viswanathan and Toland applied Tris[3-trifluoromemylhydroxyrriethylene)-(+)-camphorato]ytterbium(lll), known as *Yb(tfc)*$_3$, as a chiral lanthanide shift reagent to assess the optical purity of 1-phenylethylamine by ^{1}H NMR spectroscopy. The addition of Yb(tfc)$_3$ resulted in the formation of diastereomers which were distinct in their chemical shifts in ^{1}H and ^{13}C NMR spectra [234]. By using CDAs covalent bonds between the CDA and the enantiomers are formed resulting in diastereomers which are often analyzed by ^{1}H or ^{13}C NMR spectroscopy [230]. One of the most widely applied CDAs for the derivatization of alcohols and amines is the Mosher reagent (α-methoxy-α-trifluoromethylphenylacetic acid, Mosher's acid, MTPA) which allows the analysis of enantiopurity by ^{1}H and ^{19}F NMR spectroscopy due to the presence of the trifluoromethyl group (figure 6.1) [235].

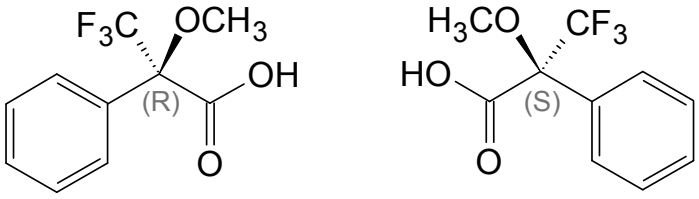

Figure 6.1: Chemical structure of (R)-Mosher's acid (left) and (S)-Mosher's acid (right).

The main drawback of MTPA is its chiral purity. MTPA can be purchased with an enantiomeric ratio of $\leq 99.5 : 0.5$ which is determined by chiral gas chromatography as labelled by the manufacturer [237]. Since the relative content of the enantiomer of interest depends on the enantiomeric purity of the derivatization reagent, the content of the examined enan-

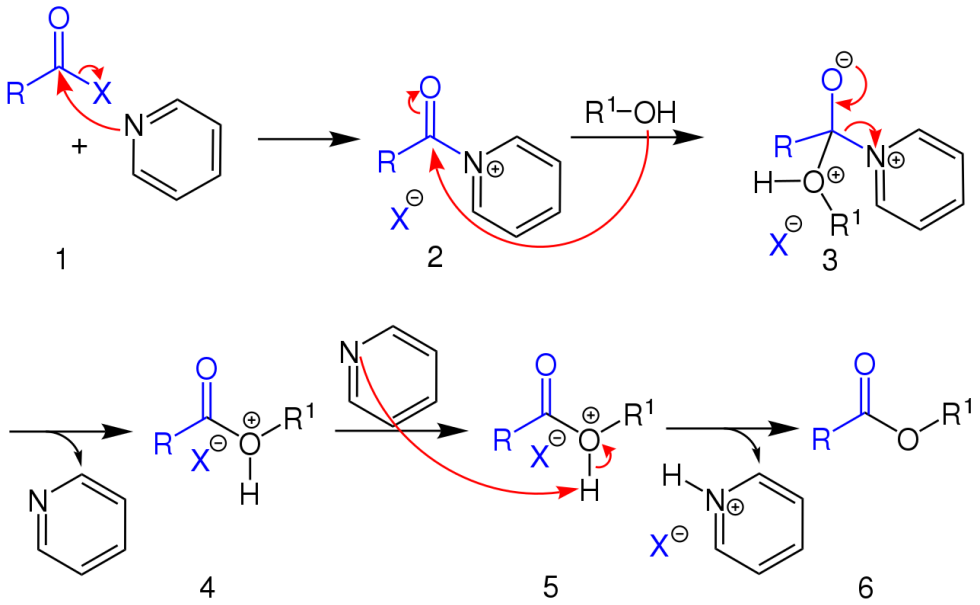

Figure 6.2: Einhorn acylation reaction mechanism of an alcohol with a carboxylic acid halide forming esters [Material has been modified [236]].

.

tiomer cannot be analyzed below an enantiomeric ratio of 0.5% by using MTPA. Thus, the demand of an alternative derivatization reagent to examine enantiomeric ratios of less than 0.5% is tremedous.

In this research, the focus is on the stereochemical analysis of alcohols. Chiral alcohols belong to an important substance class in natural and pharmaceutical products, and their enantioselective recognition represents a challenging task. To overcome this challenge and the limitation of MTPA, phosgene was examined as an alternative derivatization reagent. The reaction of alcohols using anhydrides or carboxylic acid halides in a tertiary amine such as pyridine was reported for the first time in 1898 by Alfred Einhorn and Friedrich Hollandt [238]. The reaction is called "Einhorn acylation" and it is a variant of the Schotten-Baumann method [239]. As shown in figure 6.2, the tertiary amine acts as a nucleophilic acylation catalyst and as an acid scavenger in the Einhorn acylation reaction. Initially, a nucleophilic attack on the carbon atom takes place, **1** while the halogen is split off. The next nucleophilic attack takes place through the hydroxide group of the alcohol **2**. As a result, the pyridine can split off again **3** and is ready for the uptake of the hydrogen proton **5**, which can be split off from the cationic reagent **4**. The alkylated product can then be separated [238], [240].

It is well known that phosgene reacts with R- and S-alcohols forming the respective chloroformates in the first step following the reaction constant k_r and k_s, respectively (figure 6.3) [241], [242]. Carbonates are formed as a result of further reaction of alcohol and

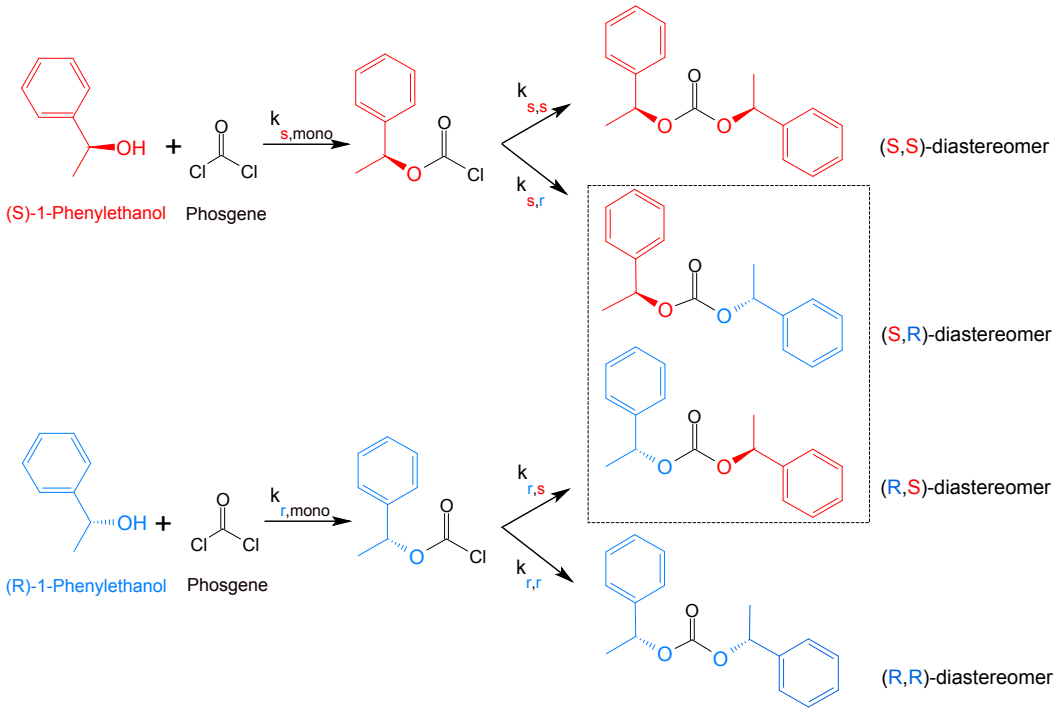

Figure 6.3: Reaction of (R)- and (S)-1-Phenylethanol with phosgene forming RR/SS diastereomers and RS/SR as *meso* compound (highlighted box), according to [241] and [242]

.

chloroformate [243]. To carry out the research study following five alcohols were explored (figure 6.4): **(1) menthol**, a monoterpene which is used as L-menthol in numerous pharmaceuticals, oral health care products, cosmetics, and tobacco products due to its flavor and cooling-anesthetic effect [244], [245]; **(2) borneol**, which is widely used in herbal medicine and whose isomers (+)- and (-)-borneol show different effects on pharmacokinetics of osthole [246]; **(3) 1-phenylethanol**, which is often used in the chemical industry as an intermediate block whose enantiomers (R)-1-phenylethanol and (S)-1-phenylethanol show different activities [247], [248], and **(4) linalool**, which is one of the most important substances to the perfume and flavor industries due to its fruity-fresh odor. Linalool has a stereogenic center at C3 and is found in two stereoisomeric forms in several plant species: as (R)-(-)-linalool, also known as licareol, in lavender, and as (S)-(+)-linalool, also known as coriandrol, in coriander [249]. The enantiomeric distribution of linalool is an important criterium for the quality control of essential oils. The chirality evaluation is routinely performed by the use of GC or multidimensional gas chromatography/mass spectrometry (MD-GC/MS) [250], [251]. In this work, the application of ^{13}C NMR spectroscopy in combination with ^{13}C-labelled and non-labelled phosgene as derivatization reagent has been evaluated for the determination of enantiomeric ratio measurement purposes for the mentioned alcohols.

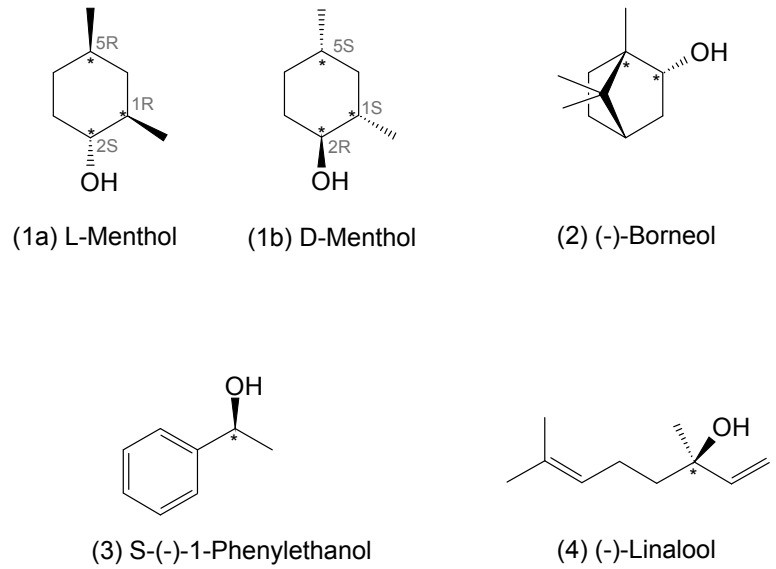

Figure 6.4: The chemical structures of chiral molecules investigated: **L-Menthol**, also known as **Levomenthol** (1a) and **D-Menthol** (1b), **(-)-Borneol** (2), **(S)-1-Phenylethanol** (3) and **(-)-Linalool** (4).

6.3 Method

6.3.1 Materials

Phosgene (15-wt% in toluene, non-labelled), ^{13}C-labelled phosgene (1.0 M in toluene), (-)-L-menthol, (-)-borneol, 1-phenylethanol and (-)-linalool were purchased from Sigma Aldrich (MERCK), (+)-D-menthol from TCI, deuterated pyridine (pyridine-d_5, 99.50 atom% D) and benzene (C_6D_6, 99.50 atom% D) from Euriso-top.

6.3.2 Sample Preparation

Method development with non-labelled phosgene

An appropriate amount of the substance of interest, which was calculated based on the molar 2:1 chemical reaction (60 mg – 90 mg), was dissolved in 1 mL benzene (C_6D_6) and 50 μL pyridine-d_5. 200 μL non-labelled phosgene was added.

Quantitative determination of ee with ^{13}C-labelled phosgene

The sample preparation was performed as described in *Method development with non-labelled phosgene*. For the quantification ^{13}C-labelled phosgene was used instead of non-labelled phosgene.

Menthol mixtures

Several menthol mixtures were prepared by mixing L-menthol and D-menthol in the following molar ratios (n=3): 100.00%; 99.86 %; 99.45%; 99.37 %; 99.04%; 98.63%; 98.08%; 97.07%; 96.02%; 89.61%; 79.62%; 69.65%; 59.68%; 53.33%; 51.52%; 50.62%; 49.71%; 49.94%; 47.90%; 46.09%; 43.38%; 36.14%; 27.09%; 16.69%; 9.03%; 4.51%; 3.61%; 2.71%; 1.80%; 0.90%; 0.45%; 0.18%, 0.00% L-menthol.

6.3.3 Experimental NMR Analysis

The ^{13}C NMR spectra were recorded on an NMR spectrometer Avance III HD 500 (Bruker, Karlsruhe, Germany) BBO Prodigy cryo probe, operating at 125 MHz and Avance III HD 600 (Bruker, Karlsruhe, Germany) BBO cryo probe, operating at 151 MHz. The acquisition ^{13}C NMR parameters were: spectral width 259 ppm, number of scans $\geq$ 256, relaxation delay 1 s, acquisition time 3.36 s.

6.4 Results and Discussion

The substances 1 to 5 in figure 6.4 reacted fast with phosgene, the derivatization agent, by using quantities of deuterated pyridine as a base to neutralize the by-product hydrogen chloride [252]. During the reaction chloroformate esters are formed in the first step and carbonate diesters in the second step. Since the alcohols are present as an R- or an S-enantiomer, diastereomeric esters are formed as RR, SS or meso (RS and SR, respectively). Some signals are influenced significantly by the configuration leading to two splitted signals in the ^{13}C NMR spectrum: a RR/SS signal and a meso signal. In this work the carbonyl signals were used for the quantification. Both carbonyl signals were integrated by deconvolution. If the reaction rate constants of the formation of the RR/SS and meso diastereomers are comparable, the curve and the respective equation in figure 6.5 are used for the determination of the molar amount and, thus of the ee (equation 6.1) [253].

$$ee[\%] = \frac{R - S}{R + S} \cdot 100 \tag{6.1}$$

In figure 6.5 the nominal correlation of the molar amount of the higher concentrated enantiomer and the integral of the RR/SS diastereomers was presented. Prerequisite was that the reaction constant k_r is equal k_s. If the interaction between the enantiomers R and R (or S and S) is not equal the interaction between R and S, a kinetic resolution will be identified where one diastereomeric formation is preferred leading to a different curve with a different equation. In this case, the lower the ee, the higher is the effect of a potential preference and, therefore the diastereoselectivity is leading to wrong calculation results. The maximum preference effect exists in racemic mixtures. Thus, the higher the ee is, the lower is

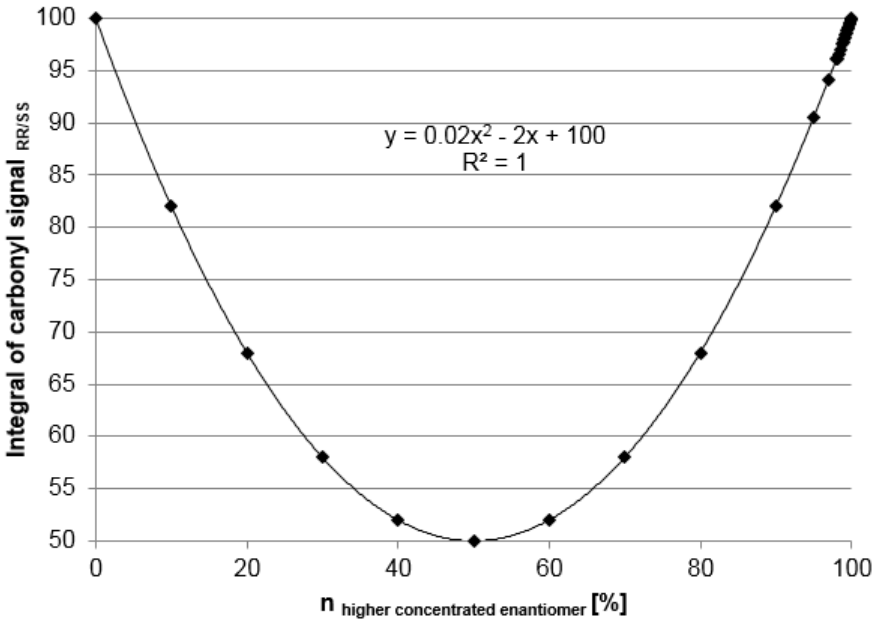

Figure 6.5: Quantification of the molar amount of the higher concentrated enantiomer n [%] by using the integral of RR/SS signal.

the influence of deviating reaction rates. Consequently, the presented method is applicable for alcohols with a high enantiomeric purity. Furthermore, the presented method does not present an approach to determine the absolute configuration. If the higher concentrated enantiomer is known, the concentrations of the R- and S-enantiomer are measurable. Otherwise, only the ee can be quantified without an assignment of the concentration of the respective enantiomer.

6.4.1 Menthol

To investigate the derivatization method, menthol (molecule **1**, figure 6.4) was used as a testing compound. Menthol is cheaply available in its enantiomerically pure natural (-)-L-form and the synthetic (+)-D-form, as well as a racemate. Menthol reacted with phosgene forming chloroformate esters in the first step and carbonate diesters in the second step (figure 6.6). Since menthol contains three chiral centres at C1, C2 and C5 (marked with *), the (1R,2S,5R)-menthol is called (-)-L-menthol and the (1S,2R,5S)-menthol is called (+)-D-menthol (figure 6.4). The derivatization of a mixture of L-menthol and D-menthol with phosgene forms LL/DD and LD/DL diastereomers, respecively, whereby the derivatized LD/DL menthol carbonate diesters are *meso* compounds. Meso compounds contain at least two chiral centers, but they are achiral because of the present internal mirror plane which makes them "superposable" on its mirror image. Before preparing artificial mixtures of natural L-menthol and synthetic D-menthol, the absolute chemical purity of both menthol samples was determined by means of quantitative NMR (qNMR) which has been described

and applied many times [22], [148]. The pre-tests to develop a powerful method as well as the quantification tests of ee $< 97\%$ were performed with the non-labelled phosgene. To increase the sensitivity, ^{13}C-labelled phosgene was used as derivatization reagent for the quantification of ee $\geq 97\%$. The advantage of the derivatization with ^{13}C-phosgene is a higher signal-to-noise ratio (S/N) and thus, a higher precision of the quantification values. Indeed, the qNMR results confirmed a chemical purity of 99.9% for D-menthol and 99.6% for L-menthol. The enantiopurity was examined by using the developed ^{13}C NMR method. D- and L-menthol were derivatized, respectively, with 200 μL phosgene and pyridine-d_5 as nucleophilic acylation catalyst and acid scavenger, forming carbonate diester (figures 6.6 and 6.7).

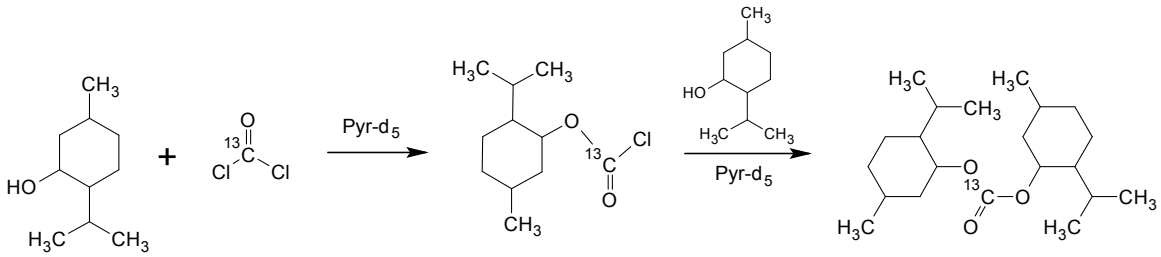

Figure 6.6: Formation of the menthol carbonate diester by using ^{13}C-phosgene as a derivatization reagent.

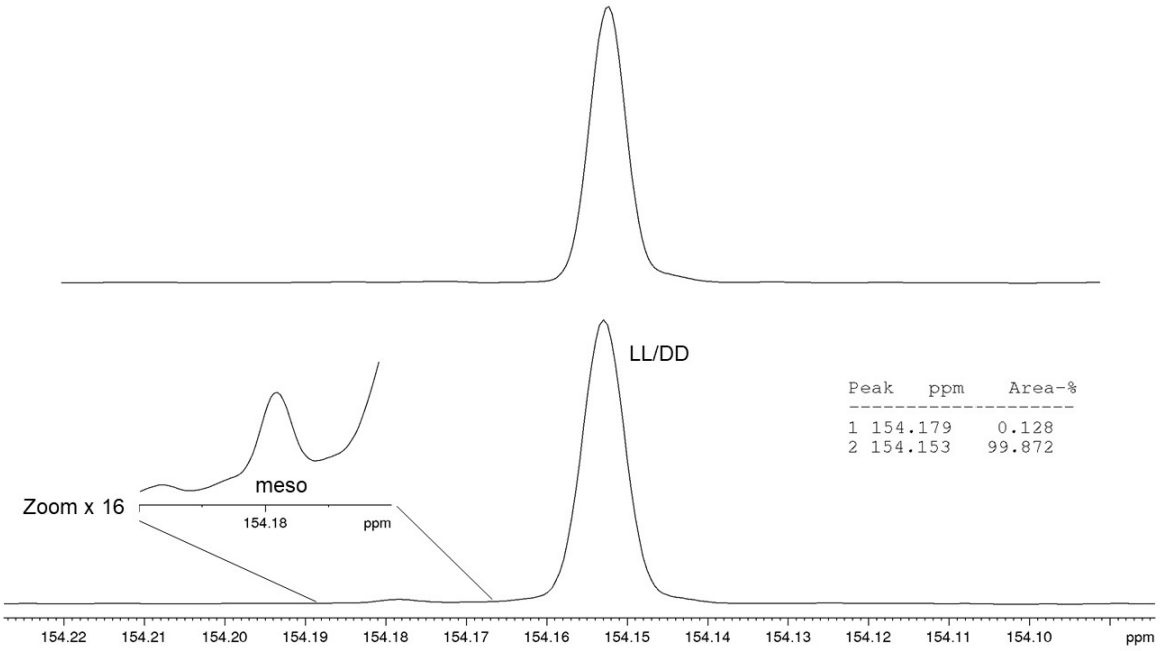

Figure 6.7: ^{13}C NMR spectra of the menthol carbonate diesters after the reaction of natural L-menthol (top) and synthetic D-menthol (bottom) with phosgene.

If the enantiopurity was less than 100%, DD-, LL-, DL- and LD-ester products were formed whose ^{13}C NMR signals were splitted into the DD/LL-form and the DL/LD-form. Here, the DL/LD-form is a meso form because it is "superposable" on its mirror image. After the derivatization of L-menthol no ^{13}C NMR signals were splitted, thus, it was stated that L-menthol was 100% entantiopure, as labelled (figure 6.7, top). In the case of D-menthol, the derivatization resulted in splitted signals which implied that the synthetic D-menthol was not enantiopure. Since good resolution is required to attain optimal results upon quantification of diastereomers in a mixture, non-overlapped signals with a large $\Delta\delta$ ($\Delta\delta = |\delta_{meso} - \delta_{DD/LL}|$) should be used for the integration. In this study, it was decided to perform the quantification on the carbonyl signal. The carbonyl signal of LL/DD menthol carbonate diester was shifted to δ =154.15 ppm and of the meso menthol carbonate diester to δ =154.18 ppm (figure 6.7, bottom), resulting in a $\Delta\delta = 0.03$ ppm. A signal separation of only 0.03 ppm was a very small separation when compared to the full ^{13}C NMR spectrum range of 200 ppm. Nevertheless, this separation is more than sufficient for the purpose of discrimination and quantitation. The separated carbonyl signals were integrated by using deconvolution. The concentration of L-menthol in D-menthol was calculated by means of a six-fold determination using the equations 6.2 to 6.9. It was calculated that D-menthol contained 1.60% L-menthol (RSD = 4.40%). Thus, the ee was determined with 96.80% which confirmed the labelled value of ee = 96%. The results of the D/L ratio and the chemical purity where implied to obtain the true theoretical (= nominal) ee value when preparing a series of different mixtures of L-menthol and D-menthol by starting from 100% to 0% L-menthol in D-menthol.

Quantification Equations

The quantification is based on the measurements shown in figure 6.5 and 6.9. The quantification of actual n of L-menthol based on carbonyl integral value is based on the general formula (figure 6.9, equation in green).

Quantification of actual n [mol] of L-menthol based on weighed amount

$$n_{L-menthol,nominal}\ [mol] = \frac{m_{L-menthol}}{M_{L-menthol}} \tag{6.2}$$

Quantification of nominal ee based on weighed [mol] of L-menthol

$$ee_{nominal}\ [\%] = \left|\frac{n_{D-menthol} - n_{L-menthol}}{n_{D-menthol} + n_{L-menthol}}\right| \cdot 100 \tag{6.3}$$

Quantification of actual n [%] of L-menthol based on carbonyl integral value

The carbonyl integral value is based on a quadratic equation, where x represents an unknown, and the coefficients of the equation a, b, and c represent known numbers, respectively, with a $\neq 0$. a represents the quadratic coefficient, b the linear coefficient and c the constant [254].

$$y = a \cdot x^2 - b \cdot x + c \tag{6.4}$$

To solve the equation, different techniques can be applied. Here, the *reduced quadratic equation* is presented, where the quadratic coefficient is reduced to one and y to zero. This produces the reduced quadratic equation (equation 6.5).

$$0 = x^2 + p \cdot x + q \tag{6.5}$$

To solve the reduced quadratic equation, equations 6.6 and 6.7 are used [254].

$$p = \frac{b}{a} \tag{6.6}$$

$$q = \frac{c - y}{a} \tag{6.7}$$

A quadratic equation has two solutions. The quadratic formula for the solutions of the reduced quadratic equation is presented in equation 6.8 and 6.9, respectively [254].

$$x_1\ [\%] = -\frac{p}{2} \pm \sqrt{\left(\frac{p}{2}\right)^2 - q} = -\frac{b}{c \cdot 2} + \sqrt{\left(\frac{b}{c \cdot 2}\right)^2 - \frac{c - y}{a}} \tag{6.8}$$

$$x_2\ [\%] = -\frac{p}{2} - \sqrt{\left(\frac{p}{2}\right)^2 - q} = -\frac{b}{c \cdot 2} + \sqrt{\left(\frac{b}{c \cdot 2}\right)^2 - \frac{c - y}{a}} \tag{6.9}$$

In our case, x is the molar amount n in percentage. Solving the quadratic equation leads to two molar amounts n_1 (equation6.8) and n_2 (equation 6.9).

Quantification of actual n [%] of D-menthol

The information about the enantiomer of the higher concentration is essential for the equation 6.10, where n_1 (equation 6.8) or n_2 (equation 6.9) are taken as $n_{L-menthol}$.

$$n_{D-menthol}\ [\%] = 100\% - n_{L-menthol}[\%] \tag{6.10}$$

Quantification of actual ee

To calculate the actual ee the actual $n_{L-menthol}$ is used as well as equation 6.10.

$$ee_{actual}\ [\%] = \frac{n_{D-menthol} - n_{L-menthol}}{n_{D-menthol} + n_{L-menthol}} \cdot 100 \tag{6.11}$$

Quantitative Determination of ee of artifical menthol mixtures

Artificial mixtures of L-menthol and D-menthol were prepared by mixing 100% to 0% L-menthol in D-menthol. By decreasing the amount of one menthol enantiomer and increasing the amount of the other menthol enantiomer, the integral of the ^{13}C NMR signal of the meso carbonate diester increased and the signal of the LL/DD-product decreased until the integral values were equal, and then the signal of the LL/DD diastereomer increased and the meso signal decreased (figure 6.8). The splitted carbonyl signals were quantified by using deconvolution. The quantification was performed as explained above, and the nominal and actual ee values were compared.

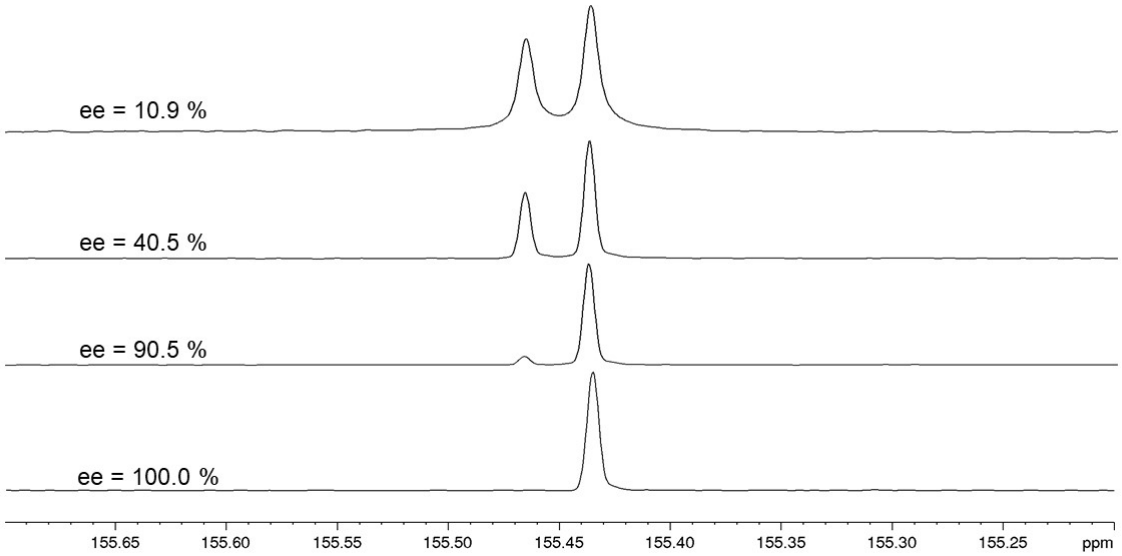

Figure 6.8: ^{13}C NMR spectra of menthol carbonate diesters after the derivatization with phosgene with the following enantiomeric excess values: 100.0%, 90.5%, 40.5% and 10.9%, ns = 512 (from bottom to top).

The ee results obtained demonstrated that the lower the ee value, the higher is the significant difference between the actual and nominal molar amount, as shown in figure 6.9. The maximal error was identified in the racemic mixture where an integral ratio of the carbonyl signals of 42 (meso) to 58 (LL/DD) was examined, resulting in an experimentally determined ee of 14% instead of 0%. These values confirmed the results presented by Vigneron

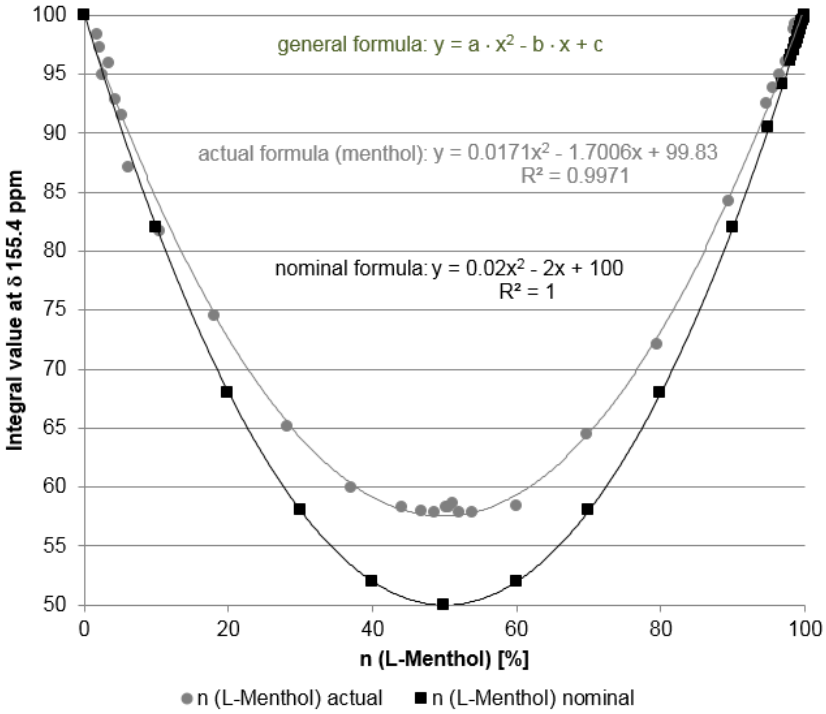

Figure 6.9: Comparison of nominal (black) and actual (grey) molar amount n of L-menthol considering the signal of the LL/DD menthol carbonate diesters.

et al. who reported a ratio of 40 (meso) to 60 (LL/DD) of the derivatization product [255]. This ratio demonstrated that the formation of LL/DD menthol carbonate diesters was preferred over the formation of meso menthol carbonate diesters, also known as *heterochiral discrimination* where a preferential interaction between same enantiomers took place [256]. The higher the concentration of one enantiomer, the lower is the influence of the discrimination. Consequently, depending on the requirements the presented ^{13}C NMR method was limited for a defined level of ee. Since the objective of the method was to ensure a relative deviation of $< 1\%$, the method was recommended for the quantification of the enantiomeric excess of menthol of expected ee $> 85\%$ or ee $< 15\%$. In these ratio ranges a correction of the ee value was not required. However, since the ratio of preference is known, the graph in figure 6.5 can be used for the determination of $85\% >$ ee $> 15\%$ by taking a correction factor into account.

Nevertheless, the method was aimed to being applied for menthol with a high enantiopurity. Thus, L/D-menthol mixtures have been prepared in the ee range of 97-100% using ^{13}C-labelled phosgene for derivatization (table 6.1). The ^{13}C labelling increased the concentration of the ^{13}C-isotope and thus, the S/N ratio of the carbonyl signal which was used for the quantification of the diastereomers and consequently of the enantiomers. By derivatizing L/D-menthol mixtures of an enantiomeric purity of $> 98\%$ (ee 96%) with ^{13}C-labelled phosgene, the nominal and actual ee values differed less than 0.1%. The LOQ,

which is defined as S/N = 10, was determined for the ^{13}C NMR analysis of ee. By using non-labelled phosgene the LOQ was determined with ee = 99.10%, and ee = 99.86% by using ^{13}C-labelled phosgene, running the experiment with 512 scans.

ee$_{nominal}$ [%]	**ee**$_{actual}$ [%]	**ee difference** [%]
100.00	100.00	0.00
99.86	99.86	0.00
99.46	99.45	0.01
99.37	99.41	0.04
99.04	99.11	0.07
98.63	98.68	0.05
98.08	98.08	0.00
97.07	97.03	0.04

Table 6.1: Comparison of nominal and actual ee > 97 % of menthol by using ^{13}C-labelled phosgene as tagging reagent based on the ^{13}C NMR carbonyl integrals

The results demonstrated a high-precise quantitative method. In general, ^{1}H and ^{13}C NMR are quantitative if a complete relaxation was performed. As well known, ^{13}C NMR spectroscopy can be used as a quantitative analysis tool, but it usually requires long relaxation delays, resulting in long measuring times to achieve sufficient S/N ratios [257]. However, in the presented study this restriction is not valid because the relaxation times of the carbon atoms of both diastereomers are equal resulting in carbon signals with the same relaxation time, which has also been shown in the study performed by Otte et al. [258]. Since the carbonyl integrals of the DD/LL ester and meso ester were compared relatively, the relaxation time did not have any influence on the quantitative results. Thus, a D1 of 1 sec was used for the analysis to make the experiment as fast as possible.

6.4.2 Borneol

The developed ^{13}C NMR tool was applied for the quantitative analysis of the enantiopurity of (1S,2R,4S)-borneol, (molecule **2**, figure 6.4), also known as (-)-borneol. An assay of $\geq$ 99.0% (sum of enantiomers, GC) was labelled, without any information about the concentrations of (-)- and (+)-Borneol. To test the quality of the enantiopurity (-)-borneol was derivatized with ^{13}C-labelled phosgene forming borneol carbonate diesters. In the ^{13}C NMR spectrum splitted carbon signals were detected which implied that (-)-borneol was not enantiopure (figure 6.10). The ^{13}C NMR carbonyl signal of the (- -)/(+ +) diastereomer was shifted to 156.81 ppm and of the meso signal to 156.78 ppm. By integrating both signals, the integral value of the meso carbonyl signal was determined with 3.24 (figure 6.10). Using the equation 6.1, an ee of 96.70% was determined. A correction of the calculation was unnecessary due to the high enantiomeric purity, where a significant impact of a potential enantiodiscrimination was negligible. Thus, by the quality control of borneol by means of ^{13}C NMR spectroscopy 1.65% of (+)-borneol were identified in (-)-borneol.

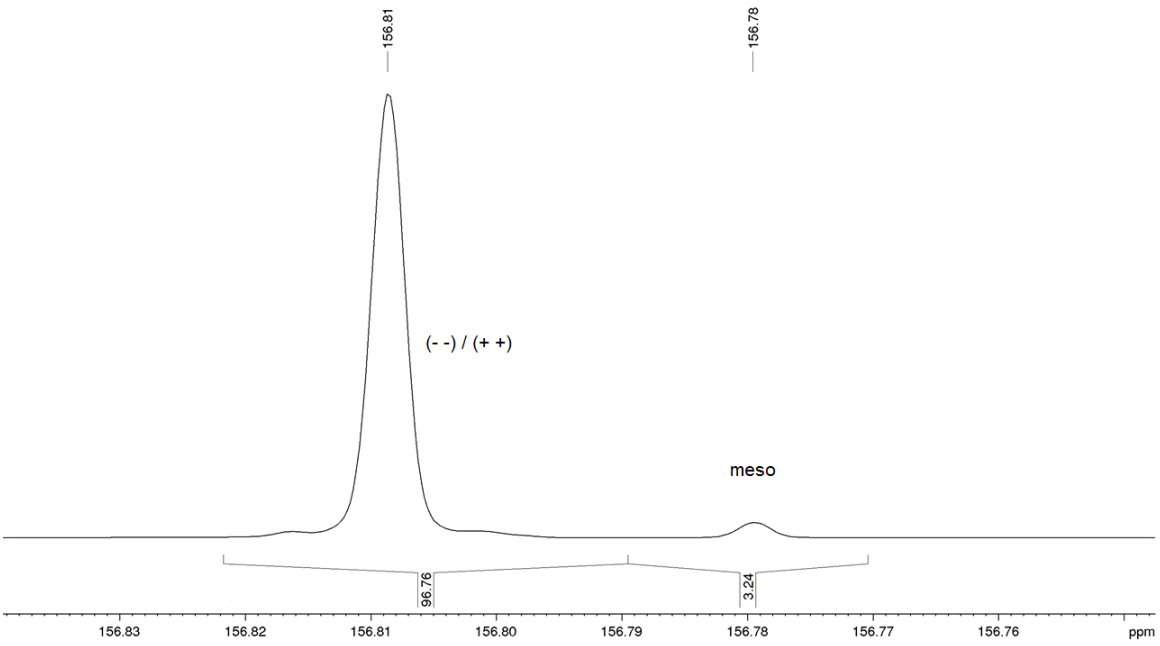

Figure 6.10: ^{13}C NMR spectra of the borneol carbonate diesters after the derivatization with ^{13}C-labelled phosgene, ns = 512.

6.4.3 1-Phenylethanol

The developed ^{13}C NMR tool was applied for the determination of the enantiomeric purity of (S)-1-phenylethanol, (molecule **3**, figure 6.4). (S)-1-phenylethanol reacted with ^{13}C-labelled phosgene forming 1-phenylethanol carbonate as diastereomer. In the ^{13}C NMR spectrum of the derivatization reaction product two carbonyl signals were detected indicating that (S)-1-phenylethanol is not entantiopure (figure 6.11). The RR/SS carbonyl signal was identified at $\delta = 155.86$ ppm and the meso diester carbonyl signal at $\delta = 155.83$ ppm. Both signals were integrated and compared. By using the equation from figure 6.5 the ee was determined with 96.54%. Consequently, the analyzed (S)-1-phenylethanol consisted of 98.27% (S)-1-phenylethanol and 1.73% (R)-1-phenylethanol. Since the enantiomeric purity is very high a potential kinetic resolution is negligible.

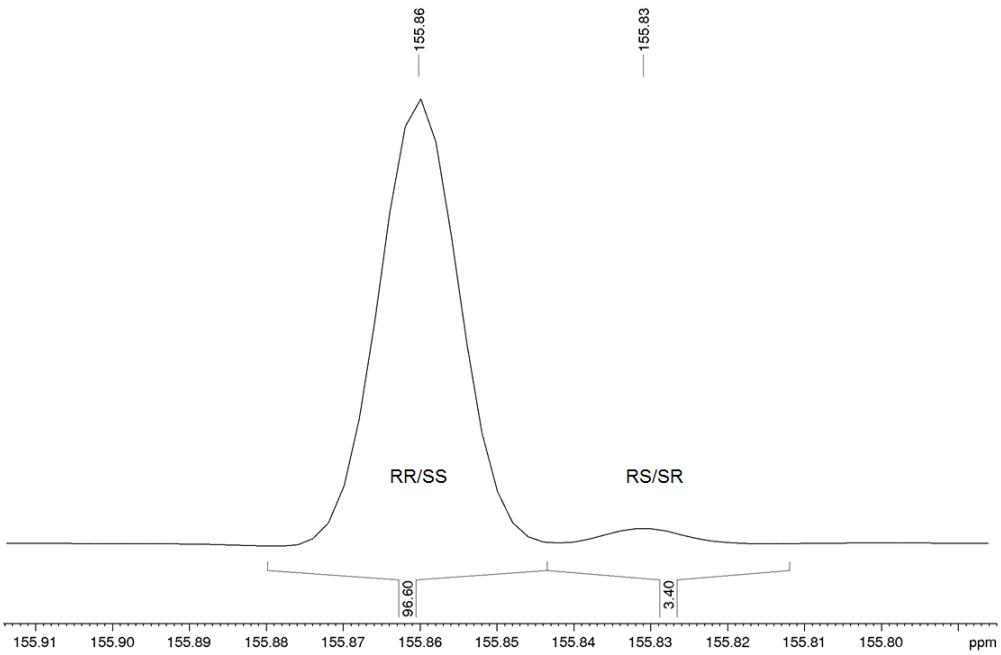

Figure 6.11: ^{13}C NMR spectrum of 1-phenylethanol carbonate diesters after the derivatization of (S)-1-phenylethanol with ^{13}C-labelled phosgene; ns=256.

6.4.4 Linalool

(-)-Linalool was examined towards its enantiomeric purity by ^{13}C NMR spectroscopy. Linalool, (molecule **4**, figure 6.4), reacted with ^{13}C-labelled phosgene forming RR/SS and meso linalool carbonate diesters as diastereomers. In the ^{13}C NMR spectrum the carbonyl signal was splitted whereby the carbonyl signal of RR/SS linalool carbonate diesters was shifted to δ = 144.36 ppm and the carbonyl signal of meso form to δ = 144.32 ppm (figure 6.12). Both signals were integrated by deconvolution. By using the equation from figure 6.5, the ee was determined with ee = 66.38%. Since the enantiomeric purity was low, a kinetic resolution was not precluded. In this case, a preparation and analysis of a calibration curve with mixtures of different ratios of (-)-linalool and (+)-linalool was required to examine the potential asymmetrical induction. However, because (+)-linalool was not available for purchase, a calibration curve could not be prepared. Consequently, the reaction constants could not be studied and the nominal and actual ee values could not be compared. Thus, a reliable quantification was not performed. Nontheless, the ^{13}C NMR results showed that the substance (-)-linalool was not enantiopure. Thus, the enantiomeric purity was refuted by the NMR results.

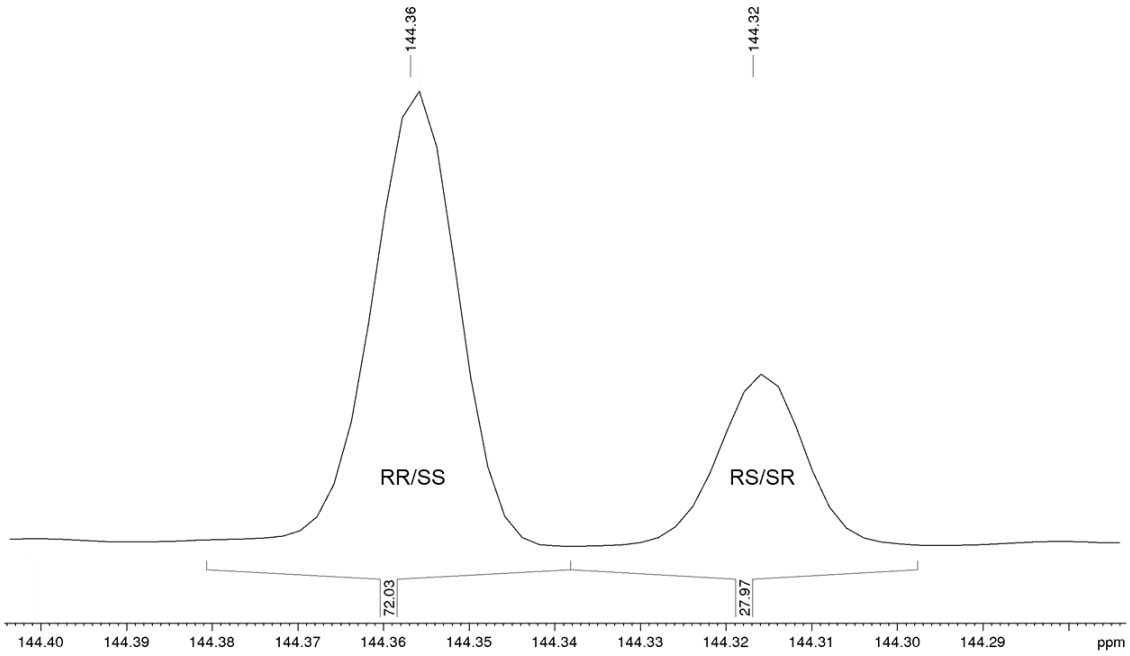

Figure 6.12: ^{13}C NMR spectra of the linalool carbonate diesters after the derivatization of (-)-linalool with ^{13}C-labelled phosgene; ns=1024.

6.5 Conclusions

In summary, ^{13}C NMR spectroscopy acquired with short relaxation delays of D1 = 1 sec is a convenient method for the quantitative determination of enantiomeric excess of chiral alcohols such as menthol, borneol, 1-phenylethanol and linalool by means of phosgene as derivatization reagent. ^{13}C NMR spectroscopy together with phosgene as derivatization reagent is a powerful tool for the accurate determination of the enantiomeric excess of chiral alcohols such as menthol, borneol, 1-phenylethanol and linalool. The derivatization of alcohols with phosgene in C_6D_6 is fast and the reaction products are stable. The ^{13}C NMR approach is advantageous with regard to the easy performance of quality control within a short time. To determine ee of $< 90\%$ a potential asymmetrical induction should be examined by preparing and analyzing artificial mixtures of both enantiomers. The appropriate calibration curve can be used for an accurate calculation of ee even if an asymmetrical induction is confirmed. Even though ^{13}C NMR is less sensitive than ^{1}H NMR, on modern 600 MHz cryo NMR instruments, the sensitivity is more than sufficient. The ^{13}C NMR spectroscopy implies the following advantages: very high resolution, good separation of signals, precise integration, and a higher chance of non-overlapped signals which are suitable for the quantification of the enantiomeric ratio. In several analytical cases, these advantages are more important than the disadvantage of a lower sensitivity or the longer measuring time. The developed ^{13}C NMR method is demonstrated to be a complimentary or alternative technique to the common used chiral chromatography for determination of enantiomeric purity.

Chapter 7

Final Discussion

This work aimed to solve analytical issues by developing new quantitative NMR methods using tagging reagents. Analytical issues have been detected in several areas such as in the food and pharmaceutical sector. Here, one interlaboratory comparison test was organized (chapter 3) and three NMR methods have been developed focusing for applications in chemical, pharmaceutical and food products (chapters 4 to 6), whose analytical details are presented in table 7.1. Each method is discussed critically in this chapter.

Analytical issue	**Peroxides in Oils**	**Divalent metal cations**	**Enantiomeric Excess**
NMR Experiment	^{1}H-^{31}P dec. NMR	^{1}H NMR	^{13}C NMR
Sample	Vegetable oil Krill oil Fish oil	Artificial Salt Solutions Food Supplements Pharmaceutical Products	Menthol 1-Phenylethanol Linalool Borneol
Tagging Reagent	Triphenylphosphine	EDTA (c = 55 mg/mL), pH = 7.2	Phosgene 1M, 15 wt-%
Sample amount	200 mg	5-20 mg	60-90 mg
Tagging amount	5-10 mg	1000 μL	200 μL
Solvent	C_6D_6	D_2O	C_6D_6
Number of Scans	16	16	256
D1	2 sec	1 sec	1 sec
Experimental time	3 min	2 min	20 min

Table 7.1: Overview of developed NMR methods

In summary, a precise quantitative determination of peroxides in low-oxidized and high-oxidized vegetable and animal oils was designed by using triphenylphosphine as tagging reagent (chapter 4). For the second method, which was presented in chapter 5, EDTA was used to chelate divalent metal ions and thus, to identify Be^{2+}, Mg^{2+}, Ca^{2+}, Sr^{2+}, Zn^{2+}, Cd^{2+}, Hg^{2+}, Sn^{2+}, and Pb^{2+} in aqueous salt solutions through their unique signal shift

and coupling pattern, and to determine Ca^{2+}, Mg^{2+}, Hg^{2+}, Sn^{2+}, Pb^{2+} and Zn^{2+} (LOQ: 5-22 μg/mL) quantitatively. The third method described a ^{13}C NMR analysis of the enantiomeric excess of menthol, 1-phenylethanol, linalool and borneol by using phosgene as tagging reagent. With this method, the determination of ee $> 99.5\%$ is possible, which represents the limit of Mosher's reagent. The results of the research were presented in detail in chapter 6.

7.1 Peroxides in Oils

The aim of the research was to identify or to develop a ^1H NMR method for a fast, accurate, precise, robust and simple quality assessment of fatty oils with a fouc on the peroxides. From my point of view, the ^1H NMR method, which was developed by Skiera et al., represented a powerful alternative method for the commonly used titration methods. Since low-oxidized oils are of high analytical interest, the performance of the ^1H NMR method should be examined. Thus, an interlaboratory comparison test (ILC) was organized with a total of 21 NMR data sets which were obtained from 17 international participant laboratories [91].

7.1.1 Conventional titration techniques

Traditionally, the quality assessment of edible oils has been performed according to official methods, including the analysis of free fatty acids, peroxides, aldehydes, di- and triglycerides as well as oil-characteristic substances such as squalene in olive oil. Therefore, numerous analytical techniques are used to examine one of many quality parameters: free fatty acids are detemined by an acid-base titration [134], [135], [136], peroxides by a visual (iodometric) titration according to ISO 3960:2007 [259] or a potentiometric endpoint titration according to ISO 27107:2008 [260], aldehydes are measured by the official AOCS method Cd 18-90(11) using a spectrophotometric analysis [138], [139], [140], [141]. These commonly used techniques imply several drawbacks which will be presented here. For the quality control, numerous analytical techniques and instruments are required, which need space, installation, qualification, maintenance and skilled personnel with experience, which results in high costs. Furthermore, some techniques require calibration curves which increase the need of reference material, solvent and occupancy of the instrument and thus, decrease the capacity of number of analyzed samples. With a focus on the titration method for the PV determination, which represnets an old wet chemistry technique, high amounts of (toxic) chemicals and solvents are required for sample preparation which increase the costs of purchase on the one hand, and for storage and disposal on the other hand. To highlight these amounts, the sample preparation must be looked at closely. For the PV determination using the official titration method, dependent on the expected peroxide concentration, 5 gram or 10 gram oil, 50 mL glacial acetic acid/isooctane solution as well as 30-100 mL water are required (figure 7.1, page 107) [137], [167]. The sample preparation *"must be carried out in diffuse daylight or in artificial light. Direct exposure to sunlight*

must be avoided. All vessels must be free from oxidising or reducing compounds" [167]. This paragraph shows how error-prone the method is. Besides that, depending on the number of sample preparation steps, waiting and analysis time, the number of examined samples per hour is very low which is not ideal for a high-throughput routine analysis.

7.1.2 Interlaboratory Comparison Test (ILC)

To overcome the drawbacks of the presented conventional titration technique, the ^{1}H NMR method developed by Skiera et al. [91], which was identified as a powerful alternative, was critically investigated within an international ILC test, which is presented in 3 [131]. The advantages and limits of the ^{1}H NMR method are discussed here.

Advantages of ^{1}H NMR method developed by Skiera et al.

The benefit of this method is the fast and simple sample preparation using only 200 mg of oil and 1 mL of the solvent $CDCl_3$/DMSO-d_6. The weighing and dissolving step needs less than one minute. For the analysis neither cost-intensive reference material nor any calibration curves are required [91]. The experimental time of the ^{1}H NMR spectrum is about three minutes and as further benefit, NMR experiments can be run automatized by using autosamplers which allow the handling of up to 480 sample tubes [261]. Consequently, in one hour about 12 samples, and in one day about 288 oil samples can be measured by NMR spectroscopy, which represents a big advantage over the titration method. Besides the PV, in the ^{1}H NMR spectrum several parameters can be investigated simultaneously including free fatty acids, anisidine value (aldehydes), iodine value (double bonds) as well as the composition of di- and triacylglyceride, and oil-characteristic compounds such as squalene in olive oil. Furthermore, adulterations, contaminations and frauds of fats and oils may be examined [262].

Drawbacks & Limits of ^{1}H NMR method developed by Skiera et al.

The ^{1}H NMR method has also some drawbacks which have been identified within the ILC test. Here, it was detected that unexperienced NMR scientists submitted results with higher deviations because of higher error-proneness of their phase and baseline corrections. It is important to highlight that the experience level in NMR spectroscopy varied of the participating laboratories from student to well-experienced NMR expert. This outcome underscores the importance of training NMR-newbies in the handling of NMR spectra focusing on phase, baseline and integration. Nonetheless, 90.5% of the participants passed successfully the ILC test [131].

Furthermore, the magnetic strength of NMR instruments had an influence on the results of the fatty acid distribution. Because of the significant difference of the integral values of the C18:3 signal in the ^{1}H NMR spectra recorded with 400 MHz spectrometer, it was stated that the analysis of triacylglycerides should be conducted on NMR spectrometers

with frequencies greater than 400 MHz. The evaluation of the C18:3 signal showed comparable results for 500 MHz and 600 MHz [131].

The results of free fatty acids, peroxides and aldehydes showed higher deviations due to a broad signal of the COOH-signal of the free fatty acids and the low concentrations and, consequently, low signal-to-noise (S/N) ratios of peroxides and aldehydes. By analyzing oils with a PV of 4.55 meq/kg, a relative standard deviation (RSD) of 15% was determined along the organized ILC test [91], [131]. In 2004/2005, an ILC test was organized by the DGF to determine the precision of the titration method for the PV analysis. Here a sample with a PV of 4.42 meq/kg was measured with a RSD of 1.51% which is one-tenth of the RSD of the alternative ^{1}H NMR method for comparable PV [167]. Consequently, the applicability of the ^{1}H NMR method by Skiera et al. is limited to higher oxidized oils which leads to a demand of a new precise NMR method with a focus on low-oxidized oils [91], [131].

7.1.3 ^{1}H NMR method by using TPP

Even though, Skiera et al. [91] developed a powerful ^{1}H NMR method, the ILC test identified that the method is not optimal for the analysis of low-oxidized oils [131]. Therefore, a new NMR method was developed using TPP as tagging reagent. The advantages, drawbacks and limits of the new method, which is presented in chapter 4, are discussed in this chapter [154].

Advantages

The presented ^{1}H NMR method using TPP as tagging reagent is a fast and robust method. Instead of a complex sample preparation as being depicted for the titration method, the developed NMR method requires only three steps including weighing sample, weighing derivatization agent TPP, and adding deuterated benzene as solvent. The sample preparation is finished within a few minutes (figure 7.1).

In opposite to the titration method, where 5 g higher oxidized oil or 10 g low-oxidized oil are needed, 200 mg sample and an appropriate amount of TPP are adequate for the ^{1}H NMR analysis. The amount of TPP depends on the concentration of the peroxides in the sample. 5-10 mg are sufficient for the analysis of PV $<$ 150 meq/kg. In comparison with the titration method, only 4% or rather 2% of the sample amount is needed for the quality analysis by using ^{1}H NMR spectroscopy, so 96% or rather 98% of the sample amount is saved with the newly developed NMR method. Furthermore, instead of 150 mL solvent (glacial acetic acid/isooctane/water), only 1 mL C_6D_6 is required to solve the oil sample resulting in about 99% less solvent waste. After the sample preparation, the samples are stable in solution for more than 24 hours making a re-analysis within this time period possible.

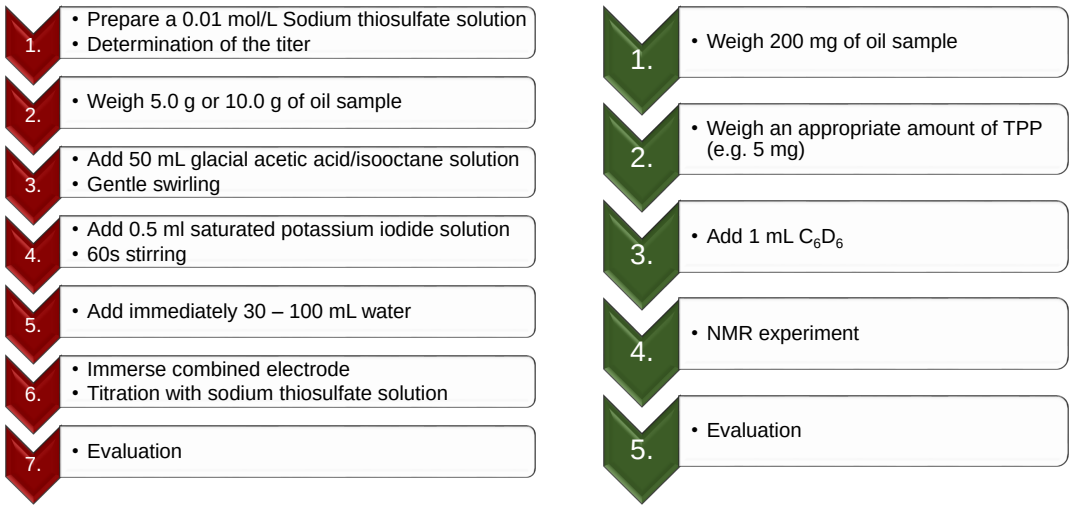

a) Conventional titration method b) ^{1}H NMR method using TPP

Figure 7.1: Comparison of the analysis process of the conventional titration technique [167] and the developed ^{1}H NMR method using TPP [154].

Additionally, as criticized by the German Society for Fat Science e.V. (DGF), PV does not relate in all types of oils directly to the oxidation status as confirmed for example for black cumin oil, where high PV can be clearly attributed to the concentration of a high natural content of essential oils and do not refer to a bad quality of the oil product. Thus, on the one hand, the PV of different oil types cannot be compared with each other, and on the other hand, the natural fluctuation of the phytonutrients has a significant influence on the PV. Consequently, DGF confirmed that the titration is methodically associated with a considerable measurement uncertainty [263]. These evidents argument against the conventional titration. Contrary to the titration, the analysis of PV by NMR spectroscopy by using TPP depends only on the concentration of the present peroxides, and is thus, not related to secondary phytochemicals like squalene in olive oil or thymochinone in black cumin oil [154].

Moreover, the official titration method is limited to oils without phospholipids, so it cannot be applied for the analysis of krill oils or lecithins because of their high phospholipid content [135]. Another advantage of the NMR method by using TPP is its applicability for various matrices of phospholipid containing and non-containing oils and fats like vegetable or krill oils. However, since the global krill oil market was valued at US $ 267.7 Mn in 2014 and is expected to reach a value of US $ 703.0 Mn by 2022, krill oil is a product of even high and still raising interest, which leads to a need of an adequate quality control where the NMR method provides an opportunity for [264].

If an oil sample with an extreme low PV of < 1 meq/kg is intended to be examined, the NMR method can be slightly modified to produce still accurate and precise results. Several options are available to receive better S/N ratios of TPPO and consequently, of the peroxide determination. One option is the modification of the sample preparation by increasing the amount of sample, or by decreasing the amount of TPP. Additionally, the solvent volume can be decreased to a minimum volume of 0.7 mL which is required for the measurement in 5 mm NMR tubes. Another option is to increase the number of scans during the NMR experiment. By quadruplying the number of scans, the measuring time increases also by a factor of four and the S/N ratio is doubled.

As demonstrated, the NMR method is much faster, less time-dependent and more economical regarding the use of resources than the titration method and hence, it represents a powerful alternative for the PV determination by unsing titration.

Drawbacks & Limits

A drawback of the NMR method which has been developed is the use of the solvent benzene. The first idea was to run the analysis in $CDCl_3$/DMSO-d_6 as presented in the ^1H NMR method developed by Skiera et al. [91]. A solvent ratio of 4:1 led to an overlap of the chloroform and the TPPO-signal which made a quantitative evaluation impossible. The advantage of the $CDCl_3$/DMSO-d_6 (3:1) approach would be a holistic control of oils including the triacylglyceride profile, free fatty acids, sterols, tocopherols and also peroxides. Unfortunately, TPP reacts with $CDCl_3$/DMSO-d_6 immediately forming 2.3% TPPO, with an increasing concentration of TPPO over time. Thus, $CDCl_3$/DMSO-d_6 was identified as a non-suitable solvent for the peroxide method. As an alternative, C_6D_6 has been examined and confirmed as a feasible solvent for the analysis. Thus, for an overall holistic control two NMR analysis are required: the NMR analysis in $CDCl_3$/DMSO-d_6, developed by Skiera et. al [91], and in C_6D_6 with TPP for the precise and accurate analysis of peroxides [154]. In contrast to the desired "all-in-one analysis", the holistic quality control of fats and oils needs two NMR methods and this, in total 400 mg sample, 1 mL $CDCl_3$/DMSO-d_6 and 1 mL C_6D_6 as well as about 7 minutes of total analysis time, which represents an advantage comparing with other methods.

Another drawback of the method is the time-dependent reaction of TPP in krill oil. A krill oil sample was analyzed directly after the sample preparation showing a PV of 7.67 meq/kg. The sample solution was re-measured after 2 hours, 4 hours, 6 hours, 7 hours, 8 hours, 9 hours, 12 hours and afterwards in 4-hours-step up to 28 hours. After 28 hours (about 1700 min) the TPPO signal increased about +55%, resulting in a PV of 11.55 meq/kg (figure 7.2). The increase of the PV over time was representative for all krill oil samples which have been examined by the new TPP NMR method within the study. This implicated a time-dependent cross-reaction of TPP and krill oil, however, the responsible krill-specific substance(s) could not be detected. Since krill oil is a natural product, it is a

complexe mixture of lipids enriched in eicosapentaenoic acid (EPA) and docosahexaenoic acid (DHA), phospholipids, cholesterol and cholesterol esters, phytinic esters as metabolites of chlorophyll, astaxanthin as the red-colored antioxidant, amino acids, homarine, ethanol and trimethylamine N-oxide as by-products of the production process if not completely removed [265], [266]. Thus, it was not possible and also not requested to find the reason for the PV increase. Additionally, the increase of the PV in the prepared krill oil samples could not be confirmed by titration, because of the following reasons:

- The official titration method is not applicable for milk fat and lecithins. The reason therefore is the amount of phospholipids. Since krill oil contains also phospholipids, this matrix cannot be analyzed by titration [167], [265];
- The increase of the PV was detected in the sample solution, meaning krill oil and TPP dissolved in C_6D_6. Since the influence of these chemicals on the titration were unknown, the measurement was not performed;
- For the titration analysis, 10 grams of krill oil were needed. However, this high amount of one batch was unavailable which made this kind of analysis impossible.

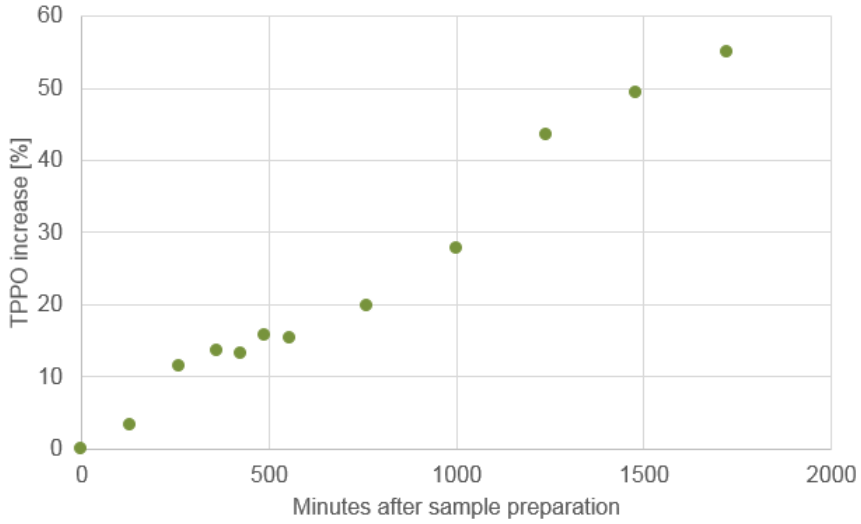

Figure 7.2: Increase of TPPO content [%] over 28 hours after sample preparation.

As a consequence of the research results, it was decided to perform the NMR experiments directly after finishing the sample preparation of krill oils. Sample solutions of vegetable oils are stable for at least 24 hours.

Prospects for future research

Oils are natural products which contain a high number of substances in various concentrations such as saturated and unsaturated tri-, di- and monoglycerides, sterols, tocopherols,

squalene in olive oil, thymochinone in black cumin oil and astaxanthin as well as phospholipids in krill oil, and many more [181], [267]. The addition of TPP results in the expected 1:1 reaction with peroxides forming TPPO, although unintentional cross-reactions with other substances may occur which is always a risk in a derivatization reaction. To confirm that no cross-reactions falsify the PV results, all reactive oil-ingredients may be examined. Furtermore, the NMR method could be applied for more matrices such as lecithins or baby formula milk powder.

7.2 Divalent metal cations by ^{1}H NMR spectroscopy

The aim of the investigation was the development of a fast and simple NMR method for the qualitative and quantitative determination of inorganic divalent cations. For this purpose, the ^{1}H NMR method, which was developed and published by Monakhova et al., was used as a basis [95]. By applying EDTA as a complexing agent Be^{2+}, Sr^{2+}, and Cd^{2+} can be determined qualitatively, and Ca^{2+}, Mg^{2+}, Hg^{2+}, Sn^{2+}, Pb^{2+} as well as Zn^{2+} can be determined qualitatively as well as quantitatively. The results of the research have been presented in chapter 5 and the advantages, drawbacks and limits of the method are discussed in this chapter.

Advantages

One of the main advantages of the developed ^{1}H NMR method is the simultanous qualitative analysis of nine cations (Be^{2+}, Sr^{2+}, Cd^{2+}, Ca^{2+}, Mg^{2+}, Hg^{2+}, Sn^{2+}, Pb^{2+}, Zn^{2+}) and the simultanous qualitative as well as quantitative analysis of six cations (Ca^{2+}, Mg^{2+}, Hg^{2+}, Sn^{2+}, Pb^{2+}, Zn^{2+}). Due to the stability of the Met-EDTA-complexes, their signals show individual multiplicities and unique chemical shifts in the ^{1}H NMR spectrum which makes an analysis of a mixture of the mentioned divalent cations possible.

A fast quantification is feasible by using EDTA as a complexation reagent with the additional function of an internal standard. If a known amount of EDTA is added to a known amount of a sample, the amount of Met-EDTA-complex is equal the amount of present divalent metal cations [212]. Thus, the comparison of the integrals of the signals of free EDTA and Met-EDTA-complexes can be recalculated into the amount of the divalent metal cations which are present in the analyzed product. Consequently, the amounts of the divalent metal cations Ca^{2+}, Mg^{2+}, Hg^{2+}, Sn^{2+}, Pb^{2+} and Zn^{2+} are quantified without the addition of further internal standards. However, the quantification is only possible if the rules of qNMR spectroscopy are followed. In this case, EDTA and the Met-EDTA-complexes should be fully relaxed before the next scan. Hence, the T1 time was determined beforehand. T1 times were determined in the millisecond-range, so a D1 time of 1 second was set which enabled a quantitative analysis within around 3 minutes. Additionally, further substances like sugars and citric acid, which are additives in numerous products, can be identified and quantified simoultaneously in the same analysis run if they are soluble in

D_2O. In these cases, it is important to study the T1 time of the substances of additional interest and, if necesseary, to increase the D1 time. The EDTA method reduces the total number of required analysis, and thus, the volume of required sample, internal standard and solvent as well as analysis time and costs.

Drawbacks & Limits

Based on the composition of the examined sample, the signals of free and chelated EDTA may be overlapped by other signals which makes the quantitative analysis more erroneous or even impossible. If the free EDTA signal is disturbed, a quantitative analysis is still possible by adding an internal standard and increasing the D1 time to receive fully relaxed signals. However, if the signals of the Met-EDTA-complex are overlapped, deconvolution can be applied to integrate them nonetheless. In some cases, the overlapping is too strong which makes the quantification impossible.

The signals of Ba^{2+}, Be^{2+} and Sr^{2+} are identified as too broad to be used for an accurate and precise quantitative analysis. In these cases, the temperature should be decreased from 298 K to 278 K or even lower to "freeze" the Met-EDTA-complex which would result in more narrow signals as shown in figure 5.8. However, cooling down and heating up is a time-consuming procedure which increases the total time of analysis on the one hand, and makes the method suboptimal for a routine analysis because the instrument needs support during the processes of temperature change on the other hand. Consequently, in most contract NMR laboratories, NMR analyses at room temperature are preferred.

Another drawback of the analysis is the pH dependency. Based on the pH, EDTA can be present in different stati of protonated and deprotonated forms which influences the complexation constant significantly. For the tagging method, EDTA should be present in its fully deprotonated $EDTA^{4-}$ form which is detected at a pH of above 7. In contrast to the research results presented by Reilley and Schmid, EDTA totally complexes with Be^{2+}, Sr^{2+}, Cd^{2+}, Ca^{2+}, Mg^{2+}, Hg^{2+}, Sn^{2+}, Pb^{2+} and Zn^{2+} at a pH of 7.2. They recommended a complexation of calcium and magnesium at a pH of 8 and 10, respectively [268]. However, since the comparison of the theoretical and measured concentrations at pH ranges of 7 to 10 did not show any significant differences (not published results), the approach is suitable at pH = 7.2. However, the rection in a too basic solution is also not recommended because here, metal hydroxides such as $Mg(OH)_2$ are formed, which are solid and, thus, precipitate.

One further limit is the quantitative analysis of lead-contaminated water. As presented in chapter 5, the LOQ of lead is determined with 0.05 mg/mL which is a factor of 5000 higher than the permitted concentration limit of lead in potable water of 0.000010 mg/mL in Germany [217]. Even with an optimization of the method, this NMR method is not sensitive enough to determine lead quantitatively in water at concentrations considered unsafe for human consumption.

Prospects for future research

In particular, the quantitative method has not been applied to Ba^{2+}, Be^{2+} and Sr^{2+} because of their broad signal shapes. As prospects for future research, besides the temperature of the NMR measurement further parameters should be tested to receive better signal shapes which make a quantitative analysis also for these three divalent cations possible. Since the pH is an important factor for the complexation reaction, its influence should be studied in detail. Furthermore, up to now the method is tested for the cations Be^{2+}, Sr^{2+}, Cd^{2+}, Ca^{2+}, Mg^{2+}, Hg^{2+}, Sn^{2+}, Pb^{2+} and Zn^{2+}, which means that numerous further cations should be studied to expand the method. Besides the pharmaceutical products and food supplements which have been presented in this work as potential applications, numerous products from the sector of food, pharmaceuticals, cosmetics and chemicals contain different metal cations that can be examined with this method representing a big pool of applications.

7.3 Enantiomeric Excess by ^{13}C NMR spectroscopy

The aim of the investigation was the development of a fast and simple NMR method for the qualitative and quantitative determination of enantiomeric excess of chiral alcohols. The results of the research have been presented in chapter 6. A detailed consideration of the advantages as well as drawbacks and limits is discussed in this chapter.

Advantages

The ^{13}C NMR spectroscopic method developed is an easy and fast approach. The reaction of phosgene and menthol, borneol, phenylethanol and linalool is completed within several seconds. For the reaction only small amounts of chemicals and solvents are required: 200 μL phosgene, 60-90 mg of the alcohol and 1 mL C_6D_6. The amounts can be further decreased by increasing the number of scans to receive a comparable S/N ratio.

The application of ^{13}C-labelled phosgene instead of non-labelled phosgene increases the S/N of the ^{13}C NMR carbonyl signal of the resulting esters significantly which makes a detection also of small concentrations of one enantiomer possible. By using ^{13}C-labelled phosgene, an enantiomeric excess can be quantified precisely in the range of 97% to 100%, especially in the region of ee $>$ 99.5%, which represents the limit for the application of Mosher's reagent. Furthermore, the evaluation of the ^{13}C NMR spectrum is simple because only two signals have to be integrated and compared. The integration can be performed manually or by using deconvolution.

The price of non-labelled phosgene is another advantage. 100 mL can be purchased at Sigma-Aldrich for 70.70 € [269]. 100 mL are sufficient for 500 analyses, leading to a cost factor for phosgene of 0.14 € per analysis. Comparing the price of the non-labelled and

^{13}C-labelled phosgene, the use of ^{13}C-labelled phosgene is more cost-intentive. 100 mL can be purchased at Sigma-Aldrich for 337 €, leading to 0.68 € per analysis which is a factor of around 5 comparing with the non-labelled phosgene.

Drawbacks & Limits

The main drawback of the new method is the use of phosgene. Phosgene is known as a hazardous, colorless gas at ambient temperature and pressure, which is commonly used in industry for the production of pesticides or polyurethanes [270]. It is an insidious gaseous poison because of the lack of an odor at < 0.4 ppm, and symptoms do not appear immediately [271]. Thus, occupational limit value is set to 0.1 mL/m^3 [272]. However, to overcome these high risks of gaseous phosgene, for the developed method 1 molar ^{13}C-labelled and 15 weight-% non-labelled phosgene in toluene solutions were used. The sampling of 0.2 mL phosgene in toluene, required for the analysis, was performed in a fume hood by using a syringe to pierce a septum. Thus, a high degree of occupational safety was ensured.

Since the developed method is based on a derivatization method, the reaction of phosgene with each substance of interest has to be studied. As presented by Babad and Zeiler, phosgene reacts with various chemicals at a nitrogen, oxygen, sulfur or carbon center as well as with inorganic compounds in various ways [273]. In the presented study a focus was set on substances with a hydroxy group. However, if an alcohol shows additional functional groups containing e. g. oxygen or nitrogen, it can react with phosgene producing various substances like a five-membered ring, as shown in figure 7.3, which makes the analysis of the enantiomeric excess impossible because no diastereomers are formed [273].

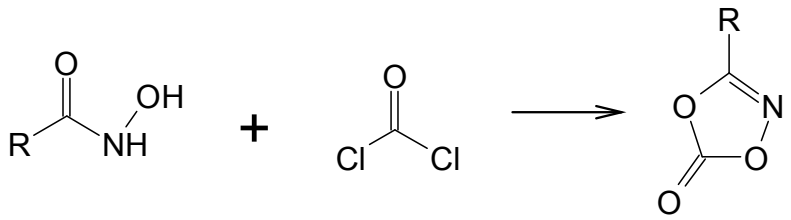

Figure 7.3: Reaction of phosgene and hydroxamic acids forming nitrile carbonates [273].

Another limit of a derivatization or a tagging reaction is the risk of a diastereoselectivity, which leads to an asymmetric formation of diastereomers and establishes a preferred relative stereochemistry. Consequently, there is a need of an examintion of a potential diastereoselectivity for each alcohol which should be analyzed according its enantiomeric composition by being tagged with phosgene. Therefore, artificial mixtures of enantiomers are prepared and measured by NMR spectroscopy. The signals of the RR/SS and RS/SR diastereomers are integrated and the expected and measured ratios are compared. If the measured values are not consistent with the expected values, a diastereoselectivity can be confirmed, as it was confirmed in the case of menthol (figure 6.9). Here, it was shown that

the diastereoselectivity was particularly pronounced among the racemic mixture, with a progressive reduction of the diastereoselectivity with increasing enantiomeric excess values. Thus, the influence of the diastereoselectivity at ee $> 95\%$, which is often the region of interest, is negligible. If samples with an ee $< 95\%$ should be examined, a preparation of a calibration curve is essential to determine the "real" enantiomeric excess without the influence of the diastereoselectivity. Thus, the developed tagging method induced the following drawbacks:

- the preparation of a calibration curve is time-consuming,
- expensive due to the need of both enantiomers,
- highly pure enantiomers cannot be purchased for all chiral products,
- the diastereoselectivity depends on several parameters such as temperature, pressure and water content [274].

Even though possibilities are presented to apply the NMR method to racemic samples, it is recommended to use this technique only for the examination of alcohols with a high enantiomeric purity. Additionally, the absolut configuration of the enantiomer of the higher concentration should be known because the method cannot be used to determine the absolut configuration of the stereoisomers. In order to be able to establish a statement about the ratio of the absolute R and the S enantiomer, an information from the manufacturer about the enantiomer of the higher concentration is required. Is this information missing, only the enantiomer excess can be determined without defining which enantiomer is present in the higher concentration.

Prospects for future research

In this research the NMR analysis was performed at 298 K. As shown by Lankhorst et al. ^{13}C NMR experiments at 300 K resulted in broader signals than measurement at 260 K, which was chosen as the optimal temperature for the quantitative enantiodiscrimination by Lankhorst et al. [275]. As a prospect for future, the presented NMR method should be performed at lower temperatures to study the line broadening effect as well as its influence on the quantitative results. Furthermore, in this study only menthol, borneol, 1-phenylethanol and linalool were examined. On-going and future studies should provide a larger set of applications. Additionally, less toxic and less cost-intensive substances should be examined as alternatives to the toxic phosgene.

7.4 Conclusions

The outcome of this entire study has demonstrated that the NMR spectroscopy is a powerful analytical tool to solve various analytical challenges. Substances which could not be detected in NMR spectra, can now be studied after being derivatized or complexed with tagging substances. Tagging is a highly effective tool to determine the peroxide value in oils, cations in artifical salt mixtures and pharmaceutical products as well as food supplements, and the enantiomeric excess of chiral alcohols. The presented NMR methods can be used as alternatives or even as replacements for obsolete official methods such as titrations or chromatography. The research studies indicated that the NMR spectroscopy is a high-performance technique for chemical analyses whose range of applications has not been exhausted yet.

Chapter 8

Zusammenfassung

Die hochauflösende Kernresonanzspektroskopie findet heute primär Anwendung in der Strukturaufklärung und der qualitativen sowie quantitativen Untersuchung von Produktinhaltsstoffen. Trotz der weltweiten Entwicklung von innovativen kernresonanzspektroskopischen Methoden sind noch zahlreiche, offiziell anerkannte Methoden zur Qualitätskontrolle von Arzneimitteln, Lebensmitteln und Chemikalien in Verwendung, die spezifische Substanzen kontrollieren und keine ganzheitliche Untersuchung darstellen. Somit können verunreinigte, qualitativ minderwertige oder gefälschte Produkte trotz vorheriger Qualitätskontrollen auf den Markt gebracht und vertrieben werden. Um dies zu verhindern, wurden im Rahmen dieser Arbeit drei kernresonanzspektroskopische Methoden entwickelt, die zur (1) Bestimmung der primären Oxidation in pflanzlichen und tierischen Ölen anhand der Peroxidzahl, (2) zur qualitativen und quantitativen Analyse von Metallkationen und (3) zur Ermittlung des Enantiomerüberschusses in chiralen Alkoholen dienen.

In der Ölanalytik werden Titrationsverfahren zur Bestimmung der Bulkqualitätsparameter wie auch der Peroxidzahl, welche die Konzentration an Peroxiden aufzeigt, eingesetzt. Da die Titration neben dem Einsatz von größeren Mengen an Probenmaterial und Lösungsmitteln, auch Kreuzreaktionen und eine geringe Robustheit aufweist, wurde eine kernresonanzspektroskopische Methode entwickelt, in der Triphenylphosphin als Derivatisierungsreagenz eingesetzt wird, welches mit Peroxiden im stöchiometrischen Verhältnis von 1:1 zu Triphenylphosphinoxid reagiert. Im ^{1}H-^{31}P entkoppelten Kernresonanzspektrum werden die Signale des nicht reagierten Triphenylphosphins bei 7,4 ppm und des reagierten Triphenylphosphinoxid bei 7,8 ppm detektiert. Das Verhältnis beider Signale wird in die Konzentration der Peroxide umgerechnet. 108 Ölproben mit einer Peroxidzahl zwischen 1 meq/kg und 170 meq/kg wurden mit der entwickelten Methode untersucht. Hierbei zeigten Öle mit einer sehr geringen Peroxidzahl von weniger als 3 meq/kg eine relative Standardabweichung von 4,9%, hochoxidierte Öle mit einer Peroxidzahl von 150 meq/kg 0,2%. Die kernresonanzspektroskopische Methode findet Anwendung in der Untersuchung von Krill- und pflanzlichen Ölen.

Eine weitere ^{1}H kernresonanzspektroskopische Methode wurde zur qualitativen Analyse

von Be^{2+}, Sr^{2+} und Cd^{2+} und zur qualitatitativen sowie quantitativen Bestimmung von Ca^{2+}, Mg^{2+}, Hg^{2+}, Sn^{2+}, Pb^{2+} und Zn^{2+} entwickelt. Hierbei wurde Ethylendiamintetraacetat (EDTA) als Komplexbildner verwendet. EDTA ist ein sechszähniger-Ligand, der stabile Chelatkomplexe mit zweiwertigen Kationen bildet. Die definierte Menge an EDTA und das Verhältnis von freier und komplexierter EDTA nach Zugabe der Probe werden für die Rückrechnung der Konzentration der Kationen verwendet. Somit ist der Einsatz eines internen Standards obsolet. EDTA komplexiert Be^{2+}, Sr^{2+}, Cd^{2+}, Ca^{2+}, Mg^{2+}, Hg^{2+}, Sn^{2+}, Pb^{2+} und Zn^{2+} zu stabilen Komplexen, deren Signale im Protonen-Kernresonanzspektrum pH-unabhängige und kationenspezifische chemische Verschiebungen und Kopplungen aufweisen, die zur Identifizierung und Quantifizierung verwendet werden. Die Koaleszenz der Δ und Λ Konfigurationen des EDTA-Komplexes mit Be^{2+}, Sr^{2+} und Cd^{2+} führt bei 298K zu einer Signalverbreiterung, die eine Quantifizierung bei den vorliegenden Parametern unmöglich macht. Die Kationen Ca^{2+}, Mg^{2+}, Hg^{2+}, Sn^{2+}, Pb^{2+} und Zn^{2+} sind ab einer Konzentration von 5-22 μg/mL quantitativ in wässriger Lösung quantifizierbar. Diese Methode kann im Lebensmittel- und Arzneimittelbereich eingesetzt werden.

Die dritte kernresonanzspektroskopische Methode stellt eine neue Bestimmung des Enantiomerüberschusses (ee) in den chiralen Alkoholen Menthol, Borneol, 1-Phenylethanol und Linalool unter Einsatz von Phosgen als Derivatisierungsreagenz vor. Phosgen reagiert mit einem chiralen Alkohol zu Carbonsäurediestern, die aus zwei gleichen (RR, SS) oder zwei unterschiedlichen Enantiomeren (RS, SR) entstehen. Diese zwei Diastereomertypen können anhand der unterschiedlichen, chemischen Verschiebungen ihrer Signale identifiziert werden. In der vorgestellten Methode wird das Carbonylsignal integriert und zur Bestimmung des Enantiomerenüberschusses eingesetzt. Die Bestimmungsgrenze ist hierbei u. a. von dem eingesetzten Phosgen und der Probe abhängig. Bei Menthol wurde eine Bestimmungsgrenze mittels nicht markiertem Phosgen von ee = 99,1% und mittels ^{13}C-markiertem Phosgen von ee = 99,9% ermittelt. Die ^{13}C Methode wurde zudem zur Qualitätskontrolle der Enantiomerreinheit von Borneol, 1-Phenylethanol sowie von Linalool eingesetzt. Hierbei enthielten die käuflich erworbenen Chemikalien (-)-Borneol und (S)-1-Phenylethanol jeweils 1,7% des anderen Enantiomers (+)-Borneol bzw. (R)-1-Phenylethanol. Bei (-)-Linalool konnte ein Enantiomerüberschuss von ee = 66,4% und somit eine größere Verunreinigung durch (+)-Linalool identifiziert werden. Bei Proben, die einen Enantiomerüberschuss von ee $<$ 95,0% aufweisen, sollte eine potentielle, asymmetrische Induktion mittels Kalibrationskurven anhand von künstlichen Enantiomerenmischungen vorab untersucht werden. Die entwickelte ^{13}C kernresonanzspektroskopische Methode präsentiert eine leistungsstarke Alternative zur Analyse mittels Mosher's Reagenz für die Untersuchung des Enantiomerüberschusses in chiralen Alkoholen.

Diese Arbeit weist eine Vielfalt an Möglichkeiten der Anwendungen der quantitativen Kernresonanzspektroskopie in der chemischen Untersuchung von Arzneimitteln, Lebensmitteln und Chemikalien unter Einsatz von Tagging, wie Derivatisierungen und Komplexierungen auf. Die hierbei entwickelten kernresonanzspektroskopischen Methoden repräsentieren leistungsstarke Alternativen zu bisher eingesetzten Techniken der Qualitätskontrolle.

Chapter 9

Abstract

High-resolution nuclear magnetic resonance (NMR) spectroscopy is used in structure elucidation and qualitative as well as quantitative examination of product components. Despite the worldwide development of numerous innovative NMR spectroscopic methods, several official methods that analyze specific substances and do not represent a holistic analysis, are still in use for the quality control of drugs, food and chemicals. Thus, counterfeit or contaminated products of inferior quality can be brought onto the market and distributed despite previous quality controls. To prevent this, three NMR spectroscopic methods have been developed within the scope of this work (1) to study the peroxide value in vegetable and animal oils, (2) for the qualitative and quantitative analysis of metal cations and (3) to determine the enantiomeric excess in chiral alcohols.

In oil analysis, titration methods are used to determine the bulk quality parameters such as peroxide value, which represents the concentration of peroxides. Titrations show several drawbacks, such as the need of a large amount of sample and solvents, cross reactions and the low robustness. Thus, an alternative NMR spectroscopic method was developed to improve the peroxide analysis by using triphenylphosphine as a derivatization reagent, which reacts with peroxides in a stoichiometric ratio of 1:1 forming triphenylphosphine oxide. In the ^{1}H-^{31}P decoupled NMR spectrum, the signals of the unreacted triphenylphosphine and the reacted triphenylphosphine oxide are detected at 7.4 ppm and 7.8 ppm, respectively. The ratio of the two signals is used for the calculation of the peroxide concentration. 108 oil samples with a peroxide value between 1 meq/kg and 150 meq/kg were examined using the developed method. Oils with a very low peroxide value of less than 3 meq/kg showed a relative standard deviation of 4.9%, highly oxidized oils with a peroxide value of 150 meq/kg of 0.2%. The NMR method was demonstrated as a powerful technique for the analysis of vegetable and krill oils.

Another ^{1}H NMR spectroscopic method was developed for the qualitative determination of Be^{2+}, Sr^{2+} and Cd^{2+}, and for the qualitative and quantitative determination of Ca^{2+}, Mg^{2+}, Hg^{2+}, Sn^{2+}, Pb^{2+} and Zn^{2+} by using ethylenediamine tetraacetate (EDTA) as complexing agent. EDTA is a hexadentate ligand that forms stable chelate complexes with

divalent cations. The known amount of added EDTA and the signal ratio of free and complexed EDTA are used to calculate the concentrations of the divalent cations, which makes the use of an internal standard obsolete. The use of EDTA with Be^{2+}, Sr^{2+}, Cd^{2+}, Ca^{2+}, Mg^{2+}, Hg^{2+}, Sn^{2+}, Pb^{2+} and Zn^{2+} result in complexes whose signals are pH-independent, showing cation-specific chemical shifts and couplings in the ^{1}H NMR spectrum that are used for identification and quantification. The coalescence of the Δ and Λ configurations of the EDTA complex with Be^{2+}, Sr^{2+} and Cd^{2+} leads to a signal broadening at 298K that make quantification difficult or even impossible. In the presented NMR method, the limit of quantification of the cations Ca^{2+}, Mg^{2+}, Hg^{2+}, Sn^{2+}, Pb^{2+}, and Zn^{2+} was determined with 5-22 μg/mL. This method is applicable in the food and drug sectors.

The third NMR spectroscopic method introduced an alternative determination of the enantiomer excess (ee) of the chiral alcohols menthol, borneol, 1-phenylethanol and linalool using phosgene as a derivatizing reagent. Phosgene reacts with a chiral alcohol to form carboxylic acid diesters, made of two identical (RR, SS) or two different enantiomers (RS, SR). These two different types of diastereomers can be examined by the difference of their chemical shifts. In the presented method, the integration values of the carbonyl signals in the ^{13}C NMR spectrum are used for the determination of the enantiomer excess. The limit of quantification depends, among others, on the sample and on the non-labelled or ^{13}C-labelled phosgene used for the analysis. In the case of menthol, a quantification limit of ee = 99.1% was determined using non-labelled phosgene and ee = 99.9% using ^{13}C-labelled phosgene. The ^{13}C NMR method was also applied for the quality control of the enantiomeric purity of borneol, 1-phenylethanol and linalool. (-)-borneol and (S)-1-phenylethanol contained 1.7% (+)-borneol and (S)-1-phenylethanol, respectively. In the case of (-)-linalool, an enantiomeric excess of ee = 66.4% was identified, demonstrating a low enantiomeric purity. In the case of samples with an enantiomeric excess of ee <95%, a potential asymmetric induction should be investigated by using calibration curves which have been prepared beforehand on artificial enantiomer mixtures. The developed ^{13}C NMR method represents a powerful alternative to Mosher's reagent for investigating the enantiomeric excess in chiral alcohols.

This work demonstrates the variety of possibilities of applications for the quantitative nuclear magnetic resonance spectroscopy in the chemical analysis of drugs, food and chemicals using tagging reactions such as derivatizations and complexations. The nuclear resonance spectroscopic methods developed in this research work represent powerful alternatives to the previously used quality control techniques.

Bibliography

[1] T. Schoenberger. Determination of Standard Sample Purity Using the High-Precision ^{1}H-NMR Process. *Anal. Bioanal. Chem.*, 403:247–254, 2012.

[2] G. F. Pauli, T. Gödecke, B. U. Jaki, and D. C. Lankin. Quantitative ^{1}H NMR. Development and Potential of an Analytical Method: an Update. *J Nat Prod.*, 75:834–851, 2012.

[3] B. Diehl, U. Holzgrabe, Y. Monakhova, and T. Schönberger. Quo Vadis qNMR? *Journal of Pharmaceutical and Biomedical Analysis.*, 177:112847–112860, 2020.

[4] T. Kuballa, Y. B. Monakhova, I. Straub, M. Kohl-Himmelseher, C. Tschiersch, and D. W. Lachenmeier. Kernresonanzspektroskopie (NMR) und Chemometrie in der amtlichen Überwachung von Lebensmitteln, Kosmetika und Arzneimitteln. *Lebensmittelchemie*, 66:135–138, 2012.

[5] U. Holzgrabe, I. Wawer, and B. Diehl. *NMR Spectroscopy in Pharmaceutical Analysis.* Oxford University Press, Oxford, United Kingdom, 2008.

[6] A. U. Rahman, M. I. Choudhary, and A. T. Wahab. *Solving Problems with NMR Spectroscopy.* Elsevier Inc., London, United Kingdom, 2016.

[7] P. A. Crooks, D. R. Worthen, G. D. Byrd, J. D. deBethizy, and W. S. Caldwell. Modern instrumentan methods for studying mechanisms of toxicology. In A. W. Hayes, editor, *Principles and Methods of Toxicology*, pages 2054–2070. Informa Healthcare, New York, United States of America, 5th edition, 2008.

[8] D. Jun, K. Ma, F. R. van de Voort, and A. A. Ismail. Stoichiometric Determination of Hydroperoxides in Oils by Fourier Transform Near-Infrared Spectroscopy. *JAOAC Int.*, 80:345–352, 1997.

[9] International Conference on Harmonisation (ICH). ICH Q2(R1) Validation of Analytical Procedures: Text and Methodology., 2005.

[10] T. D. W. Claridge. *High-Resolution NMR Techniques in Organic Chemistry.* Elsevier, Amsterdam, Netherlands, 2016. 61-132.

[11] F. Malz and H. Jancke. Validation of Quantitative NMR. *J. Pharm. Biomed. Anal.*, 38:813–823, 2005.

[12] G. Maniara, K. Rajamoorthi, S. Rajan, and G. W. Stockton. Method Performance and Validation for Quantitative Analysis by ^{1}H and ^{31}P NMR Spectroscopy. Applications to Analytical Standards and Agricultural Chemicals. *Anal. Chem.*, 70:4921–4928, 1998.

[13] A. E. Derome. *Modern NMR Techniques for Chemistry Research.* Pergamon Books Inc., Elmsford, United States of America, 1987.

[14] P. A. Hays and T. Schoenberger. Uncertainty Measurement for Automated Macroprogram-Processed Quantitative Proton NMR Spectra. *Anal. Bioanal. Chem.*, 406:7397–7400, 2014.

[15] T. D.W. Claridge. *High-Resolution NMR Techniques in Organic Chemistry.* Elsevier Ltd, Amsterdam, Netherlands, 2016.

[16] T. Schönberger. Guideline for qNMR Analysis. Technical report, Bundeskriminalamt, Wiesbaden, Germany, 2019. `https://bit.ly/34ezOIU`, accessed 02 March 2020.

[17] R. Kaarls. The Consultative Committee for Metrology in Chemistry and Biology – CCQM. *J. Chem. Metrol.*, 12:1–16, 2018.

[18] B. King. The Practical Realization of the Traceability of Chemical Measurements Standards. *Accred Qual Assur*, 5:429–436, 2000.

[19] Consultative Committee on the Quantity of Material (CCQM). Minutes from the Fifth Meeting (February 1998) of the Consultative Committee on the Quantity of Material (CCQM) of the Bureau International des Poids et Mesures (BIPM), 1998.

[20] H. Jancke, F. Malz, and W. Haesselbarth. Structure Analytical Methods for Quantitative Reference Applications. *Accred. Qual. Assur.*, 10:421–429, 2005.

[21] H. Jancke. NMR als Primäre Analytische Messmethode. *Nachr. Chem. Tech. Lab.*, 46:20–722, 1998.

[22] S. K. Bharti and R. Roy. Quantitative ^{1}H NMR Spectroscopy. *Trends Analyt. Chem.*, 35:5–26, 2012.

[23] J. Vial and A. Jardy. Quantitation by standard addition. In J. Cazes, editor, *Encyclopedia of Chromatography*, page 696. Marcel Dekker, Inc., New York, United States of America, 2001.

[24] Sigma Aldrich, St. Louis, United States of America. *Pharmaceutical Secondary Standards.*, 2015. `https://bit.ly/3kav5yP`, accessed 18 October 2020.

[25] C. A. Gonzalez. NIST PS1 Primary Standard for Quantitative NMR (Benzoic Acid)., 2018. `https://bit.ly/2SyyQ4V`, accessed 06 October 2020.

[26] P. A. Winslow and R. F. Meyer. Validating analytical methods for pharmaceutical applications: A comprehensive approach. In C. Medina, editor, *Compliance Handbook for Pharmaceuticals, Medical Devices, and Biologics*, pages 109–158. Marcel Dekker, Inc., New York, United States of America, 2004.

[27] Merck KGaA. TraceCERT(R) CRMs for Quantitative NMR (qNMR)., 2020. `https://bit.ly/34vsOYl`, accessed 06 October 2020.

[28] M. Weber, C. Hellriegel, A. Rück, R. Sauermoser, and J. Wüthrich. Using High-PerformanceQquantitative NMR (HP-qNMR) for Certifying Traceable and Highly Accurate Purity Values of Organic Reference Materials with Uuncertainties $< 0.1\%$. *Accred. Qual. Assur.*, 18:91–98, 2013.

[29] T. S. Al-Deen, D. B. Hibbert, J. M. Hook, and R. J. Wells. An Uncertainty Budget for the Determination of the Purity ofGglyphosate by Quantitative Nuclear Magnetic Resonance (QNMR) Spectroscopy. *Accred. Qual. Assur.*, 9:55–63, 2004.

[30] T. Kitayama and K. Hatada. *NMR Spectroscopy of Polymers.* Springer Verlag, Heidelberg, Germany, 2004.

[31] T. Rundlöf, M. Mathiasson, S. Bekiroglu, B. Hakkarainen, T. Bowden, and T. Arvidsson. Survey and Qualification of Internal Standards for Quantification by ^{1}H NMR Spectroscopy. *J. Pharm. Biomed. Anal.*, 52:645–651, 2010.

[32] European Directorate for the Quality of Medicines & HealthCare (EDQM). Ph. Eur. Method 01/2009:20233: Nuclear Magnetic Resonance Spectroscopy., 2009.

[33] European Directorate for the Quality of Medicines & HealthCare (EDQM). Ph. Eur. Method 07/2011:20264: Peptide Identification by Nuclear Magnetic Resonance Spectrometry., 2011.

[34] European Directorate for the Quality of Medicines & HealthCare (EDQM). Ph. Eur. Method 07/2017:2350: Medronic acid for Radiopharmaceutical Preparations., 2017.

[35] European Directorate for the Quality of Medicines & HealthCare (EDQM). Ph. Eur.Method 01/2016:1077 corrected 10.0: Buserelin., 2016.

[36] European Directorate for the Quality of Medicines & HealthCare (EDQM). Ph. Eur. Method 07/2012:2398: Cod-Liver Oil, Farmed., 2012.

[37] European Directorate for the Quality of Medicines & HealthCare (EDQM). Ph. Eur. Method 04/2018:0827 corrected 10.0: Gonadorelin Acetate., 2018.

[38] European Directorate for the Quality of Medicines & HealthCare (EDQM). Ph. Eur. Method 01/2013:1636 corrected 9.6: Goserelin., 2013.

[39] European Directorate for the Quality of Medicines & HealthCare (EDQM). Ph. Eur. Method 01/2020:0332: Heparin Calcium., 2020.

[40] European Directorate for the Quality of Medicines & HealthCare (EDQM). Ph. Eur. Method 01/2020:0333: Heparin Sodium., 2020.

[41] European Directorate for the Quality of Medicines & HealthCare (EDQM). Ph. Eur. mMethod 07/2019:0828 corrected 10.0: Heparins, Low-Molecular-Mass., 2019.

[42] European Directorate for the Quality of Medicines & HealthCare (EDQM). Ph. Eur. Method 01/2017:1804: Hydroxypropylbetadex., 2017.

[43] European Directorate for the Quality of Medicines & HealthCare (EDQM). Ph. Eur. Method 01/2020:2046: Lauromacrogol 400., 2020.

[44] European Directorate for the Quality of Medicines & HealthCare (EDQM). Ph. Eur. Method 01/2020:2414 : Octreotide., 2020.

[45] European Directorate for the Quality of Medicines & HealthCare (EDQM). Ph. Eur. Method 01/2017:2637 corrected 10.0: Pemetrexed Disodium Heptahydrate., 2017.

[46] European Directorate for the Quality of Medicines & HealthCare (EDQM). Ph. Eur. Method 07/2012:1910: Salmon Oil, Farmed., 2012.

[47] European Directorate for the Quality of Medicines & HealthCare (EDQM). Ph. Eur. Method 01/2013:2165 corrected 10.0: Starch, Hydroxypropyl., 2013.

[48] European Directorate for the Quality of Medicines & HealthCare (EDQM). Ph. Eur. Method 07/2013:2645 corrected 10.0: Starch, Hydroxypropyl, Pregelatinised., 2013.

[49] European Directorate for the Quality of Medicines & HealthCare (EDQM). Ph. Eur. Method 07/2019:2804 corrected 10.0: Sulfobutylbetadex sodium., 2019.

[50] European Directorate for the Quality of Medicines & HealthCare (EDQM). Ph. Eur. Method 07/2017:2646: Terlipressin., 2017.

[51] United States Pharmacopeia (USP). <761> Nuclear Magnetic Resonance Spectroscopy.

[52] United States Pharmacopeia (USP). <1761> Applications of Nuclear Magnetic Resonance Spectroscopy.

[53] B. Casu, A. Naggi, and G. Torri. Re-visiting the Structure of Heparin. *Carbohydr. Res.*, 403:60–68, 2015.

[54] K. Szczubiałka, K. Kaminski, K. Zasada, A. Karewicz, and M. Nowakowska. Heparin - A Key Drug in the Treatment of the Circulatory Degenerative Diseases: Controlling its Action with Polymers. *Curr. Pharm. Des.*, 18:2591–2606, 2012.

[55] A. Gómez-Outes, M. L. Suárez-Gea, G. Calvo-Rojas, R. Lecumberri, E. Rocha, C. Pozo-Hernández, A. I. Terleira-Fernández, and E. Vargas-Castrillón. Discovery of Anticoagulant Drugs: a Historical Perspective. *Curr. Drug Discov. Technol.*, 9:83–104, 2012.

[56] United States Pharmacopeia (USP). Revision Bulletin: Heparin Sodium and Heparin Calcium Monographs, 2018. `https://bit.ly/3aLcSTH`, accessed 17 July 2020.

[57] European Directorate for the Quality of Medicines & HealthCare (EDQM). Workshop On The Characterisation Of Heparin Products. `https://bit.ly/3fvR9kp`, 2008. accessed 03 June 2020.

[58] U. S. Food and Drug Administration (FDA). Information on Heparin., 2018. `https://bit.ly/2XcCrtc`, accessed 30 March 2020.

[59] European Directorate for the Quality of Medicines & HealthCare (EDQM). European Pharmacopoeia Heparin Sodium Monograph PA/PH/Exp. 6/T(0) 42 PUB Monograph Number 333., 2008. `https://bit.ly/3dUD0Ox`, accessed 30 March 2020.

[60] Pharmaceuticals and Medical Devices Agency. Japanese Pharmacopoeia (JP) XVII, Monograph: Heparin Sodium [9041-08-1]., 2016. `https://bit.ly/2RfZ1gJ`, accessed 30 March 2020.

[61] T. Beyer, M. Matz, D. Brinz, O. Rädler, B. Wolf, J. Norwig, K. Baumann, S. Alban, and U. Holzgrabe. Composition of OSCS-Contaminated Heparin Occurring in 2008 in Batches on the German Market. *Eur. J. Pharm. Sci.*, 40:297–304, 2010.

[62] M. Feliz, M. A. Molins, M. Gairí, V. Muñoz-Torrero, and T. Gonzalez. Handbook of Instrumental Techniques from CCiTUB: Nuclear Magnetic Resonance. `https://bit.ly/3fuksDK`, assessed 13 May 2020, 2012.

[63] A. W. Birley, R. J. Heath, and M. J. Scott. *Plastisa Materials - Properties and Applications.* Blackie Academic & Professional, Glasgow, United Kingdom, 1988.

[64] n.d. Vortäuschen höherer Eiweißgehalte: Grenzen der Stickstoffbestimmung nach Kjeldahl. *Süsswaren*, 11:1, 2008. `https://bit.ly/33Jdf0J`, accessed 07 August 2020.

[65] H. Ogasawara H, K. Imaida, H. Ishiwata, K. Toyoda, T. Kawanishi, C. Uneyama, S. Hayashi, M. Takahashi, and Y. Hayashi. Urinary Bladder Carcinogenesis Induced by Melamine in F344 Male Rats: Correlation Between Carcinogenicity and Urolith Formation. *Carcinogenesis*, 16:2773–2777, 1995.

[66] J. Erling. Melamin-Skandal weitet sich aus. `https://bit.ly/2RfC9xE`, 9 2008. accessed 05 April 2020.

[67] D. W. Lachenmeier, E. Humpfer, F. Fang, B. Schütz, P. Dvortsak, C. Sproll, and M. Spraul. NMR-Spectroscopy for Nontargeted Screening and Simultaneous Quantification of Health-Relevant Compoundsin Foods: The Example of Melamine. *J. Agric. Food Chem.*, 57:7194–7199, 2009.

[68] World Health Organization (WHO), Geneva, Switzerland. *Toxicological and Health Aspects of Melamine and Cyanuric Acid.*, 2009. `https://bit.ly/2VhuYGL`, accessed 05 April 2020.

[69] UN Food and Agriculture Organization. UN Strengthens Regulations on Melamine, Seafood, Melons, Dried Figs and Labelling. `https://bit.ly/2x36sRi`, 9 2008. accessed 05 April 2020.

[70] S. M. Watkins and J. B. German. Unsaturated fatty acids. In C. C. Akoh and D. B. Min, editors, *Food Lipids: Chemistry, Nutrition, and Biotechnology.*, pages 559–588. Marcel Dekker, Inc., New York, United States of America, 2002.

[71] F. Shahid. Antioxidants in Food and Food Antioxidants. *Food/Nahrung*, 44:158–163, 2000.

[72] J. Kanner and I. Rosenthal. An Assessment of Lipid Oxidation in Foods. *Pure & Appl. Chem.*, 64:1959–1964, 1992.

[73] F. Shahidi and Y. Zhong. Lipid oxidation: Measurement methods. In F. Shahidi, editor, *Bailey's Industrial Oil and Fat Products.*, pages 357–385. John Wiley & Sons, Inc., Hoboken, United States of America, 2005.

[74] M. Gordon. The development of oxidative rancidity in foods. In J. Pokorny, N. Yanishlieva, and M. Gordon, editors, *Antioxidants in Food: Practical Applications.*, pages 7–21. Woodhead Publishing, Ltd., Cambridge, United Kingdom, 2001.

[75] A. Kamal-Eldin and D. B. Min. *Lipid Oxidation Pathway.* AOCS Press, Urbana, United States of America, 2nd edition, 2008.

[76] R. J. Hsieh and J. E. Kinsella. Oxidation of Polyunsaturated Fatty Acids: Mechanisms, Products, and Inhibition with Emphasis on Fish. *Adv. Fd. Nutr. Res.*, 33:233–341, 1989.

[77] E. Choe. Effect and mechanisms of minor compounds in oil and lipid oxidation. In C. C. Akoh and D. B. Min, editors, *Food Lipids: Chemistry, Nutrition, and Biotechnology.*, pages 449–474. CRC Press, Boca Raton, United States of America, 2008.

[78] X. Huang and D. U. Ahn. Lipid oxidation and its implications to meat quality and human health. *Food Sci. Biotechnol.*, 28:1275–1285, 2019.

[79] F. R. van de Voort, A. A. Ismail, J. Sedman, J. Dubois, and T.Nicodemo. The Determination of Peroxide Value by Fourier Transform Infrared Spectroscopy. *J. Am. Oil Chem. Soc.*, 71:921–926, 1994.

[80] H. Li, F. R. van de Voort, A. A. Ismail, and R. Cox. Determination of Peroxide Value by Fourier Transform Near-Infrared Spectroscopy. *J. Am. Oil Chem. Soc.*, 77:137–142, 2000.

[81] F. D. Gustone. High resolution ^{13}c nmr spectroscopy of lipids. In W. W. Christie, editor, *Advances in Lipid Methodology - Two.*, pages 1–68. The Oily Press, Dundee, Scotland, 1993.

[82] A. W. Claxson, G. E. Hawkes, D. P. Richardson, D. P Naughton, R. M. Haywood, C. L. Chander, M. Atherton, E. J. Lynch, and M. C. Grootveld. Generation of Lipid Peroxidation Products in Culinary Oils and Fats During Episodes of Thermal Stressing: a High ^{1}H NMR Study. *FEBS Lett.*, 355:81–90, 1994.

[83] R. M. Haywood, A. W. D. Claxon, G. E. Hawkes, D. P. Richardson, D. P. Naughton, G. Coumbarides, J. Hawkes, E. J. Lynch, and M. C. Grootveld. Detection of Aldehydes and their Conjugated Hydroperoxydiene Precursors in Thermally-Stressed Culinary Oils and Fats: Investigations using High Resolution Proton NMR Spectroscopy. *Free Radic. Res.*, 22:441–482, 1995.

[84] I. Medina, R. Sacchi, I. Giudicianni, and S. Aubourg. Oxidation in Fish Lipids During Thermal Stress as Studied by ^{13}C Nuclear Magnetic Resonance Spectroscopy. *J. Am. Oil Chem. Soc.*, 75:147–154, 1998.

[85] C. J. Silwood and M. Grootveld. Application of High-Resolution, Two-Dimensional ^{1}H and ^{13}C Nuclear Magnetic Resonance Techniques to the Characterization of Lipid Oxidation Products in Autoxidized Linoleoyl/Linolenoylglycerols. *Lipids*, 34:741–756, 1999.

[86] M. D. Guillén and A. Ruiz. Formation of Hydroperoxy- and Hydroxyalkenals During Thermal Oxidative Degradation of Sesame oil Monitored by Proton NMR. *Eur. J. Lipid Sci. Technol.*, 106:680–687, 2004.

[87] M. D. Guillén and A. Ruiz. Study by Means of ^{1}H Nuclear Magnetic Resonance of the Oxidation Process Undergone by Edible Oils of Different Natures Submitted to Microwave Action. *Food Chem.*, 96:665–674, 2006.

[88] M. D. Guillén and A. Ruiz. Monitoring of Heat-Induced Degradation of Edible Oils by Proton NMR. *Eur. J. Lipid Sci. Technol.*, 110:52–60, 2008.

[89] M. D. Guillén and E. Goicoechea. Oxidation of Corn Oil at Room Temperature: Primary and Secondary Oxidation Products and Determination of Their Concentration in the Oil Liquid Matrix from ^{1}H Nuclear Magnetic Resonance Data. *Food Chem.*, 116:183–192, 2009.

[90] M. D. Guillén and P.S. Uriate. Contribution to Further Understanding of the Evolution of Sunflower Oil Submitted to Frying Temperature in a Domestic Fryer: Study by ^{1}H Nuclear Magnetic Resonance. *J. Agric. Food Chem.*, 57:7790–7799, 2009.

[91] C. Skiera, P. Steliopoulos, T. Kuballa, U. Holzgrabe, and B. Diehl. ^{1}H-NMR Spectroscopy as a New Tool in the Assessment of the Oxidative State in Edible Oils. *J. Am. Oil Chem. Soc.*, 89:1383–1391, 2012.

[92] C. Skiera, P. Steliopoulos, T. Kuballa, U. Holzgrabe, and B. Diehl. ^{1}H NMR Approach as an Alternative to the Classical p-Anisidine Value Method. *Eur. Food Res. Technol.*, 235:1101–1105, 2012.

[93] D. H. Wheeler. Peroxide Formation as a Measure of Autoxidative Deterioration. *Oil and Soap*, 9:89–97, 1932.

[94] T. N. Mitchell and B. Costisella. *NMR - From Spectra to Structures: An Experimental Approachs.* Springer, Heidelberg, Germany, 2004.

[95] Y. B. Monakhova, T. Kuballa, C. Tschiersch, and B. W. K. Diehl. Rapid NMR Determination of Inorganic Cations in Food Matrices: Application to Mineral Water. *Food Chem.*, 221:1828–1833, 2017.

[96] The Hebrew University of Jerusalem. (Cd) Cadmium NMR. `https://bit.ly/31TYR2W`, accessed 14 August 2020.

[97] A. L. Johnson, N. Hollingsworth, G. Kociok-Köhn, and K. C. Molloy. Organocadmium Aminoalcoholates: Synthesis, Structure, and Materials Chemistry. *Inorg. Chem.*, 47:9706–9715, 2008.

[98] N. Hertkorn, E. M. Perdue, and A. Kettrup. A Potentiometric and ^{113}Cd NMR Study of CadmiumComplexation by Natural Organic Matter at Two Different Magnetic Field Strengths. *Anal. Chem.*, 76:6327–6341, 2004.

[99] I. M. Armitage, T. Drakenberg, and B. Reilly. Use of ^{113}Cd NMR to Probe the Native Metal Binding Sites in Metalloproteins: An Overview. *Met Ions Life Sci.*, 11:117–144, 2013.

[100] B. Wrackmeyer. Fundamentals in tin chemistry. In A. G. Davies, M. Gielen, K. H. Pannell, and E. R. T. Tiekink, editors, *Tin Chemistry: Fundamentals, Frontiers, and Applications*, pages 17–45. Wiley, Chichester, United Kingdom, 2008.

[101] The Hebrew University of Jerusalem. (Sn) Tin NMR. `https://bit.ly/3jgCpbk`, accessed 28 August 2020.

[102] L. Wang, C. E. Kefalidis, T. Roisnel, S. Sinbandhit, L. Maron, J.-F. Carpentier, and Y. Sarazin. Structure vs ^{119}Sn NMR Chemical Shift in Three-Coordinated Tin(II)Complexes: Experimental Data and Predictive DFT Computations. *Organometallics*, 34:2139–2150, 2015.

[103] ^{119}sn-nmr parameters. volume 16 of *Annual Reports on NMR Spectroscopy*, pages 73 – 186. Academic Press, 1985.

[104] The Hebrew University of Jerusalem. (^{207}Pb) Lead NMR. `https://bit.ly/2YQpKnA`, accessed 31 August 2020.

[105] ^{207}pb-nmr parameters. volume 22 of *Annual Reports on NMR Spectroscopy*, pages 249 – 306. Academic Press, 1990.

[106] The Hebrew University of Jerusalem. (Hg) Mercury NMR. `https://bit.ly/3anFSl8`, accessed 14 August 2020.

[107] G. Moreno-Alcántar, M. Arroyo, J. L. Bautista, S. Bernès, N. Esturau-Escofet, and H. Torrens. Polyfluorinated mercury thiolates. ^{199}Hg NMR studies and the crystal structure of [Hg($SC_6H_4(CF_3)$-2)$_2$]. *J. Fluor. Chem*, 156:61–65, 2013.

[108] M. L. Helm, G. P. Helton, D. G. VanDerveer, and G. J. Grant. Mercury-199 NMR Studies of Thiacrown and Related Macrocyclic Complexes: The Crystal Structures of [Hg(18S6)]$(PF_6)_2$ and [Hg(9N3)$_2$]$(ClO_4)_2$. *Inorg. Chem.*, 44:5696–5705, 2005.

[109] Y. B. Monakhova, G. Randel, and B. W. K. Diehl. Automated Control of the Organic and Inorganic Composition of Aloe Vera Extracts Using ^{1}H NMR Spectroscopy. *J. AOAC Int.*, 99:1213–1218, 2016.

[110] K. Jozwiak, W. J. Lough, and I. W. Waine. *Drug Stereochemistry: Analytical Methods and Pharmacology (Drugs and the Pharmaceutical Sciences).* CRC Press, Boca Raton, United States of America, 3rd edition, 2012.

[111] W. Xiaowen and Z. Wu. Stereoselective Metabolic and Pharmacokinetic Analysis of the Chiral Active Components from Herbal Medicines. *Curr. Pharm. Anal.*, 6:39–52, 2010.

[112] W. Brown, C. Foote, B. Iverson, and E. Anslyn. *Organic Chemistry.* Brooks/Cole Cengage Learning, Belmont, United States of America, 2009.

[113] G. Q. Lin, Q. D. You, and J. F. Cheng. *Chiral Drugs: Chemistry and Biological Action.* Wiley, Hoboken, United States of America, 1st edition, 2011.

[114] H. Caner, E. Groner, L. Levy, and I. Agranat. Trends in the Development of Chiral Drugs. *Drug Discov. Today*, 9:105–110, 2004.

[115] S. C. Stinson. Chiral Pharmaceuticals. *Chem Eng News*, 79:79–97, 2001.

[116] V. Gulati. Differential Properties of Enantiomers of Commercially Available Racemates. *J. Indian Med. Assoc.*, 105:173–174, 2007.

[117] U.S. Food and Drug Administration (FDA). Development of New Stereoisomeric Drugs. `https://bit.ly/3ezexwZi`, 5 1992. accessed 19 July 2020.

[118] European Medicines Agency (EMA). Investigation of Chiral Active Substances. `https://bit.ly/2OIVSEB`, 4 1994. accessed 19 July 2020.

[119] B. W. K. Diehl and U. Holzgrabe. Determination of the isomeric composition of drugs. In U. Holzgrabe, I. Wawer, and B. Diehl, editors, *NMR Spectroscopy in Drug Development and Analysis.*, pages 85–100. Wiley-VCH, Weinheim, Germany, 1999.

[120] G. P. Moss. Basic Terminology of Stereochemistry (IUPAC Recommendations 1996). *Pure and Applied Chemistry*, 68:2193–2222, 1996.

[121] K. Mori. Synthesis of Optically Active Pheromones. *Tetrahedron*, 45:3233–3298, 1989.

[122] Y. Okamoto and T. Ikai. Chiral HPLC for Efficient Resolution of Enantiomers. *Chem. Soc. Rev.*, 37:2593–2608, 2008.

[123] R. Kühnreich and U. Holzgrabe. High-Performance Liquid Chromatography Evaluation of the Enantiomeric Purity of Amino Acids by means of Automated Precolumn Derivatization with Ortho-Phthalaldehyde and Chiral Thiols. *Chirality*, 28:795–804, 2016.

[124] T. J. Wenzel. Chiral derivatization agents, macrocycles, metal complexes, and liquid crystals for enantiomer differentiation in nmr spectroscopy. In V. Schurig, editor, *Differentiation of Enantiomers II*, pages 1–68. Springer, Heidelberg, Germany, 2013.

[125] R. Benshafrut and R. Rothchild. NMR Studies of Drugs. Enantiomeric Excess Determination of N-acetylcathinone with $Eu(HFC)_3$. *Spectroscopy Letters*, 25:1097–1120, 1992.

[126] J. A. Dale, D. L. Dull, and H. S. Mosher. α-Methoxy-α-Trifluoromethylphenylacetic Acid, a Versatile Reagent for the Determination of Enantiomeric Composition of Alcohols and Amines. *J. Org. Chem.*, 34:2543–2549, 1969.

[127] T. R. Hoye, C. S. Jeffrey, and F. Shao. Mosher Ester Analysis for the Determination of Absolute Configuration of Stereogenic (Chiral) Carbinol Carbons. *Nature Protocols*, 2:2451–2458, 2007.

[128] H. Friebolin. *Ein- und zweidimensionale NMR-Spektroskopie*. Wiley-VCH, Weinheim, Germany, 4th edition, 2006.

[129] B. Berendt and C. Hanser, editors. *Tags are not metadata, but 'just more content'—to some people*, Boulder, United States of America, March 2007. International Joint Conferences on Artificial Intelligence.

[130] C. Jing and V. W. Cornish. Chemical Tags for Labeling Proteins Inside Living Cells. *Acc. Chem. Res.*, 44:784–792, 2011.

[131] E. Zailer, U. Holzgrabe, and B. W. K. Diehl. Interlaboratory Comparison Test as an Evaluation of Applicability of an Alternative Edible Oil Analysis by ^{1}H NMR Spectroscopy. *J. AOAC Int.*, 100:1819–1830, 2017.

[132] M. D. Guillén and A. Ruiz. High Resolution ^{1}H Nuclear Magnetic Resonance in the Study of Edible Oils and Fats. *Trends Food Sci. Technol.*, 12:328–338, 2001.

[133] F. J. Hidalgo and R. Zamora. Edible oil Analysis by High-Eesolution Nuclear Magnetic Resonance Spectroscopy: Recent Advances and Future Perspectives. *Trends Food Sci. Technol.*, 14:499–506, 2003.

[134] European Directorate for the Quality of Medicines & HealthCare (EDQM). *Ph. Eur., Ch. 2.5.1.* Strasbourg, France, 8th edition, 2015.

[135] German Society for Fat Science e.V. DGF-C-V(06).

[136] American Oil Chemists' Society (AOCS). Official Methods and Recommended Practices of the American Oil Chemists' Society (AOCS): AOCS Cd 3d-63(09).

[137] European Directorate for the Quality of Medicines & HealthCare (EDQM). *Ph. Eur., Ch. 2.5.5.* Strasbourg, France, 8th edition, 2015.

[138] European Directorate for the Quality of Medicines & HealthCare (EDQM). *Ph. Eur., Ch. 2.5.4.* Strasbourg, France, 8th edition, 2015.

[139] German Society for Fat Science e.V. DGF C-V 11a(02) Hanus.

[140] American Oil Chemists' Society (AOCS). AOCS Cd 1e01(09) by NIR.

[141] International Organization for Standardization. ISO 3961:2009: Animal and Vegetable Fast and Oils - Determination of Iodine Value., 2009.

[142] C. Skiera, P. Steliopoulos, T. Kuballa, U. Holzgrabe, and B. Diehl. Determination of Free Fatty Acids in Edible Oils by ^{1}H NMR Spectroscopy. *Lipid Technol.*, 24:279–281, 2012.

[143] N. A. Porter, K. A. Mills, and R. L. Carter. A Mechanistic Study of Oleate Autoxidation: Competing Peroxyl H-Atom Abstraction and Rearrangement. *J. Am. Chem. Soc.*, 116:6690–6696, 1994.

[144] H. W. S Chan and G. Levett. Autoxidation of Methyl Linoleate. Separation and Analysis of Isomeric Mixtures of Methyl Linoleate Hydroperoxides and Methyl Hydroxylinoleates. *Lipids*, 12:99–104, 1977.

[145] E. N. Frankel. Review. Recent Advances in Lipid Oxidation. *J. Sci. Food Agric.*, 54:495–511, 1991.

[146] Y. Li, A. G. Webb, S. Saha, W. W. Brey, C. Zachariah, and A. S. Edison. Comparison of the Performance of Round and Rectangular Wire in Small Solenoids for High-Field NMR. *Magn. Reson. Chem.*, 44:255–262, 2006.

[147] J. L. Griffin, A. W. Nicholls, H. C. Keun, R. J. Mortishire-Smith, J. K. Nicholson, and T. Kuehn. Metabolic Profiling of Rodent Biological Fluids via ^{1}H NMR Spectroscopy Using a 1 mm Microlitre Probe. *Analyst*, 127:582–584, 2002.

[148] U Holzgrabe. Quantitative NMR Spectroscopy in Pharmaceutical Applications. *Prog. Nucl. Mag. Res. Sp.*, 57:229–240, 2010.

[149] H. de Brouwer. Evaluation of algorithms for automated phase correction of nmr spectra. *J. Magn. Reson.*, 201:230–238, 2009.

[150] D. Chang, C. D. Banack, and S. L. Shah. Robust baseline correction algorithm for signal dense nmr spectra. *J. Magn. Reson.*, 187:288–292, 2007.

[151] C. Bartels, P. Guntert, and K. Wuthrich. IFLAT-A New Automatic Baseline-Correction Method for Multidimensional NMR Spectra with Strong Solvent Signals. *J. Magn. Reson.*, A117:330–333, 1995.

[152] American Oil Chemists' Society (AOCS). Official Methods and Recommended Practices of the AOCS: AOCS Cd 8b-90.

[153] International Organization for Standardization. DIN EN ISO 3960:2007, German Version of EN ISO 3960:2010., 2010.

[154] E. Hafer, U.Holzgrabe, S. Wiedemann, K. M. Adams, and B. W. K. Diehl. NMR Spectroscopy: Determination of Peroxide Value in Vegetable and Krill Oil by using Triphenylphosphine as Tagging Reagent. *Eur. J. Lipid Sci. Technol.*, 122:1900442–1900452, 2020.

[155] B. Burlingame, C. Nishida, R. Uauy, and R. Weisell. Fats and Fatty Acids in Human Nutrition: Introduction. *Ann. Nutr. Metab.*, 55:5–7, 2009.

[156] A. M. Rabasco Alvarez and M. L. González Rodríguez. Lipids in Pharmaceutical and Cosmetic Preparations. *Grasas y Aceites*, 51:74–96, 2000.

[157] P. Kalustian. Pharmaceutical and Cosmetic Uses of Palm and Lauric Products. *J. Am. Oil Chem. Soc.*, 62:431–433, 1985.

[158] D. B. Min and J. M. Boff. Chemistry and Reaction of Singlet Oxygen in Foods. *Comp. Rev. Food. Sci. and Food Saf.*, 1:58–72, 2002.

[159] E. Choe and D. B. Min. Mechanisms and Factors for Edible Oil Oxidation. *Comp. Rev. Food. Sci. and Food Saf.*, 5:169–186, 2006.

[160] E. N Frankel. *Lipid Oxidation.* The Oily Press, Dundee, United Kingdom, 2005.

[161] E. N. Frankel. Lipid Oxidation. *Prog. Lipid Res.*, 19:1–22, 1980.

[162] J. H. Cheng. Lipid Oxidation in Meat. *J. Nutr. Food Sci.*, 6:1–3, 2016.

[163] C. H. Lea. The Dffect of Light on the Oxidation of Fats. *Proc. Soc. Lond.*, 108 B:175–189, 1931.

[164] D. Firestone. Official Methods and Recommended Practices of the AOCS, Method Cd 8b-90., 2009.

[165] International Organization for Standardization. DIN EN ISO 3960, Animal and Vegetable Fats and Oils - Determination of Peroxide Value - Iodometric (Visual) Endpoint Determination (ISO 3960:2007, corrected Version 2009-05-15); German Version EN ISO 3960:2010., 2010.

[166] European Directorate for the Quality of Medicines & HealthCare (EDQM). Ph. Eur. 9.0, 20506 (01/2008)., 2008.

[167] Deutsche Gesellschaft für Fettwissenschaft e.V. (DGF). Peroxide Value, DGF Standard Methods, C-VI 6a Part 1 (05) 10th Supplement, 10/2005., 2005.

[168] A. Ruíz and B. Lendl. A Rapid Method for Peroxide Value Determination in Edible Oils Based on Flow Analysis with Fourier Transform Infrared Spectroscopic Detection. *Analyst*, 126:242–246, 2001.

[169] M. C. Dobarganes and J. Velasco. Analysis of Lipid Hydroperoxides. *Eur. J. Lipid Sci. Technol.*, 104:420–428, 2002.

[170] H. J. Fiebig. Peroxide Value Determination. *Inform*, 14:651, 2003.

[171] V. C. Mehlenbacher. *Analysis of Fats and Oils.* The Garrard Press, Champaign, United States of America, 1960.

[172] C. Skiera, P. Steliopoulos, T. Kuballa, U. Holzgrabe, and B. Diehl. ^{1}H-NMR Spectroscopy as a New Tool in the Assessment of the Oxidative State in Edible Oils. *J. Am. Oil Chem. Soc.*, 89:1383–1391, 2012.

[173] R. H. Liu. Dietary Bioactive Compounds and Their Health Implications. *J. Food Sci.*, 78:A18–A25, 2013.

[174] Commission of the European Communities. Commission Regulation (EEC) No 2568/91 of 11 July 1991 on the Characteristics of Olive Oil and Olive-Residue Oil and on the Relevant Methods of Analysis, OJ L 248., 1991.

[175] A. Kamal-Eldin and J. Pocorny. *Analysis of Lipid Oxidation.* AOCS Press, Champaign, United States of America, 2005.

[176] G. Yildiz, R. L. Wehling, and S. L. Cuppett. Comparison of Four Analytical Methods for the Determination of Peroxide Value in Oxidized Soybean Oils. *J. Am. Oil Chem. Soc.*, 80:103–107, 2003.

[177] H. Saito. Estimation of the Oxidative Deterioration of Fish Oils by Measurements of Nuclear Magnetic Resonance. *Agric. Biol. Chem.*, 51:3433–3435, 1987.

[178] U. N. Wanasundara F. Shahidi. Natural oxidants: An overview. In F. Shahidi, editor, *Natural antioxidants—chemistry, health effects, and applications.*, pages 1–11. AOCS Press, Champaign, United States of America, 1997.

[179] H. A. Abou-Gharbia, F. Shahidi, A. A. Shehata, and M. M. Youssef. Effects of Processing on Oxidative Stability of Sesame Oil Extracted from Intact and Dehulled Seeds. *J. Am. Oil Chem. Soc.*, 74:215–221, 1997.

[180] L. Horner and W. Jürgeleit. Die Reduktion organischer Peroxyde mit tertiären Phosphinen Tertiäre Phosphine VI. *Justus Liebigs Annalen der Chemie*, 591:138–152, 1955.

[181] M. D. Guillén and A. Ruiz. High Resolution ^{1}H Nuclear Magnetic Resonance in the Study of Edible Oils and Fats. *Trends Food Sci. Technol.*, 12:328–338, 2001.

[182] M. D. Guillén and A. Ruiz. ^{1}H Nuclear Magnetic Resonance as a Fast Tool for Determining the Composition of Acyl Chains in Acylglycerol Mixtures. *Eur. J. Lipid Sci. Technol.*, 105:502–507, 2003.

[183] Thea Norveel Semb. Analytical Methods for Determination of the Oxidative Status in Oils., 2012. `https://core.ac.uk/download/pdf/52102612.pdf`, accessed 12 August 2020.

[184] T. Schönberger, Y. B. Monakhova, D. W. Lachenmeier, and T. Kuballa. Technical Report No. 01/ 2014, Guide to NMR Method Development and Validation - Part I:

Identification and Quantification. Technical Report 1, European Federation of National Associations of Measurement, Testing and Analytical Laboratories, Brussels, Belgium, 7 2014. `https://bit.ly/2ReLg1D`, accessed 04 April 2020.

[185] A. Barbosa, G. D. Silveira, I. de Menezes, J. Neto, J. Bitencurt, C. D. Estavam, A. de Lima, S. M. Thomazzi, A. G. Guimaraes, L. J. Quintans, and M. R. dos Santos. Antidiabetic Effect of the Chrysobalanus icaco L. Aqueous Extract in Rats. *J. Med. Food*, 16:538–543, 2013.

[186] European Food Safety Authority. Scientific Opinion on the Re-Evaluation of Butylated Hydroxytoluene BHT (E 321) as a Food Additive. *EFSA Journal*, 10:2588–2631, 2012.

[187] C. Deyrieux, P. Villeneuve, B. Baréa, E. A. Decker, I. Guiller, F. M. Salaun, and E. Durand. Measurement of Peroxide Values in Oils by Triphenylphosphine/Triphenylphosphine Oxide (TPP/TPPO) Assay Coupled with FTIR-ATR Spectroscopy: Comparison with Iodometric Titration. *Eur. J. Lipid Sci. Tech.*, 120:1800109, 2018.

[188] European Food Safety Authority. EFSA (European Food Safety Authority). Opinion of the Scientific Panel on Additives and Products or Substances used in Animal Feed on the Request from the European Commission on the Safety of Use of Colouring Agents in Animal Human Nutrition. *EFSA Journal*, 291:1, 2005.

[189] S. A. Jackowski, A. Z. Alvi, A. Mirajkar, Z. Imani, Y. Gamalevych, N. A. Shaikh, and G. Jackowski. Oxidation Levels of North American Over-the-Counter n-3 (Omega-3) Supplements and the Influence of Supplement Formulation and Delivery form on Evaluating Oxidative Safety. *J. Nutr. Sci.*, 4:1–10, 2015.

[190] G. Bannenberg. EPA/DHA Dietary Supplement Compliance: Content Claims and Quality. Singapore, 2019. Global Organization for EPA and DHA Omega-3s (GOED), Omega-3 Summit. accessed 02 March 2020.

[191] E. Hafer, U. Holzgrabe, K. Kraus, K. Adams, J. M. Hook, and B. W. K. Diehl. Qualitative and Quantitative ^{1}H NMR Spectroscopy for Determination of Divalent Metal Cation Concentration in Model Salt Solutions, Food Supplements and Pharmaceutical Products by Using EDTA as Chelating Agent. *Magn. Reson. Chem.*, 58:653–665, 2020.

[192] Y. Sahan. Some metals in table olives. In V. R. Preedy and R. R. Watson, editors, *Olives and Olive Oil in Health and Disease Prevention.*, pages 300–306. Academic Press, United States of America, 2010.

[193] J. L. Rodriguez-Otero, P. Paseiro, J. Simai, and A. Cepeda. Mineral Content of the Honeys Produced in Galicia (North-West Spain). *Food Chem.*, 49:169–171, 1994.

[194] R. Agrawal, R. Kumar, S. Rai, A. K. Pathak, A. K. Rai, and G. K. Rai. LIBS: A Quality Control Tool for Food Supplements. *Food Biophys.*, 6:527–533, 2011.

[195] S. Rodriguez-Stanley, T. Ahmed, S. Zubaidi, S. Riley, H. I. Akbarali, M. H. Mellow, and P. B. Miner. Calcium Carbonate Antacids Alter Esophageal Motility in Heartburn Sufferers. *Digest. Dis. and Sci.*, 49:1862–1867, 2004.

[196] M. Harada. Minamata Disease: Methylmercury Poisoning in Japan Caused by Environmental Pollution. *Crit. Rev. Toxicol.*, 25:1–24, 1995.

[197] M. M. Storelli and G. Barone. Toxic Metals (Hg, Pb, and Cd) in Commercially Important Demersal Fish From Mediterranean Sea: Contamination Levels and Dietary Exposure Assessment. *J. Food Sci.*, 78:T362–T366, 2013.

[198] T. F Christiansen, J. E. Busch, and S. C. Krogh. Successive Determinations of Calcium and Magnesium in Drinking Water by Complexometric, Potentiometric Digital Titration to Two Equivalence Points. *Anal. Chem.*, 48:1051–1056, 1976.

[199] H. A. Flaschka. *EDTA Titrations.* Pergamon Press, Oxford, United Kingdom, 1964. 9-15.

[200] F. L. Garvan. Metal chelates in ethylendiaminetetra acetic acid and related substances. In F. P. Dwyer and D. P. Mellor, editors, *Chelating Agents and Metal Chelates*, pages 283–334. Academic Press, New York, United States of America, 1964.

[201] D. C. Harris. *Quantitative Chemical Analysis.* W. H. Freeman and Company, New York,United States of America, 2007. 231.

[202] A. V. Zmozinski, A. de Jesus, M. G. Vale, and M. M. Silva. Determination of Calcium, Magnesium and Zinc in Lubricating Oils by Flame Atomic Absorption Spectrometry using a Three-Component Solution. *Talanta*, 83:637–643, 2010.

[203] J. H. Kim and J. H. Lee. Simultaneous Determination of Six Cations in Mineral Water by Single-Column Ion Chromatography. *J. Chromatogr. A*, 782:140–146, 1997.

[204] D. Pröfrock and A. Prange. Inductively Coupled Plasma–Mass Spectrometry (ICP-MS) for Quantitative Analysis in Environmental and Life Sciences: A Review of Challenges, Solutions, and Trends. *Appl. Spectrosc.*, 66:843–868, 2012.

[205] R.F. Puchyr and R. Shapiro. Determination of Trace Elements in Foods by HCl-HNO_3 Leaching and Flame Atomic Absorption Spectroscopy. *J. Assoc. Off. Ana. Chem.*, 69:868–870, 1986.

[206] S. G. Patching. NMR Active Nuclei for Biological and Biomedical Applications. *J. diagn. imaging ther.*, 3:7–48, 2016.

[207] G. A. Smith, R. T. Hesketh, J. C. Metcalfe, J. Feeney, and P. G. Morris. Intracellular Calcium Measurements by ^{19}F NMR of Fluorine-Labeled Chelators. *Proc. Natl. Acad. Sci. USA*, 80:7178–7182, 1983.

[208] S. Tran-Dinh and J. M. Neumann. A ^{31}P - NMR Study of the Interaction of Mg^{2+} Ions with Nucleoside Diphosphates. *Nucleic Acids Research*, 4:397–403, 1977.

[209] M. C. Gennaro, P. Mirti, and C. Casalino. NMR Study of Intramolecular Processes in EDTA Metal Complexes. *Polyhedron*, 2:13–18, 1983.

[210] S. Han and Y. Ba. Determination of the Concentrations of Metal Cations in Aqueous Solutions Using Proton NMR Spectral Area Integration of the EDTA Complexes. *J. Solution Chem.*, 33:301–312, 2004.

[211] B.S. Somashekar, O. B. Ijare, G. A. N. Gowda, V. Ramesh, S. Gupta, and C. L. Khetrapal. Simple Pulse-Acquire NMR Methods for the Quantitative Analysis of Calcium, Magnesium and Sodium in Human Serum. *Spectrochim. Acta A*, 65:254–260, 2006.

[212] D. C. Dash. *Analytical chemistry.* PHI Learning, United States of America, 2011. 80.

[213] Y. Ba, S. Han, L. Ni, T. Su, and A. Garcia. Dynamic NMR of Intramolecular Exchange Processes in EDTA Complexes of Sc^{3+}, Y^{3+}, and La^{3+}. *J. Chem. Educ.*, 83:296–298, 2006.

[214] H. P. Latscha. Komplexometrische titrationen (chelatometrie). In H. P. Latscha, G. W. Linti, and H. Klein, editors, *Analytische Chemie - Basiswissen III*, pages 302–305. Springer-Verlag, Heidelberg, Germany, 2013.

[215] R. H. Barton, D. Waterman, F. W. Bonner, E. Holmes, R. Clarke, J. K. Nicholson, J. C. Lindon, and P. Consortium. The Influence of EDTA and Citrateanticoagulant Addition to Human Plasma on Information Recovery from NMR-based Metabolic Profiling Studies. *Mol. Biosyst.*, 6:215–224, 2010.

[216] L. Rong, Z. Liu, M. Ma, J. Liu, Z. Xu, L. W. Lim, and T. Takeuchi. Simultaneous Determination of Inorganic Cations by Capillary Ion Chromatography with a Non-suppressed Contactless Conductivity Detector. *Anal. Sci.*, 28:367–372, 2012.

[217] Umweltbundesamt. Trinkwasser wird bleifrei. Neuer Grenzwert für Blei im Trinkwasser ab 1. Dezember 2013. `https://bit.ly/2Xifu7E`, 2013. accessed 01 February 2020.

[218] World Health Organization. Lead in Drinking-water. `https://bit.ly/2UNjGeh`, 2011. accessed 01 February 2020.

[219] R. A. Sheldon. *Chirotechnology: Industrial Synthesis of Optically Active Compounds.* CRC Press, Boca Raton, United States of America, 1993.

[220] J. McConathy and M. J. Owens. Stereochemistry in Drug Action. *Prim. Care Companion J. Clin. Psychiatry*, 5:70–73, 2003.

[221] K. Jóźwiak, J. Lough, and I.W. Wainer. *Drug Stereochemistry: Analytical Methods and Pharmacology.* Marcel Dekker., New York, United States of America, 1988.

[222] E. Tokunaga, T. Yamamoto, E. Ito, and N. Shibata. Understanding the Thalidomide Chirality in Biological Processes by the Self-disproportionation of Enantiomers. *Nature*, 8:17131–17138, 2018.

[223] E. L. Izake. Chiral Discrimination and Enantioselective Analysis of Drugs: An Overview. *J. Pharm. Sci.*, 96:1659–1676, 2007.

[224] G. Gübitz and M. G. Schmid. *Chiral Separations: Methods and Protocols.* Humana Press, Totawa, United States of America, 2004.

[225] J. Shen and Y. Okamoto. Efficient Separation of Enantiomers Using Stereoregular Chiral Polymers. *Chem. Rev.*, 116:1094–1138, 2016.

[226] N. Harada. HPLC Separation of Diastereomers: Chiral Molecular Tools Useful for Preparation of Enantiopure Compounds and Simultaneous Determination of Their Absolute Configurations. *Molecules*, 21:1328–1365, 2016.

[227] P. E. Hare and E. Gil-Av. Separation of D and L Amino Acids by Liquid Chromatography: Use of Chiral Eluants. *Science*, 204:1226–1228, 1979.

[228] H. Frank, G. J. Nicholson, and E. J. Bayer. Rapid Gas Chromatographic Separation of Amino Acid Enantiomers with a Novel Chiral Stationary Phase. *Chromatogr. Sci.*, 15:174–176, 1977.

[229] H. Wan and L. G. Blomberg. Chiral Separation of Amino Acids and Peptides by Capillary Electrophoresis. *J. Chromatogr. A*, 875:43–88, 2000.

[230] T. J. Wenzel. *Discrimination of Chiral Compounds Using NMR Spectroscopy.* John Wiley & Sons, Weinheim, Germany, 2007.

[231] G Wolf, A. M. Cook, and J. E. Dannatt. Enantiodifferentiation of Multifunctional Tertiary Alcohols by NMR Spectroscopy with a Whelk-O Type Chiral Solvating Agent. *Tetrahedron Asymmetry*, 25:163–169, 2014.

[232] D. Parker. NMR Determination of Enantiomeric Purity. *Chem Rev.*, 91:1441–1457, 1991.

[233] R. Rothchild. NMR methods for Determination of Enantiomeric Excess. *Enantiomer*, 5:457–471, 2000.

[234] T. Viswanathan and A. Toland. NMR Spectroscopy Using a Chiral Lanthanide Shift Reagent to Assess the Optical Purity of 1-Phenylethylamine. *J. Chem. Educ.*, 72:945–946, 1995.

[235] J. A. Dale and H. S. Mosher. Nuclear Magnetic Resonance Enantiomer Reagents. Configurational Correlations via Nuclear Magnetic Resonance Chemical Shifts of Diastereomeric Mandelate, O-Methylmandelate, and (*alpha*-Methoxy-*alpha*-Trifluoromethylphenylacetic Acid (MTPA) Esters. *J. Am. Chem. Soc.*, 95:512–519, 1973.

[236] Dakipabru. Einhorn-Acylierung Reaktionsmechanismus., 2019. `https://bit.ly/2YsJ4aq`, accessed 24 August 2020.

[237] Sigma Aldrich. (R)-(+)-*alpha*-Methoxy-*alpha*-Trifluoromethylphenylacetic Acid. `https://bit.ly/2Xabczf`, accessed 17 February 2020.

[238] A. Einhorn and F. Hollandt. Ueber die Acylirung der Alkohole und Phenole in Pyridinlösung. *Justus Liebigs Annalen der Chemie*, 301(1):95–115, 1898.

[239] E. Baumann. Ueber eine einfache Methode der Darstellung von Benzoësäureäthern. *Berichte der deutschen chemischen Gesellschaft*, 19(2):3218–3222, 1886.

[240] J. Falbe and M. Regitz. *RÖMPP Lexikon Chemie, 10. Auflage, 1996-1999: Band 2: Cm - G.* Thieme, New York, United States of America, 2014.

[241] J. Enquist. The Horeau Principle: The Nature of Statistical Amplification in Enantioselective Synthesis., 2006. `https://bit.ly/35yiNKJ`, accessed 01 May 2020.

[242] A. Horeau. Determination of the configuration of secondary alcohols by partial resolution. In H. B. Kagan, editor, *Steroechemistry: Fundamentals and Methods.*, page 51. Georg Thieme, Stuttgart, Germany, 1977.

[243] T.A. Ryan, E.A. Seddon, K.R. Seddon, and C. Ryan. *Phosgene: And Related Carbonyl Halides*. Elsevier, Amsterdam, Netherlands, 1996. 464–475.

[244] BASF. Menthol - BASF's menthol for fresh and minty taste. `https://bit.ly/32j5RXv`, accessed 06 October 2020.

[245] Committee of Experts on Cosmetic Products. *Active Ingredients Used in Cosmetics: Safety Survey*. Council of Europe Publishing, Strasbourg, France, 2008.

[246] D.-D. Luo, X.-Y. Chen, Z.-B. Zhang, Y.-F. Zheng C.-Y. Sun, Y.-H. Liu, X.-F. Wang, Q. Wang, J. Y.-X. Zhan, and Z.-R. Su. Different effects of (+)-borneol and (-)-borneol on the pharmacokinetics of osthole in rats following oral administration. *Molecular Medicine Reports*, 15:4239–4246, 2017.

[247] L. Xu, G. Cui, C. Ke, Y. Fan, and Y. Yan. Immobilized Burkholderia cepacia Lipase on pH-Responsive Pullulan Derivatives with Improved Enantioselectivity in Chiral Resolution. *Catalysts*, 8:69–80, 2018.

[248] H. Yamamoto and A. Matsuyama. Synthesis of chiral alcohols with carbonyl reductase library and robust nad(p)h regeneration system. In Ramesh N. Patel, editor, *Biocatalysis in the Pharmaceutical and Biotechnology Industries*, page 626. CRC Press, Boca Raton, United States of America, 2007.

[249] D. Sicker, K.-P. Zeller, H.-U. Siehl, and S. Berger. *Natural Products - Isolation, Structure Elucidation, History.* Wiley-VCH, Weinheim, Germany, 2019. 236–238.

[250] A. C. Siani, M. R. R. Tappin, M. F. S. Ramos, J. L. Mazzei, M. C. K. V. Ramos, and N. Frighetto F. R. de Aquino Neto. Linalool from Lippia alba: Study of the Reproducibility of the Essential Oil Profile and the Enantiomeric Purity. *J. Agric. Food Chem.*, 50:3518–3521, 2002.

[251] K .H. C. Baser, T. Özek, and A. Konakchiev. Enantiomeric Distribution of Linalool, Linalyl Acetate and Camphor in Bulgarian Lavender Oil. *J. Essent. Oil Res.*, 17:135–136, 2005.

[252] A. A. G. Shaikh and S. Sivaram. Organic Carbonates. *Chemical Reviews*, 96:951–976, 1996.

[253] D. G. Morris. *Stereochemistry.* The Royal Society of Chemistry, Cambridge, United Kingdom, 2001.

[254] A. A. Puntambekar. *Analysis And Design Of Algorithms.* Technical Publications Pune, Pune, India, 2008. Chapter 3.

[255] J. P. Vigneron, M. Dhaenens, and A. Horeau. Nouvelle Methode pour Porter au Maximum la Purete Optique d'un Produit Partiellement Dedouble sans L'Aide D'Aucune Substance Chirale. *Tetrahedron*, 29:1055–1059, 1973.

[256] K. J. Stine. Chirality in monolayers. In P. Somasundaran, editor, *Encyclopedia of Surface and Colloid Science, Volume 2*, page 1278. Taylor & Francis, Boca Raton, United States of America, 2006.

[257] J. N. Shoolery. Some Quantitative Applications of ^{13}C NMR Spectroscopy. *Prog. Nucl. Magn. Reson. Spectrosc.*, 11:79–93, 1977.

[258] D. A. L. Otte, D. E. Borchmann, Chin Lin, Marcus Weck, and K. A. Woerpel. ^{13}C NMR Spectroscopy for the Quantitative Determination of Compound Ratios and Polymer End Groups. *Org. Lett.*, 16,:1566–1569, 2014.

[259] International Organization for Standardization. ISO 3960:2007: Animal and Vegetable Fats and Oils – Determination of Peroxide Value – Iodometric (Visual) Endpoint Determination., 2007.

[260] International Organization for Standardization. ISO 27107:2008: Animal and Vegetable Fats and Oils – Determination of Peroxide Value – Potentiometric End-Point Determination., 2008.

[261] Bruker. The Versatile Sample Changer. `https://bit.ly/3ocxZFK`. accessed 21 October 2020.

[262] L. Mannina, M. D'Imperio, D. Capitani, S. Rezzi, C. Guillou, T. Mavromoustakos, M. D. M Vilchez, A. H. Fernández, F. Thomas, and R. Aparicio. ^{1}h nmr-based protocol for the detection of adulterations of refined olive oil with refined hazelnut oil. *J. Agric. Food Chem.*, 57:11550–11556, 2009.

[263] German Society for Fat Science e.V. Gemeinsame Stellungnahme der Fachgruppe Produkte und Produktsicherheit sowie des Gemeinschaftsausschuss für die Analytik von Fetten, Ölen, Fettprodukten, verwandten Stoffen und Rohstoffen „GA Fett" der Deutschen Gesellschaft für Fettwissenschaft zur Neufassung der Leitsätze für Speisefette und Speiseöle vom 30.5.2011 und 3.11.2011., 2011. `https://bit.ly/2Zv7Ne2`, accessed 02 July 2020.

[264] Reportlinker. Global Market Study on Krill Oil: Effective Than Other Marine Oils Since Safer, Healthier, More Potent and More Absorbable., 2016. `https://bit.ly/31z1atQ`, accessed 02 July 2020.

[265] L. Burri, N. Hoem, Y. B. Monakhova, and B. W. K. Diehl. Fingerprinting Krill Oil by ^{31}P, ^{1}H and ^{13}C NMR Spectroscopies. *J. Am. Oil Chem. Soc.*, 93:1037–1049, 2016.

[266] L. Burri, K. Berge, K. Wibrand, R. K. Berge, and J. L. Barger. Differential effects of krill oil and fish oil on the hepatic transcriptome in mice. *Front Genet*, 2:1–8, 2011.

[267] R. Ebermann and I. Elmadfa. *Lehrbuch Lebensmittelchemie und Ernährung.* Springer-Verlag/Wien, Germany, 2nd edition, 2011.

[268] C. N. Reilley and R. W. Schmid. Chelometric Titrations with Potentiometric End Point Detection. *Analytical Chemistry*, 30:947–953, 1958.

[269] Sigma-Aldrich. Phosgene Solution. `https://bit.ly/3jGV29p`. accessed 12 July 2020.

[270] P. Limaye. Methyl isocyanate. In Philip Wexler, editor, *Encyclopedia of Toxicology.*, pages 306–309. Academic Press, Oxford, United Kingdom, 3rd edition, 2014.

[271] J. Borak and W. F. Diller. Phosgene Exposure: Mechanisms of Injury and Treatment Strategies. *J. Occup. Environ. Med.*, 43:110–119, 2001.

[272] Institut für Arbeitsschutz. GESTIS-Stoffdatenbank: "Phosgen". `https://bit.ly/39knzNs`, 01 2011. accessed 21 July 2020.

[273] H. Babad and A. G. Zeiler. The Chemistry of Phosgene. *Chemical Reviews*, 73:75–91, 1973.

[274] A. Lubineau and J. Augé. Water as solvent on organic synthesis. In Paul Knochel, editor, *Modern Solvents in Organic Synthesis.*, pages 1 – 40. Springer, Berlin, Germany, 1st edition, 1999.

[275] P. P. Lankhorst, J. H. J. van Rijn, and A. L. L. Duchateau. One-Dimensional ^{13}C NMR Is a Simple and Highly Quantitative Method for Enantiodiscrimination. *Molecules*, 23:1785–1795, 2018.

Appendix

List of publications, documentation and individual contribution for each author to the publication reprinted in this thesis are presented in this chapter.

Paper#1: Interlaboratory Comparison Test as an Evaluation of Applicability of an Alternative Edible Oil Analysis by ^{1}H NMR Spectroscopy

Elina Zailer[1], Ulrike Holzgrabe[2], Bernd Diehl[3]
Journal of AOAC INTERNATIONAL, 100: 1819-1830, 2017.

Author	**1**	**2**	**3**
Study Design	x	-	x
Experimental Work	x	-	x
Data Analysis	x	-	x
Manuscript Planning	x	x	x
Manuscript Writing	x	x	x
Correction of Manuscript	x	x	x
Supervision of Elina Hafer	-	x	x

Oral & Poster Presentation:

- Performance Assessment in Quantitative NMR Analyses of Edible Oils, AOCS Annual Meeting and Short Courses, April 30 – May 03, 2017, Orlando, Florida, USA.
- ^{1}H NMR Interlaboratory Test for Edible Oil Characterization, AOCS Annual Meeting and Short Courses, May 01-04, 2016, Salt Lake City, Utah, USA.
- Das "q" in quantitative NMR, 42. Tagung Praktische Probleme der Kernresonanzspektroskopie 2020, March 17 - March 18, 2020, Berlin, Germany (postponed).

Paper#2: NMR Spectroscopy: Determination of Peroxide Value in Vegetable and Krill Oil by Using Triphenylphosphine as Tagging Reagent

Elina Hafer[1], Ulrike Holzgrabe[2], Sascha Wiedemann[3], Kristie M. Adams[4], Bernd Diehl[5]
European Journal of Lipid Science and Technology, 122: 1900442-1900452, 2020.

Author	**1**	**2**	**3**	**4**	**5**
Study Design	x	x	-	x	x
Experimental Work	x	-	x	-	x
Data Analysis	x	-	x	-	x
Manuscript Planning	x	x	-	-	-
Manuscript Writing	x	x	-	-	-
Correction of Manuscript	x	x	-	x	x
Supervision of Elina Hafer	-	x	-	-	x

Oral & Poster Presentatio:

- Holistic Control of Edible and Fish Oils Based on NMR Spectroscopy, AOCS Annual Meeting and Short Courses, May 01-04, 2016, Salt Lake City, Utah, USA.
- Holistic Control of Fish Oils Based on NMR Spectroscopy, 14th Euro Fed Lipid Congress, September 18-21, 2016, Ghent, Belgium.
- Determination of Peroxide Values of Edible and Marine Oils by Nuclear Magnetic Resonance Spectroscopy, AOCS Annual Meeting and Short Courses, April 30 – May 03, 2017, Orlando, Florida, USA.
- Determination of Peroxide Values of Krill Oil and Lecithins by Nuclear Magnetic Resonance Spectroscopy, AOCS Annual Meeting and Short Courses, April 30 – May 03, 2017, Orlando, Florida, USA.
- Performance Assessment in Quantitative NMR Analyses of Edible Oils, AOCS Annual Meeting and Short Courses, April 30 – May 03, 2017, Orlando, Florida, USA.
- Determination of Peroxide Values of Edible and Marine Oils by Nuclear Magnetic Resonance Spectroscopy, 15th Euro Fed Lipid Congress, August 27-30, 2017, Uppsala, Sweden.
- Holistic control of edible oils based on NMR spectroscopy, Innovations in Food Analytics, September 19-21, 2018, Erding, Germany.
- Das "q" in quantitative NMR, 42. Tagung Praktische Probleme der Kernresonanzspektroskopie 2020, March 17 - March 18, 2020, Berlin, Germany (postponed).

Paper#3: Qualitative and Quantitative ^{1}H NMR Spectroscopy for Determination of Divalent Metal Cation Concentration in Model Salt Mixtures, Food Supplements and Pharmaceutical Products by Using EDTA as Chelating Agent

Elina Hafer[1], Ulrike Holzgrabe[2], Katharina Kraus[3], Kristie M. Adams[4], James M. Hook[5], Bernd Diehl[6]
Magnetic Resonance Chemistry, 58: 653-665, 2020

Author	**1**	**2**	**3**	**4**	**5**	**6**
Study Design	x	x	x	x	-	x
Experimental Work	x	-	x	-	x	x
Data Analysis	x	x	x	-	x	x
Manuscript Planning	x	x	-	-	-	x
Manuscript Writing	x	x	-	-	-	x
Correction of Manuscript	x	x	-	x	x	x
Supervision of Elina Hafer	-	x	-	-	-	x

Oral & Poster Presentation:

- NMR as a powerful alternative for complexometric titration to analyze metal ions qualitatively and quantitatively, 7th Annual Practical Applications of NMR in Industry Conference (PANIC), March 02 – March 07, 2019, Hilton Head Island, SC, USA.
- Das "q" in quantitative NMR, 42. Tagung Praktische Probleme der Kernresonanzspektroskopie 2020, March 17 - March 18, 2020, Berlin, Germany (postponed).

Paper#4: A Rapid ^{13}C NMR Assay for Enantiomeric Excess of Alcohols by using Phosgene as Tagging Agent

Elina Hafer[1], Ulrike Holzgrabe[2], Bernd Diehl[3]
unpublished

Author	**1**	**2**	**3**
Study Design	x	x	x
Experimental Work	x	-	x
Data Analysis	x	-	x
Manuscript Planning	x	x	-
Manuscript Writing	x	x	-
Correction of Manuscript	x	x	x
Supervision of Elina Hafer	-	x	x

Oral & Poster Presentatio:

- Das "q" in quantitative NMR, 42. Tagung Praktische Probleme der Kernresonanzspektroskopie 2020, March 17 - March 18, 2020, Berlin, Germany (postponed).